eco.mont

Journal on Protected Mountain Areas Research and Management

Vol. 14 No. 2 – July 2022

eco.mont – Journal on Protected Mountain Areas Research and Management
is published by Austrian Academy of Sciences Press and *innsbruck* university press

Publishers
eco.mont – Journal on Protected Mountain Areas Research and Management is published by
• Austrian Academy of Sciences Press, Postgasse 7, 1011 Vienna (online version), ISSN 2073-106X
in cooperation with
• *innsbruck* university press (*i*up), Technikerstraße 21a, 6020 Innsbruck (print version), ISSN 2073-1558

Editors
Valerie Braun (Austrian Academy of Sciences), Martin Coy (University of Innsbruck) and
Günter Köck (Austrian Academy of Sciences)

Editorial Board
The Editorial Board is nominated in cooperation with ISCAR and ALPARC.

Serena Arduino (CIPRA International)
Carole Birck (Asters Conservatoire d'espaces naturels Haute-Savoie, France)
Cédric Dentant (Parc National des Écrins, France)
Leopold Füreder (University of Innsbruck, Austria)
Matej Gabrovec (Anton Melik Geographical Institute, Slovenia)
Florian Knaus ((ETH Zurich, Department of Environmental Systems Science,
Institute of Terrestrial Ecosystems and UNESCO Biosphere Entlebuch, Switzerland)
Guido Plassmann (Task Force Protected Areas AC / ALPARC)
Roland Psenner (Eurac Research, Italy)
Clara Tattoni (Università degli Studi dell'Insubria, Italy)
Herbert Wölger (National Park Gesäuse, Austria)

Senior consultant: Kristina Bauch, Axel Borsdorf, Thomas Scheurer and Bernd Stöcklein

Editorial Policy
The geographic focus is on Alpine and other European (or global) protected mountain areas.

Publication Policy
eco.mont – Journal on Protected Mountain Areas Research and Management publishes peer-reviewed research articles by authors who work on protected mountain areas and articles about management approaches within these areas.
eco.mont is published twice a year. We only accept previously unpublished articles (including on the internet). Manuscripts submitted for publication are blind peer-reviewed by a member of the editorial board (to ensure a good fit with the mission of the journal and the scientific quality) and independently by a peer (to guarantee the scientific quality).
Article processing fee: non-mandatory charges are levied for papers published in eco.mont to help defray production costs. Authors, especially those with institutional and grant support, are urged to take all reasonable steps to pay the charges. The article processing charge is currently EUR 450 per article.

Please submit your article through our Open Journal System
http://ecomont.vlg.oeaw.ac.at/index.php/ecomont/login

Subscriptions and Back Issues
• electronic: open access
• prints: EUR 50 p.a.

Copyright Rules
Please contact: valerie.braun@oeaw.ac.at

Design
Logo and basic layout of the journal developed by Sigrun Lange
Cover photograph: © C. Körner

Content

Published by:

ÖAW AUSTRIAN ACADEMY OF SCIENCES

IGF

universität innsbruck

Publisher:

AUSTRIAN ACADEMY OF SCIENCES PRESS

innsbruck university press
peer reviewed

Initiated by:

ISCAR

alparc

ISSN 2073-106X print version
ISSN 2073-1558 online version: http://epub.oeaw.ac.at/eco.mont

eco.mont – Volume 14, Number 2, July 2022
ISSN 2073-106X print version – ISSN 2073-1558 online version: http://epub.oeaw.ac.at/eco.mont
https://dx.doi.org/10.1553/eco.mont-14-2s3

Editorial

Alpine protected areas (PAs) play a key role in the conservation of biodiversity but also in the monitoring of species and habitats. Only PAs can ensure long-term monitoring, over many years, far beyond normal scientific project durations, with professional equipment and staff on the ground. This feature makes PAs especially precious for the sciences, for the development of management measures and their testing, and for political decisions concerning the conservation of biodiversity.

Intact habitats and ecosystems provide greater chances for a healthier and more resilient environment. In the coming decades, PAs in the Alps should join forces to develop a common transboundary monitoring system of species and habitats, allowing the evolution of alpine ecosystems and biodiversity to be evaluated under the light of climate change. If the indicators and species are well chosen, an Alps-wide monitoring system could play an important role as an early warning system for biodiversity loss in the region.

To be realistic and acceptable to PA managers, a common monitoring system should be based on relevant species, using simple indicators which can be easily harmonized and used for scientific evaluations. The goal is to define a common minimum standard, among PAs, of existing monitoring methods.

Since its first issue, *eco.mont* has published articles about long-term monitoring programmes in various areas in the Alps (see e.g. Robinson & Oertli 2009; Robinson et al. 2011; Güsewell & Klötzli 2012; Bohner et al. 2012; Mayer & Erschbamer 2014; Fischer et al. 2014; Bonet et al. 2016; Battisti et al. 2019). To further underline the importance of monitoring programmes in PAs, after an internal review the editors and the Editorial Board decided to accept and publish in this issue a long paper by Körner et al. The 17 authors present the conceptual framework and a summary of the first five years of findings of the broad, interdisciplinary, long-term monitoring programme of terrestrial and aquatic alpine biota in the Hohe Tauern National Park (NPHT) in the Alps (Austria, Italy and Switzerland). The concept was developed in 2011 by the Scientific Advisory Board of the NPHT, on the initiative of the three NPHT directors, and finally realized in 2016. It consists of a total of eight research modules and uses highly standardized observation and analysis methods. The unusual comprehensiveness of this monitoring programme and the fact that it is a practice of use potentially to all PA managers, led us to accept the paper, in spite of its length. We are very excited to offer it to our readers, and would be interested to read and learn more in the future about long-term studies in the Alps and globally.

The other articles in this issue highlight once again the many topics within mountain PAs, but also the need to protect species living in mountain areas which are not yet protected.

A further long-term monitoring study, by Christopher T. Robinson, Christa Jolidon, Gabriele Consoli, Simon Bloem & Christian Ebi, takes us to the Macun lakes in the Swiss National Park. This study started in 2001 and was followed by annual monitoring of the physico-chemistry as well as of the temperature of the water at 10 primary sites in various basins and outlet streams (see also Robinson & Oertli 2009; Robinson et al. 2011).

Another study in this issue is concerned with the threatened ungulates *Ammotragus lervia* and *Gazella cuvier* in the semi-arid North African Nador Mountains. Farid Bounaceur, Aoued Boualem, Abdelkader Abdi, Fatima Zohra Bissaad, Mohamed Amine Kaddouri, Mohamed Djilali, Azeddine Zenati, Yahia Belgarssa & Stéphane Aulagnier assess the local distribution and estimate the abundance and population composition of the ungulates, which are listed as Vulnerable in the IUCN list. The results indicate that new conservation measures in the region are required.

Hilal Turgut & Bülent Turgut examine the effects of landforms and climate on vegetation dynamics in the Caucasus over a period of three years. The study area is characterized by high mountains and high biodiversity. The results may serve practitioners in gauging the possible consequences of climate change and managing sites accordingly.

Huiying Xue, Da Qing Luo, Bu Duo, Qing Xue, Xing Le Qu & Wen Wen Guo studied the community structure and diversity of soil nematodes at twelve selected plots around Lake Paiku in the Mount Qomolangma National Nature Reserve in Tibet, China. Due to the region's high altitude, cold dry climate and slow plant growth, it is difficult for an ecosystem to recover if it is degraded. The results show that the soil nematode community around Lake Paiku is rich in diversity but low in population density.

Sony Lama, Saroj Shrestha, Ang Phuri Sherpa, Munmun Tamang & Dinesh Ghale present the avifaunal diversity in a district in Western Nepal. Illegal hunting and trapping, hydropower projects, habitat fragmentation as well as the Covid-19 pandemic pose threats to the avifauna, which has already decreased in numbers due to human interference. The authors give an update on the bird checklists, the first since 2015.

With this issue, we once again hope to raise awareness of the importance of mountain protected areas, and with the publication of long-term studies we support and outline the interaction of scientists and PA managers.

Finally, we would like to take this opportunity to introduce and welcome two new members of the eco.mont Editorial Board: Clara Tattoni and Florian Knaus. Clara Tattoni is a research fellow at the Environment Analysis and Management Unit (*Unità di Analisi e Gestione delle Risorse Ambientali*, UAGRA), a research unit of the Department of Theoretical and Applied Sciences of the University of Insubria in Varese, Italy. She has published on various topics including land-use change, forestry, biodiversity and Alpine ecosystems. Florian Knaus is currently a lecturer at the ETH Zurich, Department of Environmental Systems Science, Institute of Terrestrial Ecosystems, where he holds the Chair of Ecosystem Management. He is also the Scientific Coordinator of the Entlebuch UNESCO Biosphere.

At the same time, Astrid Wallner and Massimo Bocca are leaving the Editorial Board of eco.mont. We wish them both all the best for the future and thank them warmly for their engagement with the journal.

Valerie Braun, Guido Plassman & Günter Köck

Battisti, A., R. Vodă, M. Gabaglio, C. Cerrato, R. Bionda, P. Palmi & S. Bonelli 2019. New data concerning the butterfly fauna (Lepidoptera, Papilionoidea) of Veglia – Devero Natural Park and its surroundings (northwestern Italian Alps). *eco.mont* 11(1): 5–15.

Bohner, A., F. Starlinger & P. Koutecky 2012: Vegetation changes in an abandoned montane grassland, compared to changes in a habitat with low-intensity sheep grazing – a case study in Styria, Austria. *eco.mont* 4(2): 5–12.

Bonet, R., F. Arnaud, X. Bodin, M. Bouche, I. Boulangeat, P. Bourdeau, M. Bouvier, L. Cavalli, P. Cholert, A. Delestrade, C. Dentant, D. Dumas, L. Fouinat, M. Gardent, S. Lavergne, S. Lavorel, E. Naffrechoux, Y. Nellier, M.-E. Perga, C. Saot, O. Senn, E. Thibert & W. Thuillert 2016. Indicators of climate: Ecrins National Park participates in long-term monitoring to help determine the effects of climate change. *eco.mont* 8(1): 44–52.

Fischer, A., M. Stocker-Waldhuber, B. Seiser, B. Hynek & H. Slupetzky 2014. Glaciological monitoring in Hohe Tauern National Park. *eco.mont* 6(1): 49–56.

Güsewell, S. & F. Klötzli 2012. Local plant species replace initially sown species on roadsides in the Swiss National Park. *eco.mont* 4(1): 23–33.

Mayer, R. & B. Erschbamer 2014. Ongoing changes at the long-term monitoring sites of Gurgler Kamm Biosphere Reserve, Tyrol, Austria. *eco.mont* 6(1): 5–14.

Robinson, C.T., M. Doering & L. Seelen 2011. Use of protected areas for freshwater biomonitoring – case studies in Switzerland. *eco.mont* 3(2): 13–22.

Robinson, C.T. & B. Oertli 2009. Long-term biomonitoring of alpine waters in the Swiss National Park. *eco.mont* 1(1): 23–34.

eco.mont – Volume 14, Number 2, July 2022
ISSN 2073-106X print version – ISSN 2073-1558 online version: http://epub.oeaw.ac.at/eco.mont
https://dx.doi.org/10.1553/eco.mont-14-2s5

ERRATA

Monitoring threatened ungulates (*Gazella cuvieri* and *Ammotragus lervia*) in the semi-arid North African Nador Mountains

Farid Bounaceur, Aoued Boualem, Abdelkader Abdi, Fatima Zohra Bissaad, Mohamed Amin Kaddouri, Mohamed Djilali, Azeddine Zenati, Yahia Belgarssa & Stéphane Aulagnier

Keywords: Gazella cuvieri, Ammotragus lervia, survey, conservation

Abstract

Cuvier's gazelle (*Gazella cuvieri*) and aoudad (*Ammotragus lervia*) are listed as *Vulnerable* in the IUCN red list, and any population should be the subject of scientific attention. Both ungulates were monitored for a year in the Nador Mountains (western Algeria). This is the first record of aoudad in this part of Tiaret province. Both species are partly sympatric. However, the aoudad was sighted only in small numbers in the roughest valleys in the north. The gazelle population is larger, but with few juveniles. The future of these wild ungulates is therefore worrying, and new conservation measures are required, including protecting this area.

Introduction

At the beginning of the 20th century, mountains of northwest Africa were still inhabited by large carnivores such as lion (*Panthera leo*) and leopard (*Panthera pardus*) and their main preys, aoudad or Barbary sheep (*Ammotragus lervia*) and Cuvier's gazelle (*Gazella cuvieri*) (Trouessart 1905). The last lions were sighted in 1912 in Kabylia for Algeria (De Smet 1989), and 1942 in the High Atlas for Morocco (Cuzin et al. 2017a), where the species was suspected to be extinct in the 1950s (Lee et al. 2015). The last leopards were reported at the turn of the 21st century in the High Atlas and Saharan Atlas (Cuzin 2003; Purroy 2010). The main causes of extinction were hunting in order to protect livestock, and the decline of the two wild mountain ungulates (Cuzin 2003).

This decline was assessed by the IUCN, whose red list until 2016 categorized Cuvier's gazelle as *Endangered*, with sub-populations of fewer than 250 mature individuals (C2a(i)). The species was then recategorized as *Vulnerable*, as two sub-populations were found with well above 250 mature individuals (IUCN SSC Antelope Specialist Group 2016). The aoudad is also listed as *Vulnerable* (C1) at international level (Cassinello et al. 2021). Formerly distributed in all craggy terrains of northwest Africa, both species retreated to the mountains under the increasing pressure of human activities at lower altitudes (e.g. Aulagnier 1992; Gil-Sánchez et al. 2017). Nowadays, poaching and habitat loss due to overgrazing by livestock are the main causes of decline (DGF 2017; Cassinello et al. 2021). Habitat fragmentation is another risk, as some sub-populations may fall below the viable population size (Wacher et al. 2002; Aulagnier et al. 2015; Ramzi et al. 2018; El Alami 2019).

In Algeria, the status of these species has recently been updated (Bounaceur et al. 2016a, b); the picture is now quite different, at least in the northern part of the country, where there is a relatively large and stable population of Cuvier's gazelle (Bounaceur et al. 2016b) and only five remaining small populations of aoudad (Bounaceur et al. 2016a). These sub-populations should therefore be monitored in order to evaluate their dynamics and so that management steps can be taken to improve the species' probability of survival.

We surveyed one of the last areas inhabited by both ungulate species in northwestern Algeria in order to (1) assess their local distribution and (2) estimate their abundance and population composition.

Methods

Study area

The Nador Mountains cover an area of 14,181 ha in Tiaret province (western Algeria) between 34° 04' and 35° 11' N, 1° 33' and 1° 53' E (Figure 1). This massif of limestone and dolomites includes, from west to east, a low-altitude plateau (126 m), high summits reaching 1,493 m at Djebel Chemakh, and an inclined plane sloping down to 883 m. The topography is very complex, with steep cliffs and deep valleys; there are no permanent watercourses and only a few springs.

The climate is Mediterranean continental according to the Debrach Continental Index (1953). Rainfall (which occurs from late autumn to spring) is around 300 mm / year. The dry period, estimated by the ombrothermal diagram of Bagnouls & Gaussen (1953), extends from March to November. The average daily temperature varies from 4.8°C in winter to 38.2°C in summer. According to Emberger's quotient (1930) of Q2 = 26.35, the area belongs to the upper arid stage, with cool winters.

Most of the plateau is covered by a steppe of *Stipa tenacissima*. The vegetation on the slopes is dominated either by *Juniperus oxycedrus* or by a mix of *Juniperus oxycedrus* and *Stipa tenacissima*; the most north-easterly parts are covered mainly by *Pistacia lentiscus* and *Tetraclinis articulata*. *Pinus halepensis* or *Quercus ilex* occupy the northern summits. A total of 79 plant species are found, which include *Cupressus sempervirens*, *Juniperus*

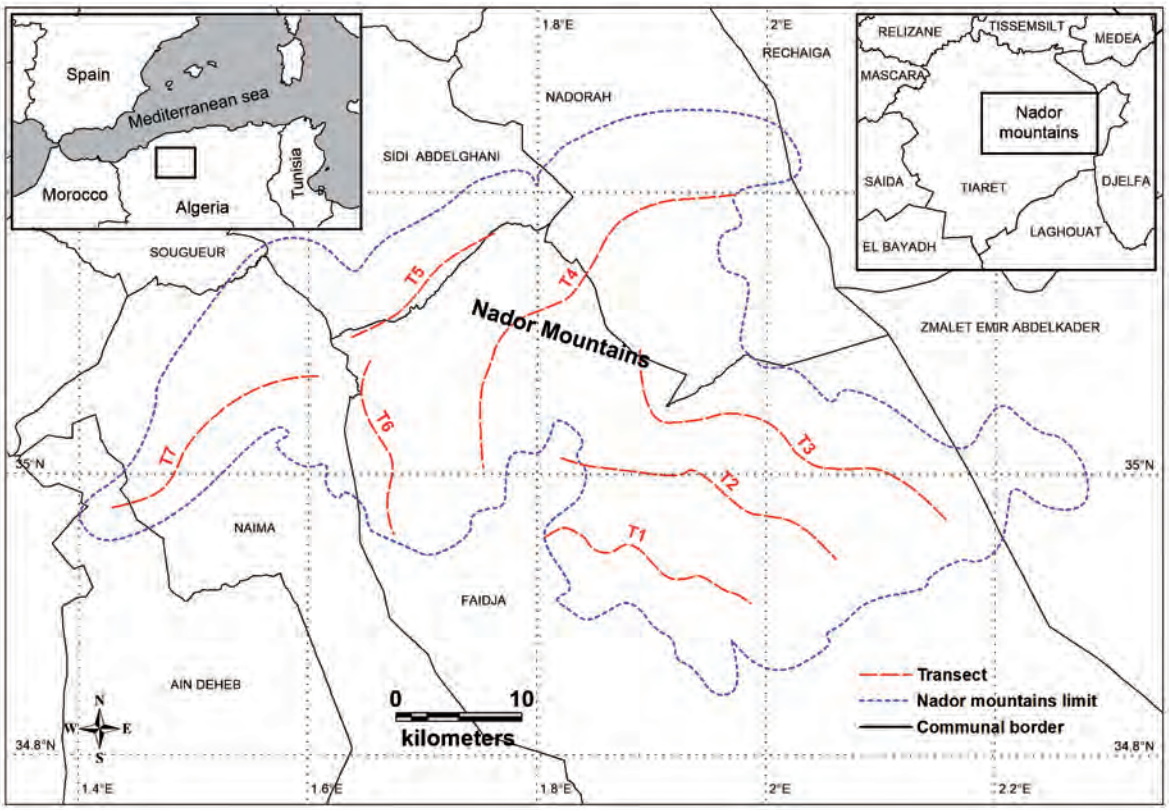

Figure 1 – Transects (T1 to T7) surveyed on foot and by car to monitor the threatened populations of Cuvier's gazelle (Gazella cuvieri) and aoudad (Ammotragus lervia) in the Nador Mountains (Tiaret province, northwestern Algeria).

phoenicea, *Pistacia terebinthus*, *P. atlantica*, *Olea europea*, *Phillyrea latifolia*, *Artemisia herba-alba*, *Ampelodesma mauritanica* and *Asparagus acutifolius* (Benkhattou et al. 2015).

Human activities are limited in the area because the nearest villages are located 15 to 20 km away. Hunting is prohibited, but poaching occurs.

Survey methods

The same team of three people, aided by local guides, conducted opportunistic surveys from January to December 2014 by car or on foot. From January to May and October to December, we also sampled seven transects on foot, over a total distance of 180 km (Figure 1), in the main habitats of the region, avoiding the vicinity of villages and areas of intense cultivation (Attum et al. 2014). These surveys were conducted each month on consecutive days. Following Abáigar et al. (2005), we recorded two types of field data: (1) direct observations or sightings, using binoculars Barska 10x50 and a telescope x20–60, in early morning and late afternoon; (2) photographs using a Canon camera (EOS 1200D 18–55 mm lens). For each ungulate group, we recorded the GPS coordinates and the number of animals; as far as possible, sex and age were estimated from body size, and from horn shape and length. GPS coordinates of all sightings were processed using MapInfo v 8.0in order to map the distribution of the two species.

Results

We recorded 13 sightings (raw total of 58 individuals) of Cuvier's gazelle over the study period (Figure 2). Two main areas of occurrence were identified: (1) the northern mountains, near the Oued el Mouilah and Oued Mkaber valleys (transect 4), and between Oued er Reem and Oued Besbassa (transect 5); (2) the southern inclined plane, mainly near Oued er Remel (transect 1), Oued el Euch el Guelbi and Oued Souffiguig (transect 2). No gazelle was sighted along transects 3, 6 or 7. Encounter rates (maximum number of individuals during one survey / transect) were 0.33, 0.20, 0.14 and 0.33 for transects 1, 2, 4 and 5 respectively.

Group sizes were between 2 and 7 individuals (4.5 ± 1.5), mainly females with one male or with sub-adults (or juveniles, in October only). The two largest groups, one comprising 6 females and one male, and the other 7 females, were observed along transect 1 in February and transect 2 in May, respectively. Most groups, including sub-adults and juveniles, were observed in transect 4. One or two groups of gazelles were sighted every month during which surveying took place at altitudes varying between 960 and 1,290 m (1,147.84 ± 94.99 m), with no seasonal pattern.

Aoudad was recorded in just 8 localities (raw total of 20 individuals), mainly in Djebel Chemakh (transect 5), in the rocky valleys of Oued El Mouilah and Oued Souffiguig, and near the southernmost valley

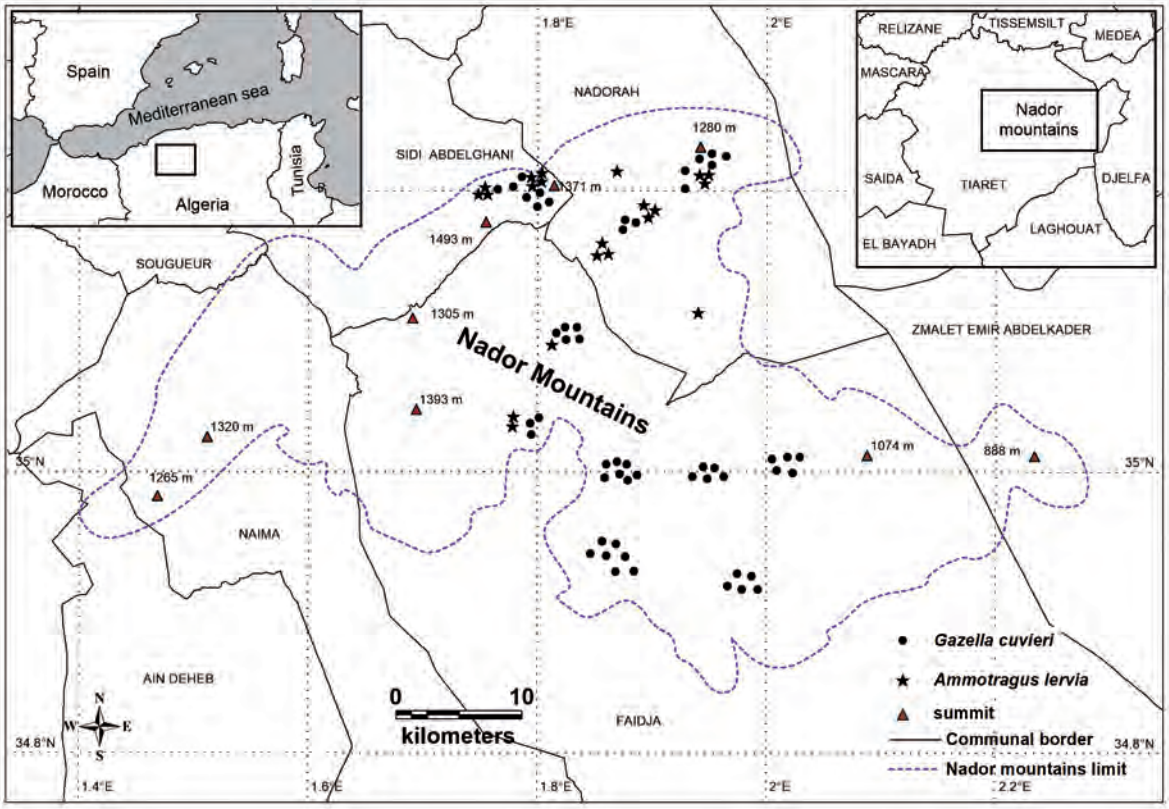

Figure 2 – Spatial distribution of Gazella cuvieri and Ammotragus lervia in the Nador Mountains (Tiaret gouvernorate, northwestern Algeria) in 2014.

of Oued Mkaber (transect 4) (Figure 2). One isolated male was sighted near Oued Mkaber (transect 3) in May. No aoudad was sighted along transects 1, 2, 6 or 7. Group sizes were between 1 and 4 individuals (2.5 ±1.1), mainly females with one male, with no seasonal pattern; no juvenile or kid was recorded. The altitudes at which animals were sighted ranged from 1,010 to 1,290 m (1097.75 ±105.69 m).

Discussion

Our results rely mainly on direct sightings as the most practical and efficient survey method in the study area. In quite similar conditions, Gil-Sánchez et al. (2017) reported that distance sampling, which requires considerable effort, does not provide additional information or improvement in the results in terms of distribution data and relative abundance for Cuvier's gazelle. Additionally, Manor & Saltz (2003) consider that distance results are affected by the shy and vigilant behaviour of gazelles. In the absence of additional techniques, such as ones using genetics on droppings, direct sightings remain a major source of information for surveying wild ungulate populations and identifying both the sex and the age of animals.

The occurrence of Cuvier's gazelle in the Nador Mountains confirms previous records (De Smet 1989; 1991; Boualem et al. 2016). This gazelle, which is not a *mountain* species (Abaigar et al. 2005), is, however, widely distributed in Tiaret province (De Smet 1989; Sellami et al. 1990; Bounaceur et al. 2015; Boualem et al. 2016). Aoudad, in contrast, was sighted for the first time in these mountains only recently (Bounaceur et al. 2016a), and we report the first year-long monitoring allowing the status of this small isolated population to be evaluated.

Spatial distribution

The spatial patterns of the Cuvier's gazelle and aoudad sighted in the Nador Mountains show similarities and differences. Both were recorded in the same altitudinal range, both species forsaking the low western plateau and inhabiting the northern mountains and rocky valleys, but only Cuvier's gazelle ranged in the southern inclined plane. This distribution cannot be related to altitude, as both species are known in Morocco at lower and at higher altitudes, from close to sea level up to 3,100 m for Cuvier's gazelle, and up to 4,100 m for aoudad (Cuzin et al. 2017b). In Algeria north to the Sahara, where the mountains are lower (Debel Chelia, 2,328 m, is the highest peak), both species ranged from 200 up to 2,000 m (De Smet 1989). The largest population was recorded in Djebel Boukahil (south of M'Sila, adjacent to Djelfa and Laghouat provinces), a mountain ranging between 1,415 and 1,675 m (Bounaceur et al. 2016a).Vegetation cannot explain this distribution either, as both species usually live in open forests, maquis and steppes (Beudels et al. 2013; Cassinello 2013), including the steppe of *Stipa tenacissima* (De Smet 1991; Sellami 1999) that cov-

ers most of the low western plateau. The main difference is more subtle: Cuvier's gazelles live on stony and sandy terrain on hills and plateaus (Beudels et al. 2013), such as the slopes of the southern inclined plane; aoudads require more rocky and precipitous terrain (Cassinello 2013), found only in the northern mountains and rocky valleys. The absence of Cuvier's gazelle in the low western plateau is quite surprising, as this species, which avoids areas of dense vegetation where visibility is limited (De Smet 1991; Boualem 2017), frequently forages in crop fields in the vicinity of Tiaret, 70 km from the Nador Mountains (Boualem 2017). This difference of habitat may also explain the respective distributions of each species in Algeria (Bounaceur et al. 2106a, b), and support the present difference in abundance.

Abundance and group size

The raw number of Cuvier's gazelle was higher than the raw number of aoudad, partly due to a larger range and probably a larger population size. The more open habitat of Cuvier's gazelle also facilitates sightings in comparison with aoudad, which lives in more inaccessible areas. However, the encounter rate of Cuvier's gazelle is low, even in the southern inclined plane, when compared to data from the Tiaret region (0.67–2.00, Bounaceur et al. 2016b). It is closer to the encounter rate in the M'sila region (0.21 for 136 km) or near Bezaz (0.20 for 77 km) (Bounaceur et al. 2016b). Habitat and food availability could explain these differences of encounter rate. First, sighting gazelles is easier in flat open areas than in the open pine forests or the rough maquis of the Nador Mountains, or in the M'sila and Bezaz regions. Second, foraging in crop fields near Tiaret (Boualem et al. 2016; Boualem 2017), Cuvier's gazelle benefit from a more abundant and nutritive food source, supporting a larger population. For aoudad, a recent survey showed that only five very small natural populations remain in northern Algeria, the Djebel Chemakh population probably being the smallest (Bounaceur et al. 2016a). On the other hand, Cuvier's gazelle has many remaining larger populations in southwestern Algeria, where they retreated to the optimum habitats (Bounaceur et al. 2016b).

Such differences in abundance may also be related to local group size, which is larger in the case of Cuvier's gazelle than for aoudad. The aoudad, however, is known to form larger groups (2–63, mean 14.7, for introduced aoudad populations in the USA (Valdez, 2011), vs 1–8, mean 3.71 for native populations of Cuvier's gazelle (Huffman 2011)). In fact, most sightings of Cuvier's gazelle were of harems, including sometimes sub-adults and occasionally juveniles, as in Mergueb reserve (Sellami & Bouerdjil 1992). Aoudad were recorded alone or in small groups of adults. Groups of 1 to 10 animals were observed in Chaambi National Park (Tunisia), but sub-adults accounted for 25.0% and 38.4% of sighted animals depending on the season (Ben Mimoun & Nouira 2013). The absence of juveniles may be associated with a low reproduction rate and / or with the protective behaviour of females with kids, which favour the most inaccessible habitats (Cuzin 2003). In a growing introduced population in Texas, juveniles accounted for 30–42% of individuals depending on the year of (aerial) survey (Gray & Simpson 1983).

Conclusion

Whereas both Cuvier's gazelle and aoudad still occur in the Nador Mountains, their statuses are quite different. Occupying a wider ecological niche, the gazelle is more extensively distributed and its population appears locally larger. Moreover, this population is more or less connected with other populations ranging in the Tiaret region. Cuvier's gazelle currently benefits from particular protection; hunting and poaching are prohibited, because this species is associated with local myths (Bounaceur et al. 2016b; Boualem 2017). The aoudad population, on the other hand, is isolated and restricted to the rougher parts of the mountain; its low numbers render it critically endangered, like most of the remaining populations in northern Algeria (Bounaceur et al. 2016a). Like all small, isolated populations, they are threatened by the loss of genetic diversity and possible inbreeding depression (Berger 1990; Nunney & Elam 1994; Schwartz et al. 1989), negative stochastic events, and habitat loss due to global change (Frankel & Soulé 1981). In order to avoid extinction in the near future, aoudad require the effective enforcement of legal protection and a funded national action plan, including establishing new protected areas and a captive breeding programme to enhance the size and genetic diversity of some populations. Cuvier's gazelle, on which the IUCN focused (2018), could also benefit from such an action plan where it lives sympatrically with aoudad, and more widely from raising conservation awareness of wild ungulates, which have declined heavily during recent decades. The Nador Mountains, which are relatively accessible, could be the first site for implementing this action plan, the first step being the regular monitoring of both species' populations.

Acknowledgements

This study was supported by MESRS Project of university research-training PRFU (ex. CNEPRU) Number: D00L02CU380120200001.

References

Abáigar, T., M. Cano & M. Sakkouhi 2005. Evaluation of habitat use of a semi-captive population of Cuvier's gazelles (*Gazella cuvieri*) following release in Boukornine National Park, Tunisia. *Acta Theriologica* 50(3): 405–415.

Attum, O., U. Ghazali, S.K. El Noby & I.N. Hassan 2014. The effects of precipitation history on the kilo-

metric index of dorcas gazelles. *Journal of arid Environments* 102: 113–116.

Aulagnier, S. 1992. Zoogeography and status of the Moroccan wild Ungulates. In: Spitz, F., G. Janeau, G. Gonzalez & S. Aulagnier (eds.), *Ongulés / Ungulates 91*. S.F.E.P.M.-I.R.G.M., Paris-Toulouse: 365–369.

Aulagnier, S., A. Bayed, F. Cuzin, M. Thévenot 2015. Mammifères du Maroc : extinctions et régressions au cours du XXème siècle. *Travaux de l'Institut Scientifique, Série générale* 8: 53–67.

Bagnouls, F. & H. Gaussen 1953. Saison sèche et indice xérothermique. *Bulletin de la Société d'histoire naturelle de Toulouse* 88: 193–239.

Ben Mimoun, J. & S. Nouira 2013. Social organization of Barbary sheep *(Ammotraguslervia)* population in the Chambi National Park, Tunisia. *International Journal for Biodiversity Conservation* 5(1): 15–19.

Benkhattou, A., B. Azouzi, K. Djili, M. Benkhattou, M. Zadek & R. Saadi 2015. Diversité floristique du massif du Nador en zone steppique (Tiaret, Algérie). *European Scientific Journal* 11(21): 401–419.

Berger, J. 1990. Persistence of different-sized populations: an empirical assessment of rapid extinctions in bighorn sheep. *Conservation Biology* 4(1): 91–98.

Beudels, R.C., P. Devillers & F.Cuzin 2013. *Gazella cuvieri* Cuvier's gazelle (Atlas gazelle, Edmi gazelle). In: Kingdon, J. & M. Hoffmann (eds.), *Mammals of Africa. Volume VI. Pigs, hippopotamuses, chevrotain, giraffes, deer and bovids*. London: 349–352.

Boualem, A. 2017. *Distribution spatiale, structure des populations, écoéthologie et conservation de* Gazella cuvieri *(Mammalia, Bovidae) dans la région de Tiaret*. Ph.D. thesis, Université Ibn Khaldoun, Tiaret.

Boualem, A., F. Bounaceur & M. Maatoug 2016. Structure des populations de *Gazella cuvieri* (Ogilby, 1841) dans la région de Tiaret, nord-ouest algérien. *Bulletin de la Société zoologique de France* 141(3): 141–152.

Bounaceur, F., N. Benamor, F.Z. Bissaad, A. Abdi & S. Aulagnier 2016a. Is there a future for the last populations of aoudad (*Ammotragus lervia*) in Northern Algeria? *Pakistan Journal of Zoology* 48(6): 1727–1731.

Bounaceur, F., A. Boualem, N. Benamor, A. Fellous, A. Benkheira, F.Z. Bissaad & S. Aulagnier 2016b. Updated distribution and local abundance of the endangered Cuvier's gazelle (Mammalia, Bovidae) in Algeria. *Folia Zoologica* 65(3): 233–238.

Bounaceur, F. A. Boualem, A. Fellous, M. Sallai, F. Douba, N. Benaboucha, K. Chérif, D. Arab Said & K. De Smet 2015. Latest news of Cuvier's gazelle *Gazella cuvieri* (Ogilby, 1841) in northern Algeria. *Gnusletter* 32(2): 11–13.

Cassinello, J. 2013. *Ammotragus lervia* Aoudad (Barbary sheep, Arrui). In: Kingdon, J. & M. Hoffmann (eds.), *Mammals of Africa. Volume VI. Pigs, hippopotamuses, chevrotain, giraffes, deer and bovids*. London: 595–599.

Cassinello, J., F. Bounaceur, J.C. Brito, E. Bussière, F. Cuzin, J. Gil-Sánchez, F. Herrera-Sánchez & T. Wacher 2021. *Ammotragus lervia. The IUCN Red List of ThreatenedSpecies*: e.T1151A22149987.

Cuzin, F. 2003. *Les grands Mammifères du Maroc méridional (Haut Atlas, Anti Atlas et Sahara): distribution, écologie et conservation*. Ph.D. thesis, E.P.H.E., Montpellier, France.

Cuzin, F., S. Aulagnier & M. Thévenot 2017a. Carnivora. In: Aulagnier, S., F. Cuzin & M. Thévenot (eds.), *Mammifères sauvages du Maroc. Peuplement, répartition, écologie*. S.F.E.P.M., Paris: 155–196.

Cuzin, F., S. Aulagnier & M. Thévenot 2017b. Cetartiodactyla. In: Aulagnier, S., F. Cuzin & M. Thévenot (eds.), *Mammifères sauvages du Maroc. Peuplement, répartition, écologie*. S.F.E.P.M., Paris: 207–232.

De Smet, K. 1989. *Studie van de verspreiding en biotoopkeuze van de grote Mammalia in Algerie in het kader van het natuurbehoud*. Doct. Landbouwkundige Wetenschappen, Rijksuniv. Gent.

De Smet, K. 1991. Cuvier's gazelle in Algeria. *Oryx* 25(1): 99–104.

DGF 2017. *Stratégie et plan d'action pour la conservation du mouflon à manchettes en Tunisie 2018–2027*. UICN Méditerranée, Málaga.

El Alami, A. 2019. A survey of the vulnerable Cuvier's gazelle (*Gazella cuvieri*) in the mountains of Ait Tamlil and Anghomar, Central High Atlas of Morocco. *Mammalia* 83(1): 74–77.

Emberger, L. 1930. Sur une formule applicable en géographie botanique. *Comptes rendus de l'Académie des Sciences* 191(8): 389–391.

Frankel, O.H. & M.E. Soulé 1981. *Conservation and Evolution*. Cambridge.

Gil-Sánchez, J.M., F.J. Herrera-Sánchez, B. Álvarez, Á. Arredondo, J. Bautista, I. Cancio, S. Castillo, M.A. Díaz-Portero, J. de Lucas, E. McCain, J. Pérez, J. Rodríguez-Siles, J.M. Sáez, J. Martínez-Valderrama, G. Valenzuela, A. Qninba & E. Virgós 2017. Evaluating methods for surveying the Endangered Cuvier's gazelle *Gazella cuvieri* in arid landscapes. *Oryx* 51(4): 648–655

Gray, G.G. & C.D. Simpson 1982. Group dynamics of free-ranging Barbary sheep in Texas. *Journal of Wildlife Management* 46(4): 1096–1101.

Gray, G.G., C.D. Simpson 1983. Populations characteristics of free ranging Barbary sheep in Texas. *Journal of Wildlife Management* 47(4): 954–962.

Huffman, B.A. 2011. Cuvier's gazelle *Gazella cuvieri*. In: Wilson, D.E. & R.A. Mittermeier (eds.), *Handbook of the Mammals of the World. 2. Hoofed mammals*. Lynx, Barcelona: 637–638.

IUCN SSC Antelope Specialist Group 2016. *Gazella cuvieri. The IUCN Red List of Threatened Species 2016*: e.T8967A50186003.

Lee, T.E., S.A. Black, A. Fellous, N. Yamaguchi, F.M. Angelici, H.Al Hikmani, J.M. Reed, C.S. Elphick & D.L. Roberts 2015. Assessing uncertainty in sighting records: an example of the Barbary lion. *PeerJ–Life and Environmanet* 3: e1224.

Manor, R. & D. Saltz 2003. Impact of human nuisance disturbance on vigilance and group size of a social ungulate. *Ecological Applications* 13(6): 1830–1834.

Nunney, L. & D.R. Elam 1994. Estimating the effective population size of conserved populations. *Conservation Biology* 8(1): 175–184.

Purroy, P. 2010. Buscando un felino 'extinto'. El leopardo del Atlas. 'Salsero' y otrasandanzas. *Edilesa, Trabajo del Camino*: 99–255.

Ramzi, H., M. Qarro, A. Zine El Abidine & A. Abrioui 2018. Conservation d'une population de Mouflon à manchettes (*Ammotragus lervia* Pallas, 1777) (Mammalia, Bovidae) dans un espace clos: cas de la réserve d'Amassine dans le Haut-Atlas (Parc National du Toubkal, Maroc). *Revue d'Ecologie (La Terre et la Vie)* 73(4): 474–481.

Schwartz, O.A., V.C. Bleich & S.A. Holl 1989. Genetics and the conservation of mountain sheep *Ovis canadensis nelsoni*. *Biology Conservation* 37(2): 179–190.

Sellami, M. 1999. *La Gazelle de Cuvier* Gazella cuvieri *(Ogilby, 1841) en Algérie. Statut et premiers éléments d'écologie, données sur le régime alimentaire dans la Réserve naturelle de Mergueb (M'Sila)*. Thèse Doctorat. Inst. Natn. Agro. El Harrach.

Sellami, M. & H.A. Bouredjli 1992. Preliminary data about the social structure of Cuvier's gazelle, *Gazella cuvieri* (Ogilby, 1841) of the reserve of Merghueb (Algeria). In: Spitz, F., G. Janeau, G. Gonzalez & S. Aulagnier (eds.), *Ongulés / Ungulates 91*. S.F.E.P.M.-I.R.G.M., Paris-Toulouse: 357–360.

Sellami, M., H.A. Bouredjli & J.L. Chapuis 1990. Répartition de la Gazelle de Cuvier (*Gazella cuvieri* Ogilby, 1841) en Algérie. *Vie Milieu* 40 (2-3): 234–237.

Trouessart, E.L. 1905. La faune des Mammifères de l'Algérie, du Maroc et de la Tunisie. *Causeries scientifiques de la Société Zoologique de France* 1: 353–410.

UICN[IUCN] 2018. *Stratégie et plan d'action pour la conservation de la gazelle de Cuvier* (Gazella cuvieri) *en Afrique du Nord 2017–2026*. UICN, Gland-Málaga.

Valdez, R. 2011. Aoudad *Ammotragus lervia*. In: Wilson, D.E. & R.A. Mittermeier (eds.), *Handbook of the Mammals of the World. 2. Hoofed mammals*. Lynx, Barcelona: 714–715.

Wacher, T., S. Baha El Din, G. Mikhail & M. Baha Eldin 2002. New observations of the 'extinct' Aoudad *Ammotragus lervia ornate* in Egypt. *Oryx* 36: 301–304.

Authors

Farid Bounaceur – corresponding author

professor of Conservation Biology at the Tissemesilt University in Algeria. Équipe de recherche Biologie de la conservation en zones arides et semi arides. Laboratoire Agronomie Environnement. Faculté des Sciences, Département des Sciences de la Nature et de la Vie. Université de Tissemsilt, 38000, Algérie. E-mail: fbounaceur@yahoo.fr

Aoued Boualem

Conservation des Forêts de la wilaya de Tiaret

Abdelkader Abdi

Conservation des Forêts de la wilaya de Tiaret

Fatima Zohra Bissaad

Laboratoire de recherche de bioinformatique, microbiologie appliquée et biomolécules (LBMAB), Faculté des Sciences, Université M'Hamed Bougara, Boumerdès, Algérie

Mohamed Amin Kaddouri

Département d'Agronomie. Faculté des Sciences. Université Telidji Amar Laghouat. Algérie

Mohamed Djilali

Équipe de recherche Biologie de la conservation en zones arides et semi arides. Laboratoire Agronomie Environnement. Faculté des Sciences, Département des Sciences de la Nature et de la Vie. Université de Tissemsilt, 38000, Algérie

Azeddine Zenati

Conservation des Forêts de la wilaya de Tiaret

Yahia Belgarssa

Conservation des Forêts de la wilaya de Tiaret

Stéphane Aulagnier

professor of Conservation Biology at the Paul Sabatier University (Toulouse) has been working on mammals in north-western Africa for 40 years, starting from Morocco and then supervizing Ph.D students in Algeria and Tunisia. Comportement et Écologie de la Faune Sauvage, INRAE, Université de Toulouse, CS 52627, 31326 Castanet-Tolosan cedex, France

eco.mont – Volume 14, Number 2, July 2022
ISSN 2073-106X print version – ISSN 2073-1558 online version: http://epub.oeaw.ac.at/eco.mont
https://dx.doi.org/10.1553/eco.mont-14-2s11

Temporal dynamics in the physico-chemistry of a high-alpine stream network in the Swiss National Park

Christopher T. Robinson, Christa Jolidon, Gabriele Consoli, Simon Bloem & Christian Ebi

Keywords: rock glacier, glacial stream, climate change, season, ecohydrology, groundwater

Abstract

The Macun lakes form a high-alpine (> 2,600 m asl) cirque landscape (3.6 km^2) in the Swiss National Park, comprising 26 small lakes together with a number of temporary ponds. Streams interconnect the four largest lakes, forming the drainage network that flows into the Inn River at the town of Lavin. The drainage network of Macun consists of a north and a south basin that overlie an ortho-gneiss, meta-granitoid bedrock. The south basin is influenced by various rock glaciers. The physico-chemistry of surface waters at 10 sites has been monitored annually in mid-summer since 2001. Further, an YSI EXO2 Multiparameter Sonde (Exosonde) with various water quality sensors has been employed since 2016 at the last lake in the network to examine seasonal and diel patterns in physico-chemistry. Results showed clear physico-chemical differences between the two basins, which mostly reflect rock-glacier inputs in the south basin. Nitrogen values were two-fold higher and particulate phosphorus values two-fold lower in the south basin than in the north basin. Over time, the physico-chemistry in the two basins became more homogeneous, with a reduction in rock-glacial inputs in the south basin and an overall decrease in nitrogen in the catchment. Data from 30 springs and tributaries sampled in 2002 and 2017 reflected the basin differences and temporal changes observed at the primary study sites. Continuous temperature records showed north basin streams to be ca. 3°C warmer than south-basin streams, but with high inter-annual variation that reflected annual differences in weather and no evidence of a general change over time (increase or decrease). Exosonde data revealed strong seasonality in measured parameters as well as seasonality in diel patterns (e. g., dissolved oxygen, temperature, chlorophyll-a); diel fluctuations were most pronounced in summer and least in winter. The results highlight the importance of long-term monitoring for understanding ecosystem state changes in alpine freshwaters, especially during periods of rapid environmental change.

Profile

Protected area

Swiss National Park

Mountain range

Alps

Country

Switzerland

Introduction

High-elevation environments are sentinels of climate change (Federal Office of the Environment (FOEN) 2021). These alpine landscapes house the glaciers of the world, most of which have been receding rapidly over recent decades under a warming climate (IPCC 2013). Alpine surface waters, comprising both standing and running waters, have experienced changes in physico-chemistry in response to climate-induced alterations in water inputs (quantity, quality and timing) (Scherrer et al. 2016; Brunner et al. 2019). In particular, alterations in water inputs act concomitantly with changes in the seasonal patterns of precipitation. For instance, most of the winter snowfall in the European Alps now occurs later in the season, sometimes as spring precipitation events, and most areas experience extreme drying in late summer followed typically by autumn increases in precipitation (FOEN 2021). In fact, flow intermittency in late summer affects a high proportion (up to 90%) of tributary streams in alpine landscapes (Robinson & Matthaei 2007; Paillex et al. 2020). Lastly, over time, human-related environmental changes also have caused some degree of change in atmospheric deposition of certain trace substances and pollutants. For example, nitrogen deposition in some areas of the European Alps has decreased due to changes in industrial activities in neighbouring countries (Rogora et al. 2006; Magnuz et al. 2017).

Rock glaciers are common landforms associated with high-mountain periglacial landscapes such as the Macun cirque. Rock glaciers comprise a mix of debris (e. g. talus) and ice, and typically move slowly downwards into valleys. Rock-glacier movement is seasonal, beginning with snowmelt in spring, with highest velocities in summer; movement can be particularly rapid after intense rainfall. However, rock glaciers globally have been moving faster in recent decades due to climate change (Kenner et al. 2020). For example, the horizontal displacement of the large rock glacier in Macun has increased markedly since 1988 (Zick 1996; Barsch & King 1998; Fehr & Reich 2015). Rain and meltwater can penetrate rock glaciers more easily today because ice has become warmer with climate

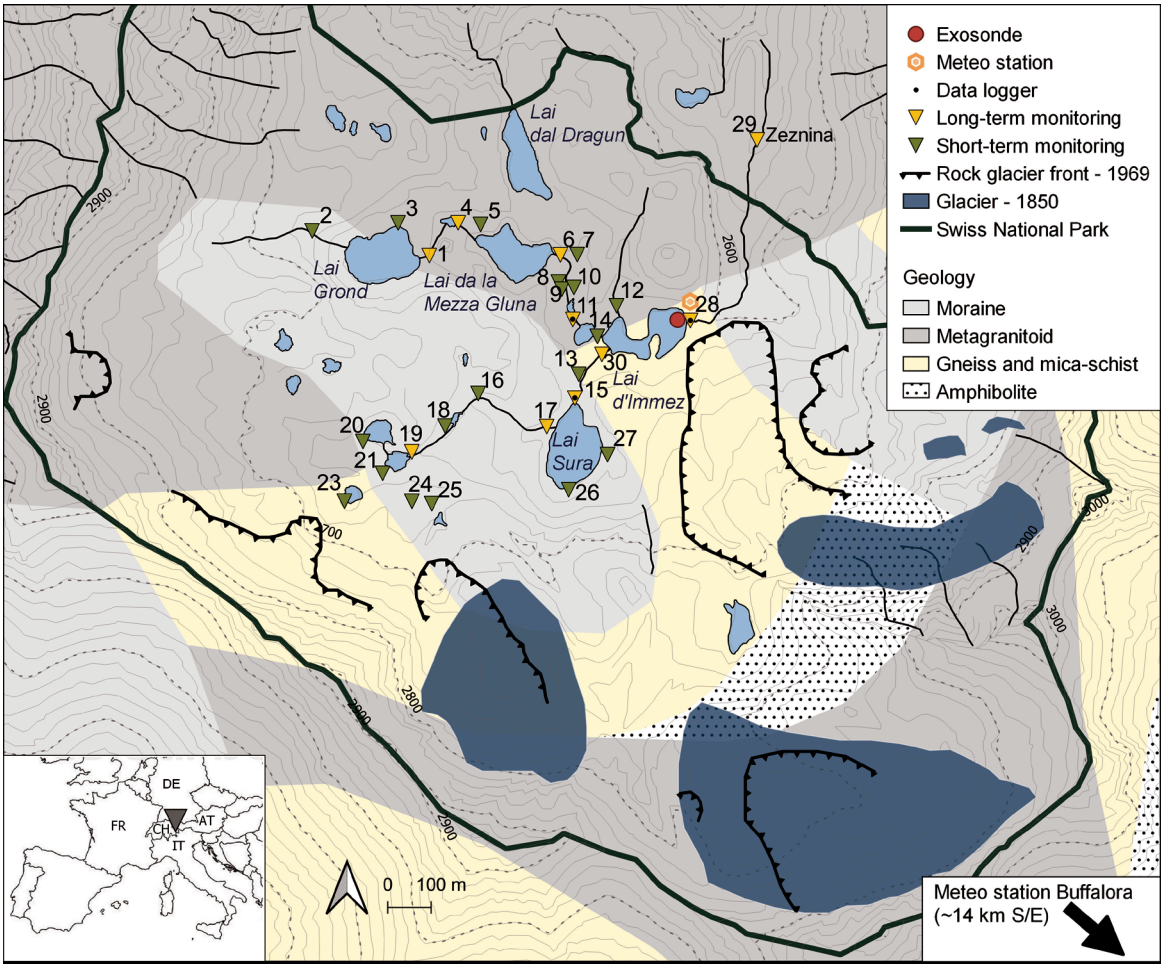

Figure 1 – Map of the Macun Lakes area. Note the rock glaciers that influence the hydrology of the south basin and outlet stream (Barsch 1969), and the associated glacial coverage from 1850 (www.swisstopo.admin: Glacial Monitoring in Switzerland GLAMOS).

change (Haberkorn et al. 2021). Indeed, long-term monitoring has shown progressive warming (rising air temperatures), increasingly intense precipitation, and accelerating rock-glacier velocities, such as those in the Macun cirque.

Monitoring is an essential component for understanding and projecting environmental change. It provides fundamental information for environmental decision-making, policy development, and guidelines in the management of natural resources. The Alps are the water tower of Europe (Tockner et al. 2009), and thus monitoring of alpine surface waters is imperative for the wellbeing of human populations inhabiting downstream landscapes. Changes in water availability in the Alps have already affected the tourist landscape, with human interventions being continuously necessary to sustain economic stability (Zarrineh et al. 2020). Other changes have occurred with respect to hydropower generation (e.g. increases in small head hydropower facilities, Lange et al. 2018; Crnobrnja-Isailovic et al. 2021), and the ongoing switch to alternative energy sources. Lastly, water-quality monitoring provides baseline environmental information in understanding changes in the ecology of water resources such as aquatic biodiversity (Jacobsen et al. 2014). Monitoring data are clearly important in understanding changes in aquatic environments in response to the rapid and ongoing changes in alpine landscapes globally (FOEN 2021).

The primary aim of this paper was to summarize long-term physico-chemical data from a high-elevation stream-lake network, the Macun Lakes, in the Swiss National Park, eastern Switzerland. A second objective was to compare the water physico-chemistry of 30 springs and tributaries in the network between 2002 and 2017. A final objective was to examine seasonal and diurnal patterns of specific physico-chemical parameters, which were recorded continuously between 2016 and 2019 using an Exosonde (YSI EXO2) near the outlet of the last lake in the fluvial network in the catchment. The data demonstrate the importance of long-term ecohydrological monitoring of alpine aquatic systems in the context of environmental change. This paper follows up on an earlier paper (Robinson & Oertli 2009), adding to that database and showing that surface waters in Macun are experiencing decreasing influence of (rock-)glacier waters.

Site description

The Macun Lakes region (46°44'N, 10°08'E) is a high-alpine cirque (>2,600 m asl) in the Graubunden Canton, Switzerland (Figure 1). The 3.6 km^2 region, annexed to the Swiss National Park in 2000, is an area designated for long-term monitoring of Alpine streams and lakes. The drainage network of Macun consists of a north and a south basin (Figure 1). The region comprises 26 small lakes and ~10 small temporary ponds; the four largest lakes, excluding lake Dragun, are interconnected by stream segments, each <500 m long (Robinson & Oertli 2009). The large lakes cover ca. 0.12 km^2 each and are <10 m deep. The surrounding peaks reach elevations of 2,800 to 3,000 m asl, and the outlet stream (Zeznina) drains north to the Inn River near the village of Lavin, Switzerland, in the lower Engadine. The elevations of the study sites were between 2,610 and 2,650 m asl. Water sources in the catchment originate from precipitation (mostly as snow in winter) and seven rock glaciers (Barsch 1969) associated with the south basin. Specifically, inputs from a large rock glacier (Macun1 in Barsch 1969; Fehr & Reich 2015; Derungs & Tischhauser 2017) affect only the surface waters assessed at Zeznina (site 29), although the six other small rock glaciers provide meltwaters to the south-basin stream network (see Figure 1). Recent assessment of the large rock glacier (Macun1) has indicated substantial activity over recent decades (Fehr & Reich 2015; Derungs & Tischhauser 2017).

Precipitation is low, around 850 mm / y^{-1}, and air temperature ranges from 20°C in summer to −25°C in winter (Buffalora meteorological station, ~14 km southeast of Macun). Our newly installed meteorological station at Macun (at site 28 in Figure 1) recorded a maximum temperature of 18.7°C in July 2019 and a minimum of −23.2°C in January 2019. Bedrock geology is slow-weathering crystalline (ortho-gneiss, meta-granitoid) rock (see Figure 1). The area is above the treeline, and terrestrial vegetation is typical alpine grasses and low-lying herbs with areas of bare rock. The area is remote and, being in the national park, is accessible only on foot. Aquatic vegetation is present in some lakes, with Bryophyta (7 taxa) being predominant (Oertli et al. 2008). Helophytes were found in a lower-elevation lake, consisting of *Eleocharis* sp., *Eriophorum scheuzeri, Glyceria* sp., and *Saxifraga stellaris*. No other assessment of the vegetation has so far been made. The large lakes have fish (*Salmo trutta fario*, *Salvenius namaycush*, *Phoxinus phoxinus*), and were last stocked in 1993 (P. Rey, personal communication).

In contrast to proglacial streams, glacial flour is essentially non-existent in these streams and turbidity is low. Even so, the annual flow regime differs between basins: the south basin experiences more extreme channel contraction from the freezing of water associated with rock glaciers in autumn (Robinson & Matthaei 2007). The stream network, as a whole, contracts by up to 60% in winter. The water source in each basin also causes differences in water chemistry and in water temperature, being warmer in the north basin than the

*Table 1 – Summary of physico-chemical data from spot collections at the end of July, from 2001 to 2019 (n = 19 years), except PP 2001–2011 (n = 11 years) and TP 2012–2019 (n = 8 years). Values expressed are means (*pH is given as median), SD = standard deviation, CV = coefficient of variation, Max = maximum, and Min = minimum, NA = not applicable.*

		Conductivity	Turbidity	Temperature	pH*	NO_3-N	DN	PN	PO_4-P	PP	GP	DOC	TIC	POC	SiO_2	Alkalinity
		µs/cm	NTU	°C		µg/l	µg/l	µg/l	µg/l	µg/l	µg P/L	mg/l	mg/l	mg/l	mg/l	mmol/L
North Basin	Mean	6.5	1.9	12.2	6.5	69.1	179.5	102.4	2.0	8.6	10.5	0.9	0.9	1.0	2.2	0.11
	SD	0.9	2.6	3.3	NA	20.3	91.6	55.0	1.3	4.1	6.5	0.5	0.4	0.5	0.6	0.03
	CV	13	134	27	NA	29	51	54	65	47	61	53	48	52	28	30
	Max	9.5	18.2	19.5	8.0	108.0	614.0	231.0	4.9	17.1	44.6	2.5	2.5	2.3	4.0	0.21
	Min	4.9	0.2	3.9	5.3	45.0	100.0	0.1	0.4	2.2	6.7	0.5	0.2	0.0	1.4	0.08
South Basin	Mean	10.3	2.0	9.3	6.4	177.6	260.3	33.8	2.3	3.4	7.0	0.7	0.8	0.3	2.4	0.09
	SD	3.1	2.2	3.2	NA	83.2	108.7	26.0	0.7	2.2	2.9	0.6	0.4	0.2	0.8	0.02
	CV	30	108	35	NA	47	42	77	32	64	42	88	47	71	33	21
	Max	24.0	10.7	14.6	7.7	470.0	520.0	157.0	3.6	9.1	17.2	3.6	1.6	1.0	4.1	0.1
	Min	5.3	0.1	2.1	5.2	53.4	101.0	9.2	1.0	0.7	3.8	0.2	0.2	0.1	1.3	0.1
Immez outlet	Mean	9.6	2.6	10.4	NA	113.1	200.9	50.7	4.5	6.7	6.7	0.8	0.8	0.5	2.3	0.10
	SD	1.5	3.5	2.9	NA	38.2	89.6	20.2	5.8	10.8	1.5	0.4	0.5	0.2	0.7	0.02
	CV	15	132	28	10	34	45	40	131	161	23	52	56	50	31	18
	Max	12.6	12.3	15.4	7.7	184.0	360.0	92.0	13.2	48.1	9.4	1.8	1.5	0.9	3.7	0.13
	Min	6.9	0.3	3.6	5.4	69.0	100.0	14.7	1.3	1.4	4.5	0.3	0.0	0.1	1.4	0.08
Zeznina	Mean	19.8	7.9	7.7	6.5	198.1	302.7	33.9	1.9	6.1	8.9	0.6	1.2	0.4	2.7	0.12
	SD	13.9	7.9	2.5	NA	68.0	100.8	34.6	0.7	3.3	5.3	0.3	0.4	0.2	0.8	0.01
	CV	71	99	32	NA	34	33	102	37	54	59	52	35	49	29	12
	Max	26.5	27.9	12.5	7.3	399.0	470.0	147.0	2.9	13.5	21.6	1.3	2.0	0.7	4.1	0.15
	Min	10.5	0.8	2.8	5.5	124.0	155.0	0.1	1.1	1.6	5.1	0.2	0.5	0.2	1.6	0.11

NO_3-N = nitrate-nitrogen, DN = dissolved nitrogen, PN = particulate nitrogen, PO_4-P = ortho-phosphorus, PP = particulate phosphorus, TP = total phosphorus, DOC = dissolved organic carbon, TIC = total inorganic carbon, POC = particulate organic carbon, and SiO_2 = silicate.

south basin. Stream channels in each basin have low gradients and contain mostly stable cobble substrate.

Methods

The study began in September 2001, followed by annual monitoring in late July (summer period) each year during the study period at 10 primary sites (yellow sites in Figure 1). Of these 10 sites, 4 were in the north basin, 4 in the south basin, and 2 in the outlet stream (Immez outlet and Zeznina). The sites were situated at the inlets and outlets of the prominent lakes in each basin along the drainage network. Meltwater from a large rock glacier enters the outlet stream between Immez outlet (site 28) and Zeznina (site 29); Immez outlet represents the outlet of both basins. In 2002 and 2017, all springs and tributaries feeding the lakes and main channel in each basin were sampled around every 3 weeks during the open-water season (typically late June to mid-October), resulting in 30 different sites being sampled (see Figure 1).

A 0.5 L water sample was collected from each site on each visit for analysis of nitrogen constituents (nitrate: NO_3-N; particulate nitrogen: PN; dissolved nitrogen: DN), phosphorus constituents (orthophosphate: PO_4-P; particulate phosphorus: PP; total phosphorus: TP), dissolved organic carbon (DOC), particulate organic carbon (POC), total inorganic carbon (TIC), silicate (SiO_2) and alkalinity, following methods in Tockner et al. (1997) and Robinson & Matthaei (2007) (see Table 1 for summaries of measured parameters). Micro-nutrients and heavy metals were sampled in 2002 and 2017 during the more extensive sampling campaigns in those years. Aluminium (Al, detection limit <0.5 µg/L), manganese (Mn, <0.01 µg/L), iron (Fe, <0.02 µg/L), cobalt (Co, <0.1 µg/L), nickel (Ni,<0.10 µg/L), copper (Cu, <0.10 µg/L), zinc (Zn, <0.1 µg/L), molybdenum (Mo, <0.1 µg/L), cadmium (Cd, <0.1 µg/L), and lead (Pb, <0.2 µg/L) were analysed by inductively coupled plasma mass spectrometry (ICP-MS). All (except Al, range 38–71 µg/L) were near or below analytical detection limits during the period of study and are not discussed further in this paper (Robinson & Matthaei 2007; Vogler 2018). Spot measures of temperature and conductivity (WTW LF 323, Germany), turbidity (Cosmos, Züllig AG, Switzerland), and pH (WTW pH 330, Germany) were taken at around midday on each visit, using portable field meters. Lastly, temperature loggers (Hobo tidbits) were installed at 3 main sites to continuously record data on an hourly basis during the study period. These sites included the outlets of each basin (north basin at site 11, south basin at site 15, and Immez outlet at site 28; see Figure 1). Tidbits were exchanged and downloaded each year. However, temperature data are missing from August 2007 to August 2009 at all sites due to dead batteries, and for 2019 at site 15 due to a faulty startup of the logger.

Figure 2 – (Top) The Exosonde, with stainless steel shell and support legs for installation in the lake. The shell and support legs protect the Exosonde from heavy snow/ice and avalanche impact during winter. (Bottom) Instruments set up for recording data from the Exosonde as well as the meteorological station; energy from the solar panel is stored via two batteries in the box. © C. Ebi

In July 2016, an YSI EXO2 Multiparameter Sonde (Exosonde) was installed near the outlet of lake Immez at a depth of ca. 1.5 metres. The lake is ice-covered in winter, but the probe is functional all winter. The probe is connected by cable to a separate data-logging station with an ensured power supply (solar panel, 0.27 m^2) and data communication capability. In March 2017, the Exosonde was damaged (compacted by heavy snow on ice) and replaced in July 2017 using a modified external stainless steel shell and support rods for better protection (Figure 2). The Exosonde records hourly, transmitting data via satellite twice per day to the National Park headquarters in Zernez, Switzerland. The data are also downloaded at the Eawag Sensor lab. The sensors embedded in the Exosonde are cleaned (sensors also self-clean during operation) and calibrated in spring and autumn of each year; they are replaced when required. In this paper, we report typical diurnal patterns over 7 days during summer,

autumn and winter 2018, and spring 2019 for continuously recorded data of specific conductance, temperature, dissolved oxygen, turbidity, pH and chlorophyll-a.

Data Analysis

Our previous assessments revealed clear basin differences in water physico-chemistry (Robinson & Matthaei 2007; Robinson & Oertli 2009). Thus we first examined the current long-term dataset by statistically summarizing the measured physico-chemical parameters, comparing the south basin, the north basin, Immez outlet and Zeznina. Summary statistics (in tabular form) included the mean, standard deviation and coefficient of variation. Next, spatial patterns were examined using principal component analysis (PCA) with log(X+1) transformed data. Here, sites were summarized in the PCA scatterplot by basin, Immez outlet and Zeznina averaged across time (years) to better illustrate the variation in physico-chemistry within each area over the study period. Temporal changes in physico-chemistry were then assessed by plotting the PCA scores of each basin, Immez outlet and Zeznina, for axis-1 and axis-2 of the PCA used above, across time (years). Simple regression was used to test for any clear temporal change (increase or decrease) in PCA scores from 2001 to 2019.

The long-term continuous temperature data were plotted to visualize differences among the two basins and Immez outlet over the study period. These data revealed seasonal as well as inter-annual differences in water temperature among the three sites. Temperature data were summarized as mean, median, maximum and minimum water temperatures experienced over the study period, and revealed the number of relatively warm days each year that probably influenced the primary and secondary production of surface waters. The number of relatively warm days each year was estimated starting from the distinct temperature inflexion increase in spring to the inflexion decrease in autumn.

Physico-chemistry measured at all sites that had surface flow (N = 30) in 2002 and 2017 was summarized using principal components analysis (PCA) on log(X+1) transformed data. PCA results were plotted as means and standard errors for each basin (north, south) and year (2002, 2017). All PCAs were conducted using SPSS (vers. 25).

The Exosonde recorded a variety of parameters near the outlet of lake Immez at a depth of ca. 1.5 m. Data were initially summarized by plotting over the period of operational time (2017–2019). This assessment revealed strong seasonality as well as strong diel patterns for the parameters measured. 7-day data patterns typical for each season (spring, summer, autumn, winter) were chosen to best illustrate the observed seasonal dynamics in diel patterns. Selected 7-day periods in spring and autumn were used to show the rapid transition in seasonality (i.e., spring to summer, autumn to winter) of the surface waters of lake Immez; the representative 7-day periods for summer and winter were at mid-summer and mid-winter. These data were summarized as means, standard deviations, coefficients of variation, and maximum and minimum values to further illustrate the seasonal differences and the diel nature of the different parameters during the different seasons.

Table 2 – Summary statistics of the long-term water temperature (°C), recorded hourly and continuously, using Hobo Tidbit data loggers. SD = standard deviation, NA = not applicable. Days refer to the summer growth period, which is the (approximate) period between the inflection date of increase in spring and that of decrease in autumn. See map for locations of sites.

	2002	2004	2005	2006	2009	2010	2011	2012	2013	2014	2015	2016	2017	2018	2019
Immez inlet north (site 11)															
Maximum	18.1	18.0	18.5	23.0	18.0	20.6	20.9	21.7	20.9	23.6	22.0	21.8	20.0	NA	19.7
Minimum	0.6	0.1	0.0	0.1	1.9	0.0	0.1	0.2	0.1	0.3	−0.1	0.0	0.0	NA	0.6
Mean	9.0	7.1	7.1	8.4	8.4	8.0	7.7	8.3	7.5	7.4	7.2	7.8	9.1	NA	8.2
Median	8.9	7.0	7.1	7.8	8.0	7.8	8.2	8.1	7.5	7.4	6.5	8.0	9.2	NA	8.3
SD	3.6	4.4	4.2	4.3	2.9	4.3	4.8	4.6	4.9	3.6	5.2	5.0	4.5	NA	4.4
Days	120	126	145	136	NA	128	163	126	135	130	154	135	127	NA	94
Immez inlet south (site 15)															
Maximum	11.4	12.3	16.4	15.3	18.9	12.8	NA	16.4	19.2	15.5	23.4	15.1	16.6	NA	12.7
Minimum	0.7	0.3	0.2	0.5	0.2	0.5	NA	0.4	0.5	0.0	0.3	0.2	0.4	NA	0.6
Mean	5.1	6.4	6.6	7.3	8.9	6.3	NA	6.6	5.9	2.3	6.6	6.8	8.2	NA	6.8
Median	5.0	7.0	6.9	7.3	9.1	6.4	NA	6.1	5.9	5.9	5.3	7.2	8.6	NA	7.6
SD	2.5	2.8	3.4	3.2	3.5	2.4	NA	4.1	3.5	2.6	4.0	3.5	3.3	NA	2.9
Days	143	120	157	134	NA	NA	NA	NA	135	141	153	134	109	NA	94
Immez outlet (site 28)															
Maximum	14.0	13.6	16.3	17.7	19.2	13.7	17.8	18.2	15.5	14.3	17.1	17.4	15.3	17.5	14.6
Minimum	1.1	0.5	0.3	−0.8	0.8	0.6	0.8	0.8	0.9	0.1	0.5	0.5	0.5	0.7	0.5
Mean	8.7	7.5	6.9	7.8	8.2	6.5	7.6	7.5	7.1	6.4	7.1	7.7	6.3	9.3	7.1
Median	9.2	7.9	7.4	7.9	8.6	6.8	8.2	7.6	6.9	6.7	5.9	7.8	4.8	10.0	7.2
SD	2.6	3.2	3.7	3.7	4.7	3.1	4.3	4.1	4.0	2.7	4.5	3.8	4.1	3.7	3.6
Days	139	118	156	139	NA	NA	165	138	133	131	162	138	NA	140	193

Results

Spatio-temporal patterns in basin physico-chemistry (2001–2019)

Surface waters of the Macun catchment are relatively pristine, reflecting the underlying geology and influence of rock-glacier inputs, which are essentially absent in the north basin but present in the south basin. Because the local geology is predominantly orthogneiss and granite, the electrical conductivity of the waters is low (mean = 6.5 µs / cm in the north basin, 10.3 µs / cm in the south basin) (Table 1). Mean conductivity at Immez lake outlet was 9.6 ms / cm, whereas it increased to 19.8 µs / cm at Zeznina due to the input of rock-glacier water between the two sites. Water turbidity (NTUs) was low (ca. 2.5 NTUs or less), increasing to a mean of 7.9 at Zeznina. The median pH of waters was ca. 6.5–6.6 at all sites, again reflecting the slow-weathering bedrock in the area.

Nitrate (NO_3-N) and dissolved nitrogen (DN) values were higher for the south basin and Zeznina than for the north basin and Immez outlet:

- mean NO_3-N = 177.6 (south basin) and 198.1 µg / L (Zenina)
- mean NO_3-N = 69.1 (north basin) and 113.1 µg / L (Immez outlet)
- mean DN = 260.3 (south basin) and 302.7 µg / L (Zenina)
- mean DN = 179.5 (north basin) and 200.9 µg / L (Immez outlet).

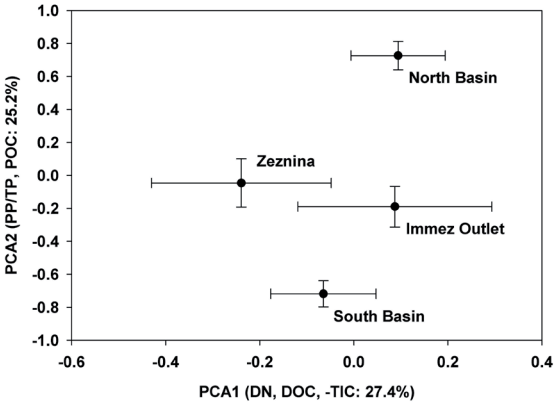

Figure 3 – Scatterplot of the first two axes of a principal components analysis (PCA1, PCA2) using the physico-chemical data collected each year at the end of July. Site loadings are summarized as means and standard errors along each axis for sites located in the North Basin (n = 4), South Basin (n = 4), lake Immez outlet and Zeznina. DN = dissolved nitrogen, DOC = dissolved organic carbon, TIC = total inorganic carbon, PP = particulate phosphorus, TP = total phosphorus, POC = particulate organic carbon.

In contrast, particulate nitrogen (PN) averaged 102.4 µg / L in the north basin but only 33.8 µg / L in the south basin and Zenina (Table 1).

Ortho-phosphorus (PO_4-P) concentrations were similar among surface waters, averaging between 1.9 and 4.5 µg / L (Table 1). In contrast, particulate phos-

*Table 3 – Summary of data for physico-chemical parameters for a representative time period (7 days) in each season in 2018. Parameters were recorded hourly by individual sensors embedded in the Exosonde near the outlet of Lake Immez. See Figure 6 for graphical presentation of the continuous data. Values expressed are means (*pH is given as median), SD = standard deviation, CV = coefficient of variation, Min = minimum, Max = maximum, NA = not applicable.*

Season		Temperature	Conductivity	Turbidity	Dissolved Oxygen	Chlorophyll-a	pH*
		(°C)	(µS / cm)	(FNU)	(mg / L)	(µg / L)	
Spring	Mean	0.6	5.2	0.68	10.74	−0.02	6.4
30 May–6 June	SD	0.39	0.19	0.08	0.14	0.08	NA
	CV	64.0	3.6	11.8	1.3	327.2	NA
	Min	0.1	4.9	0.53	10.27	−0.19	6.2
	Max	1.5	5.9	0.89	10.89	0.23	6.5
Summer	Mean	13.2	10.4	1.31	8.41	4.80	7.4
7–15 August	SD	0.56	0.30	0.17	0.23	1.65	NA
	CV	4.3	2.9	13.3	2.8	34.4	NA
	Min	11.8	9.9	0.88	7.70	1.21	6.8
	Max	14.9	11.0	1.69	8.94	11.08	8.6
Autumn	Mean	1.7	11.0	1.11	10.24	11.59	6.9
26 October–2 November	SD	0.70	0.36	0.37	0.21	3.60	NA
	CV	41.2	3.3	32.9	2.1	31.0	NA
	Min	0.8	10.5	0.80	9.05	0.92	6.7
	Max	3.8	11.9	5.78	10.54	19.96	7.1
Winter	Mean	0.1	13.6	0.43	7.84	0.08	6.1
19–26 February	SD	0.01	0.36	0.04	0.11	0.08	NA
	CV	14.2	2.7	9.2	1.4	92.1	NA
	Min	0.1	12.9	0.36	7.67	−0.14	6.1
	Max	0.1	14.1	0.89	8.08	0.32	6.1

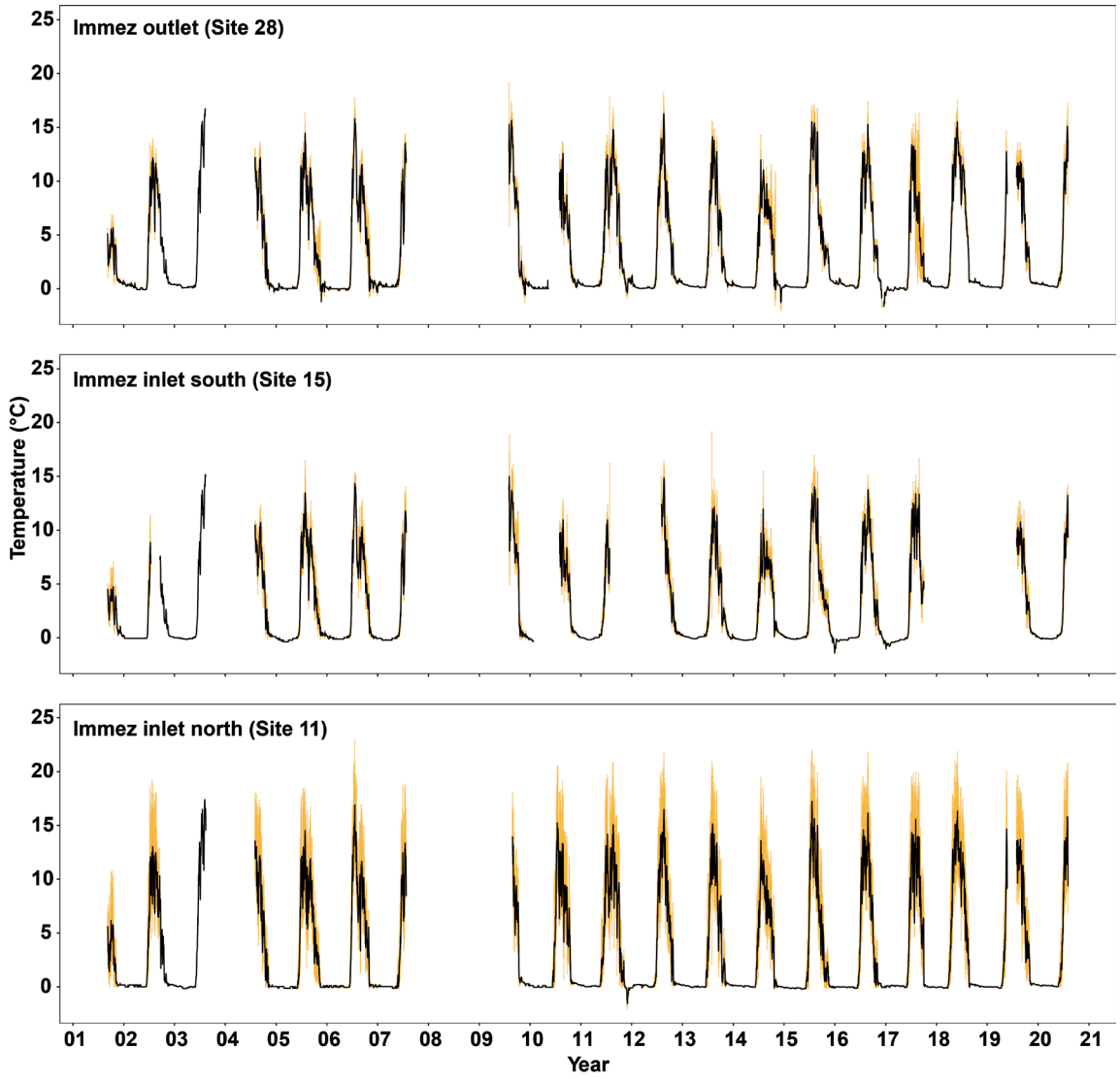

Figure 4 – Long-term temperature (°C) data recorded hourly with data-loggers installed at the north inlet of lake Immez (North Basin network), south inlet of lake Immez (South Basin network), and the outlet of lake Immez. The bold line is the average; the grey line represents minima and maxima. Data is missing from August 2007 to July 2009 because of dead batteries.

phorus (PP) and total phosphorus (TP) were higher in the north basin (8.6 µg / L and 10.5 µg / L, respectively) than in the south basin (3.4 µg / L and 7.0 µg / L, respectively). Further, PP and TP at Zeznina were 6.1 and 8.9 µg / L, respectively; phosphorus values at Immez lake outlet fell between the values of the two basins.

Mean dissolved organic carbon (DOC) and total inorganic carbon (TIC) values were relatively low, averaging 0.65–0.95 m / L for DOC and 0.80–1.21 m / L for TIC. Particulate organic carbon (POC) was generally low, but was higher in the north basin (mean = 0.96 m / L) than in the other sites (mean = 0.34–0.52 m / L). Silicate, a typical indicator of glacial waters, was similar among waters, averaging 2.2–2.7 m / L; mean alkalinity ranged from 0.09 to 0.12 mmol / L (Table 1).

Results from the PCA summarizing the physico-chemical data collected during the 19-year study period clearly separated sites in the north and south basins of the Macun catchment (Figure 3). PCA axis-1 explained 27.4% of the variation among sites and was loaded most highly by measures of dissolved nitrogen (DN), dissolved organic carbon (DOC) and total inorganic carbon (TIC). PCA axis-2 explained 25.2% of the variation among groups and was loaded highest with measures of particulate phosphorus (PP), total phosphorus (TP) and particulate organic carbon (POC). The data from Immez lake outlet fell mid-way between the basin groups along both PCA axes in the scatterplot. The Zeznina site downstream of Immez outlet, fed by meltwaters from a large rock-glacier, was located the farthest left on axis-1, clearly showing the influence of rock-glacier inputs on its physico-chemistry. PCA axis-2 showed north-basin sites having higher values of PP, TP and POC than south-basin sites, with the values for Immez lake outlet and Zeznina somewhere between those for the two basins.

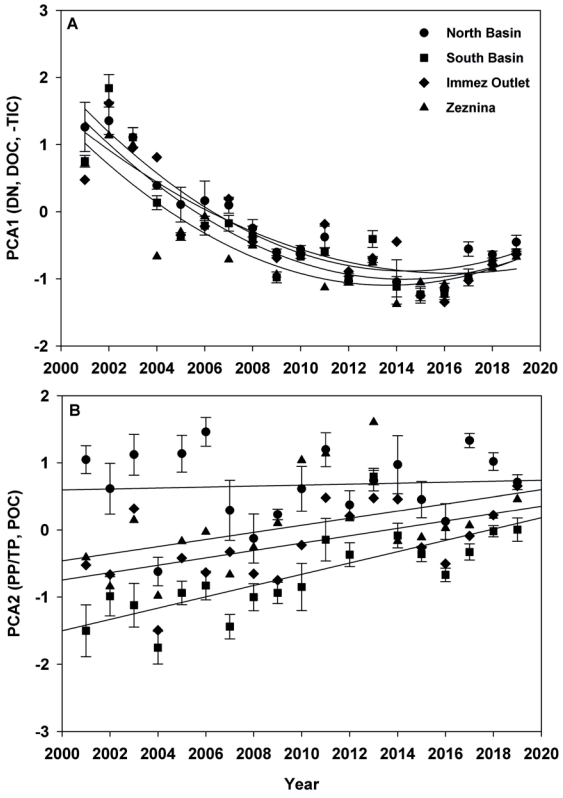

Figure 5 – Long-term trend lines (regression lines) in physico-chemical parameters that best explained PCA1 and PCA2 of the scatterplot shown in Figure 3. Plots represent temporal changes in North Basin sites (n = 4), South Basin sites (n = 4), lake Immez outlet and Zeznina, from 2001 to 2019. DN = dissolved nitrogen, DOC = dissolved organic carbon, TIC = total inorganic carbon, PP = particulate phosphorus, TP = total phosphorus, POC = particulate organic carbon.

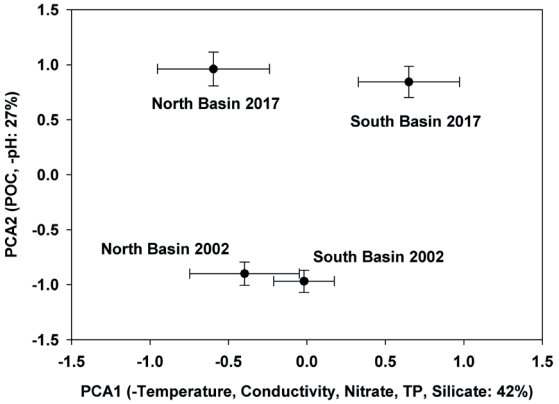

Figure 6 – Scatterplot of the first two axes of a principal components analysis (PCA1, PCA2) using the physico-chemical data collected at spring sites in the North Basin and South Basin in 2002 and 2017. Site loadings are summarized as means and standard errors along each axis for sites located in the North Basin (n = 7) and South Basin (n = 10). TP = total phosphorus, POC = particulate organic carbon.

Another evident pattern in the PCA scatterplot was the much higher spread in the data loading axis-1 than in the data loading axis-2.

Continuous long-term records at the outlet of each basin and Immez lake outlet revealed inter-annual differences in temperature patterns but no overall increase or decrease from 2001 to 2019 (Figure 4). Basins clearly differed in temperature: in summer, the north basin always had higher values (most years above 20°C, mean = 12.2°C) than the south basin (less than 20°C, mean = 9.3°C) (Table 1). Immez outlet temperatures were somewhere between those of the two basins or cooler, depending on the year (mean = 9.1°C), reflecting the general contribution and mixing of waters from each basin. In winter, waters in each basin and Immez outlet decreased to near 0°C, and possibly even froze at the recorded sites. The number of days per year with relatively warm waters (> 1.0°C) differed among basins and the outlet, ranging from 120 days (ca. 4 months) to a maximum of 165 days (ca. 5–6 months) (Table 2).

Long-term patterns in physico-chemistry were illustrated by plotting the PCA scores of axis-1 and axis-2 over time (Figure 5). PCA axis-1 showed a decrease from 2001 to 2009, then a general flattening in the data from 2009 to 2019 (albeit a slight increase occurred in 2019). These data indicate a general decrease in DN and DOC, and an increase in TIC, from 2001 to 2009, with little change in values from 2009 to 2019. In contrast, data from PCA axis-2 showed a general increase in PP, TP and POC over the study period for south-basin sites, Immez lake outlet and Zeznina. North-basin sites remained relatively unchanged in PCA axis-2 scores during the study period and, as mentioned above, had the highest PCA axis-2 scores among groups. Of note is that the variation among data loading on PCA axis-2 decreased from 2001 to 2019 (the variation was less on PCA axis-2 than for PCA axis-1 scores), suggesting a temporal homogenization in the physico-chemistry of waters in the Macun catchment overall (Figure 5).

Long-term physico-chemistry of springs and tributaries (2002 versus 2017)

PCA based on the physico-chemistry of springs and tributaries in the Macun catchment (see Figure 1, map) revealed differences between basins and between years (here, 2002 versus 2017) (Figure 6). PCA axis-1 explained 42% of the variation among sites and was loaded with measures of temperature, conductivity, nitrate, TP and silicate. PCA axis-2 explained an additional 27% of the variation among sites and was loaded with POC and pH. PCA axis-1 best represented the differences observed between the north-basin springs and the tributaries lying left of those from the south basin. PCA axis-2 best represented the temporal differences between 2002 and 2017 within each basin, with 2002 being lower on the plot than 2017 (Figure 6). The patterns shown in the PCA support the differences between basins evident in the physico-chemistry of the main channel sites as well as the tem-

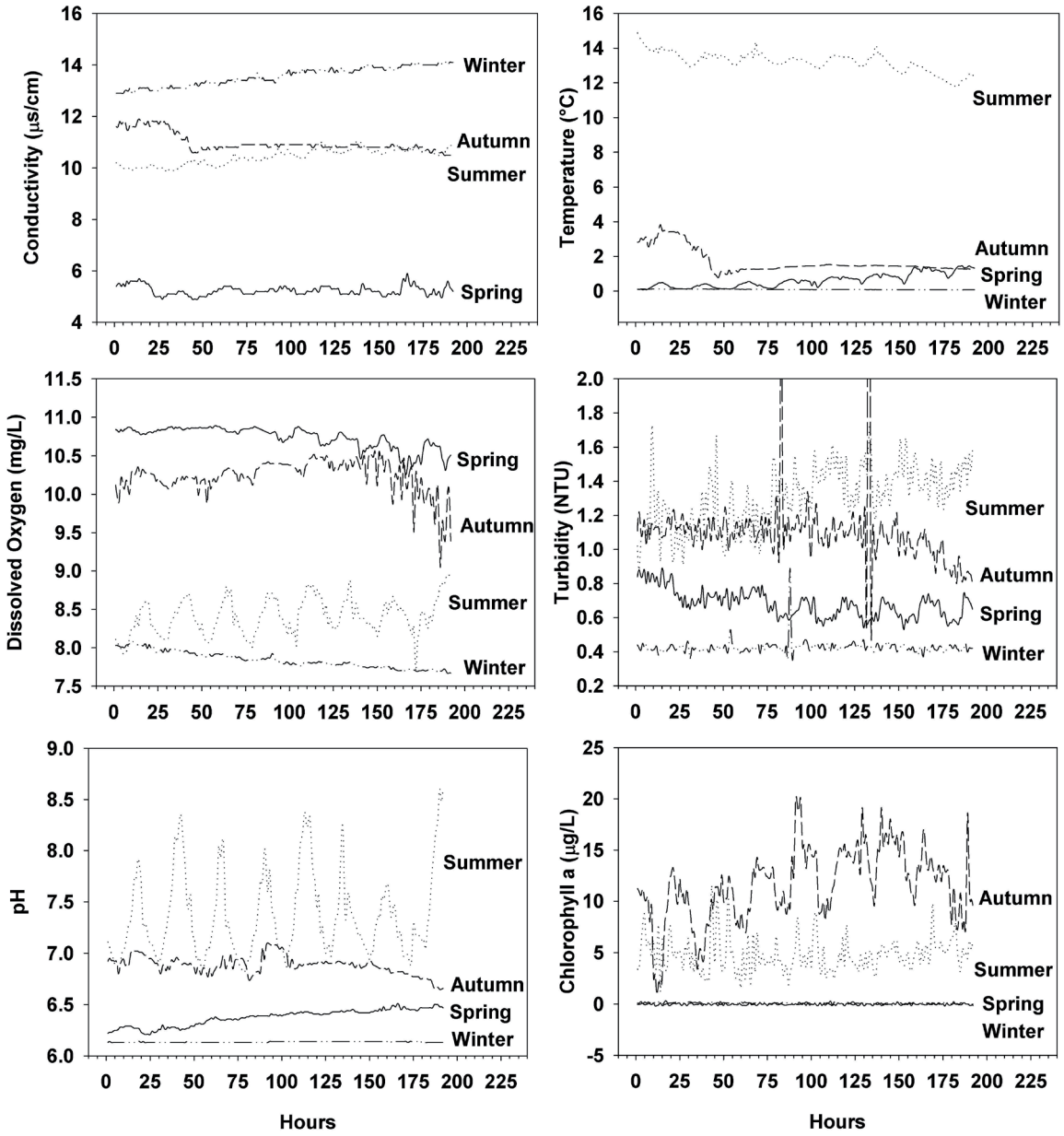

Figure 7 – Plots of continuously recorded (hourly) physico-chemical variables from individual sensors embedded in the Exosonde located near the outlet of lake Immez. Plots show a representative time period (7 days, as noted in Table 3) for each season in 2018.

poral changes in some physico-chemical parameters in the catchment overall.

Seasonal and diel physico-chemistry at the basin outlet in 2018

The Exosonde near the outlet of lake Immez continuously recorded data for conductivity, temperature, dissolved oxygen, turbidity, pH and chlorophyll-a. Typical patterns of one selected week in each season are shown in Figure 7. Conductivity values in general were low in Macun (< 16 µs / cm), where maximum values were observed in winter (12–14 µs / cm) and minimum values in spring (< 6 µs / cm) (Table 2). Some minor diel variation in conductivity was evident in spring and summer, with higher values during the day than night. Maximal temperatures were observed in summer (14–16°C) and minimal temperatures in winter (near 0°C) (Table 3). Maximum temperatures in spring and autumn ranged from 2 to 4°C. Diel variation in temperature was notable in spring and summer, when temperatures were warmer during the day than at night (Figure 7). Dissolved oxygen concentrations were highest in spring and autumn (10–11 mg / L), and lowest in winter (ca. 8 mg / L). Strong diel variation in DO was present in summer (ca. 1 mg / L change between day and night), being maximal during the day. In general, the summary of data in spring showed the transition from essentially no diel variation in winter to relatively strong diel curves in summer. In contrast, the summary of data in autumn depicted the rapid decrease in diel variation as winter became dominant in the catchment (Figure 7).

Water clarity, shown as turbidity, was low, but also showed strong seasonality, being highest in summer (ca. 1.3 NTUs) and lowest in winter (ca. 0.4 NTUs) (Figure 7, Table 3). The data summary also revealed some peaks in turbidity associated with local rainstorms; diel patterns were visible in spring. The seasonal patterns in pH showed the lowest values in winter (ca. pH 6.1); values were highest in summer, when strong diel patterns were evident (pH value minima ca. 7.0; maxima 8.0–8.5) (Table 3). Water chlorophyll-a values (sonde accuracy was 0.01 µg / L) were minimal in winter and spring (close to 0 µg / L), intermediate in summer (ca. 4.8 µg / L), and maximal in autumn (11.6 µg / L) (Table 3). The autumn values showed the greatest diel variation (from ca. 1.0 µg / L during the night to a maximum of 19.9 µg / L during the day) (Figure 7).

Discussion

The Macun Lakes are in an alpine cirque. They encompass a variety of water sources, from groundwater springs to rock glaciers, and drain into two separate basins. Various lakes along the main outflow channels are interconnected. The Macun Lakes area also comprises a number of intermittent ponds and small tributaries. As such, it represents an excellent area for the long-term monitoring of the effects of environmental change on alpine waters. The results clearly showed between-basin differences as well as temporal changes in the physico-chemistry of surface waters during the 19 years of monitoring. The assessment of springs and tributaries between 2002 and 2017 reflected the spatio-temporal changes observed in the main-channel study sites. Lastly, Exosonde data revealed strong diel and seasonal shifts in the physico-chemistry of surface waters, emphasizing the active functional role of lakes in alpine fluvial networks.

Rock-glacier input is the primary explanation for physico-chemical differences between the north basin (no rock glacier) and south basin (presence of rock glaciers). In fact, the south basin lies mostly over moraine deposits, and rock glaciers are still active contributors of water to the system (Robinson & Oertli 2009). In contrast, the north basin lies mostly over local bedrock and relatively thin soils, and glacial-water inputs are minimal or absent. A glacial-water signature, or lack of, is clearly visible in the colour of lake water (even with the low turbidity values): the colour is more greyish-blue in the south, while the lake waters in the north basin are browner (authors' personal observation). A glacial-water signature is also seen in physico-chemistry differences between the basins. For instance, in the north basin particulate forms of nitrogen and phosphorus were ca. 2–3x higher than in the south basin, and water temperature in the south basin was ca. 3°C lower (see also Robinson & Matthaei 2007). One possible explanation for the differences is that rock glaciers are typically associated with permafrost areas. Climate warming may have increased the amounts of solutes from permafrost / rock glacier in the surface waters of the south basin. Further, these relatively small rock glaciers in the south basin may be more sensitive to precipitation events than larger rock glaciers. As the basins lie over gneiss and granitic bedrock, ion concentrations of the waters in both basins were generally low, with mean electrical conductivities typically being below 10 µs / cm.

The physico-chemistry of the catchment changed over the study period. Around 2007, dissolved nitrogen in the catchment was lower than in 2001 (Robinson & Oertli 2009), and decreased further between 2007 and 2019 (see Figure 5). The pH of waters in both basins also increased, from < 6.0 in the late 1970s (Schanz 1984) to 6.5–7.0. Over time, other parameters, such as PP and POC, have changed more in the south basin than in the north basin, probably reflecting the general decrease in rock-glacier inputs in the south basin. Importantly, over the study period, the changes in physico-chemistry of the south basin have shifted the basin's chemical signature closer to that of the north basin. This change suggests that the physico-chemistry of surface waters in the catchment are becoming more similar over time. As both basins lie over similar geology, the ongoing reduction in rock-glacial waters will continue the process of homogenization. The question remains as to how long a glacial legacy effect will be present in south-basin waters (a glacial legacy has been observed in other alpine streams in the area, see Sertic Peric et al. 2015).

The springs and tributaries monitored in 2002 and 2017 also revealed temporal changes in both basins, while the basin-level differences observed at main-channel sites remained. The temporal changes revealed in the PCA were subtle differences in pH (lower in 2017) and POC (higher in 2017); basin-level differences were for the same variables as in the main dataset. It is important to note that most tributaries (ca. 70%) are precipitation-fed and intermittent, typically drying up in late summer (Robinson & Matthaei 2007), as also documented in the nearby catchment Val Roseg (Paillex et al. 2020).

The records for temperature, which was logged hourly at the outlets of each basin and in the outlet of the catchment, clearly demonstrate the sensitivity of alpine surface waters to local climate conditions. The area is relatively small. Thus, differences in solar radiation exposure between the basins are minimal. The warming of alpine waters under climate change has been documented (Webb & Nobilis 2007), but our data also show that inter-annual differences in weather play a significant role in dictating surface-water temperatures in the Macun catchment. For instance, although a 3°C difference occurred between basins (due to the rock-glacial water inputs in the south basin), strong inter-annual differences were observed over the study period and in both basins. Maximum temperatures between 2002 and 2019 ranged from 18.0

to 23.6°C in the north basin, from 11.4 to 23.4°C in the south basin, and from 13.7 to 19.2°C at the catchment outlet at Immez; no general warming trend was observed over the study period (at 19 years long, however, it was relatively short for the detection of trends) (see Table 2). Although streams are fairly shallow, slow-flowing and interconnected by small lakes, the high maximum temperatures in some years (> 23°C) is alarming. The network of lakes and streams increases water residence times and further enhances the potential for heating via intense solar radiation, even though rock-glacial inputs maintain cooler waters in the south basin (e. g. Lissi et al. 2015). Piccolroaz et al. (2018) showed that the temperatures of glacial-fed streams during heatwaves may be buffered by glacial water inputs that keep the waters cool. For Macun, this finding suggests that north-basin streams lacking glacial inputs are probably more sensitive to solar heating than south-basin streams, and will continue to be so until rock-glacial inputs diminish, as is expected to happen in the near future (see e. g. Woodward et al. 2016).

Sensor development has enhanced the potential for continuous remote monitoring. The Exosonde used in the present study recorded data, for a number of physico-chemical parameters, which were downloaded via satellite twice a day and displayed in real time at the Swiss National Park visitor centre (www.nationalpark.ch). The unit is solar-powered (with backup batteries), and was recently coupled to a meteorological station. The Exosonde was placed near the outlet of the last lake in the network, at 2,600 m asl. The data clearly demonstrated both strong seasonal patterns and diel dynamics for recorded variables (see Figure 7).

Values for conductivity, temperature, turbidity and pH displayed extremes between summer and winter; temperature, turbidity and pH were maximal in summer, and conductivity was maximal in winter (see Figure 7). In contrast, dissolved oxygen was maximal in spring and autumn; chlorophyll-a was maximal in autumn and intermediate in summer. These seasonal patterns reflect the ecosystem processes and functioning of the alpine waters during the annual cycle. Little or virtually no activity was evident in winter, as the system is completely snow-covered and water inputs come solely from groundwater. Spring activity reflects renewed biological functioning of the waters and benthic processes; summer and autumn reveal seasonality in ecosystem production (e. g., phytoplankton and benthic biofilms) and respiration (decomposition of benthic organic matter). Dissolved oxygen levels were lower in summer than in spring and autumn, probably due to the increased microbial activity (respiration) in the decomposing organic matter accumulated during winter. Interestingly, such patterns were similar to those of an earlier study assessing the ecosystem metabolism of Macun's streams: this study found that respiration was higher in early summer than in the autumn, due to the metabolic processing of accumulated organic matter by microbes (Logue et al. 2004).

The diel data from the Exosonde indicated how rapidly ecosystem processes start up in spring and slow down in autumn. For example, strong diel patterns in dissolved oxygen became evident during the week of recording in spring, whereas a breakdown of the DO diel pattern was evident in the 7-day record for the autumn (see Figure 7). A diel pattern was also evident for temperature in spring and summer; no diel temperature pattern was evident in the autumn or winter data. The chlorophyll-a data showed a strong diel pattern in the autumn, and a weaker one in summer. These data suggest seasonal changes in phytoplankton dynamics in alpine waters, and in lakes in particular. One explanation for the difference between summer and autumn could be changes in grazing activity by zooplankton (which is greater in summer than in autumn); this needs to be examined further. The diel phytoplankton variation in summer, when changes in dissolved oxygen reached almost 1.0 m / L between day and night, was also reflected in the large diel curves in pH (a difference of almost one pH unit between day and night). Although the data shown are for a typical week of any given season, long-term continuous monitoring will provide even greater insights into how alpine surface water functions in relation to environmental change. The coupling of other sensors (e. g., biotic) with physico-chemical sensors is recommended for future studies and monitoring networks.

To summarize, long-term monitoring helps to predict future environmental changes in ecosystem properties (here, those of alpine surface waters). These data, in turn, assist resource managers in environmental decision-making. Long-term data also provide important information towards understanding the drivers of environmental change, and the triggers for ecosystem state changes at tipping points. In particular, long-term data allow us to identify and focus on those parameters that are critical in comparative studies, and to avoid having to run the full suite of measures recorded in this study. Further, the development of new sensors will add to the toolbox of monitoring possibilities, and could enhance our mechanistic understanding of environmental change as well, especially when different types of sensors (e. g., abiotic and biotic) are evaluated together.

The physico-chemistry data from Macun show the sensitivity of alpine waters to environmental change, as well as to annual differences in weather. An important finding was the overall homogenization of surface waters as glacial inputs have diminished over time – a process that is likely to be a response of many glaciated alpine catchments globally. Lastly, the Exosonde data from the last lake in the fluvial network also revealed the strong metabolic patterns at seasonal and diel scales. The combination of lakes and streams in alpine landscapes should be considered in future surface-water monitoring programmes.

Acknowledgments

This study began in 2001 following the annexation of the Macun Lakes area within the Swiss National Park. Data are collected annually from 10 stream sites, supplemented over the years by more intensive and extensive studies conducted by Master's students (Sebastian Matthaei, Helena Vogler) interested in high-mountain landscapes and their waters. Each year, students, scientific collaborators, guest researchers and even artists get involved in the monitoring of the system. The authors graciously thank the Swiss National Park for logistical support (Flurin Filli, Ruedi Haller, Not Armon Willi) towards the annual expeditions over the last 20 years, and for supporting the installation of the Exosonde in more recent years. We owe a debt of gratitude to the chemical lab at Eawag for analysing the water samples each year. Two anonymous reviewers provided constructive comments that improved the paper. All data are available on request from the senior author or the data repository of the national park.

References

Barsch, D. 1969. Studien und Messungen an Blockgletschern in Macun, Unterengadin. *Zeitschrift für Geomorphologie, Annals of Geomorphology, Annales de Geomorphologie* 8: 11–30.

Barsch, D. & L. King 1998. *Rock glacier Macun 1, Lower Engadin, Switzerland, Version 1*. Boulder, Colorado USA. NASA National Snow and Ice Data Center Distributed Active Archive Center. Available at: https://doi.org/10.7265/3w9k-nv64 (accessed 17/02/2022)

Brunner, M., D. Farinotti, H. Zekollari, M. Huss & M. Zappa 2019. Future shifts in extreme flow regimes in Alpine regions. *Hydrology and Earth System Sciences* 23: 4471–4489. Doi: 10.5194/hess-23-4471-2019

Crnobrnja-Isailovic, J., B. Jovanovi , M. Ili, J. Corovic, T. Cubri, D. Stojadinovi & N. Cosic 2021. Small hydropower plants proliferation would negatively affect local herpetofauna. *Frontiers in Ecology and Evolution* 9: 610325. Doi: 10.3389/fevo.2021.610325

Derungs, D. & M. Tischhauser 2017. *Blockgletscher Macun – Dritte Folgemessung*. Bachelor-Thesis FHNW Fachhochschule Nordwestschweiz Hochschule für Architektur, Bau und Geomatik Institut Vermessung und Geoinformation.

Fehr, M. & R. Reich 2015. *Blockgletscher Macun - Zweite Folgemessung*. Bachelor Thesis, HNW Fachhochschule Nordwestschweiz Hochschule für Architektur, Bau und Geomatik, Institut Vermessung und Geoinformation.

FOEN (ed.) 2021. *Effects of climate change on Swiss water bodies. Hydrology, water ecology and water management.* Federal Office for the Environment FOEN, Bern, Switzerland. Environmental Studies No. 2101.

Haberkorn, A., R. Kenner, J. Noetzli & M. Phillips 2021. Changes in ground temperature and dynamics in mountain permafrost in the Swiss Alps. *Frontiers in Earth Science* 9: 626686. Doi: 10.3389/feart.2021.626686

IPCC 2013. *Climate Change 2013. The Physical Science Basis.* Contribution of Working Group I to the Fifth Assessment Report of the Intergovernmental Panel on Climate Change. Cambridge, United Kingdom and New York, NY, USA.

Jacobsen, D., S. Cauvy-Fraunie, P. Andino, R. Espinosa, D. Cueva & O. Dangles 2014. Runoff and the longitudinal distribution of macroinvertebrates in a glacier-fed stream: implications for the effects of global warming. *Freshwater Biology* 59: 2038–2050. Doi: 10.1111/fwb.12405

Kenner, R., L. Pruessner, J. Beutel, P. Limpach & M. Phillips 2020. How rock glacier hydrology, deformation velocities and ground temperatures interact: examples from the Swiss Alps. *Permafrost and Periglacial Processes* 31: 3–14. Doi: 10.1002/ppp.2023

Lange, K., P. Meier, C. Trautwein, M. Schmid, C.T. Robinson, C. Weber & J. Brodersen 2018. Basin-scale effects of small hydropower on biodiversity dynamics. *Frontiers Ecology Environment* 16: 397–404. Doi: 10.1002/fee.1823

Lissi, P.J., D.E. Schindler, T.J. Cline, M.D. Scheuerell & P.B. Walsh 2015. Watershed geomorphology and snowmelt control stream thermal sensitivity to air temperature. *Geophysical Research Letters* 42: 3380–3388.

Logue, J.B., C.T. Robinson, C. Meier & J.R. Van der Meer 2004. Relationship between sediment organic matter, bacteria composition, and the ecosystem metabolism of alpine streams. *Limnology and Oceanography* 49: 2001–2010. Doi: 10.4319/lo.2004.49.6.2001

Magnuz, E., D. Simpson, M. Schwikowski & L. Granat 2017. Deposition of sulphur and nitrogen in Europe 1900–2050. Model calculations and comparison to historical observations. *Tellus B: Chemical and Physical Meteorology* 69: 1328945. Doi: 10.1080/16000889.2017.1328945

Oertli, B., N. Indermuehle, S. Angelibert, H. Hinden & A. Stoll 2008. Macroinvertebrate assemblages in 25 high alpine ponds of the Swiss National Park (Cirque of Macun) and relation to environmental variables. *Hydrobiologia* 597: 29–41. Doi: 10.1007/s10750-007-9218-7

Paillex, A., A.R. Siebers, C. Ebi, J. Mesman & C.T. Robinson 2020. High stream intermittency in an alpine fluvial network: Val Roseg, Switzerland. *Limnology and Oceanography* 2019: 1–12. Doi: 10.1002/lno.11324

Piccolroaz, S., M. Toffolon, C.T. Robinson & A. Siviglia 2018. Exploring and quantifying river thermal response to heatwaves. *Water* 10: 1098. Doi: 10.3390/w10081098

Robinson, C.T. & S. Matthaei 2007. Hydrological heterogeneity of an alpine stream/lake network in Switzerland. *Hydrological Processes* 21: 3146–3154.

Robinson, C.T. & B. Oertli 2009. Long-term biomonitoring of alpine waters in the Swiss National

Park. *eco.mont - Journal on mountain protected areas research and management* 1(1): 23–34.

Rogora, M., R. Mosello, S. Arisci, M.C. Brizzio, A. Barbieri, R. Balestrini, P. Waldner, M. Schmitt, M. Stàhli, A. Thimonier, M. Kalina, H. Puxbaum, U. Nickus, E. Ulrich & A. Probst 2006. An overview of atmospheric deposition chemistry over the Alps: present status and long-term trends. *Hydrobiologia* 562: 17–40.

Scherrer, S.C., E.M. Fischer, R. Posselt, M.A. Liniger, M. Croci-Maspoli & R. Knutti 2016. Emerging trends in heavy precipitation and hot temperature extremes in Switzerland. *Journal of Geophysical Research: Atmospheres* 121: 2626–2637. Doi: 10.1002/2015JD024634

Schanz, F. 1984. Chemical and algological characteristics of five high mountain lakes near the Swiss National Park. *Verhandlungen des Internationalen Verein Limnologie* 22: 1066–1070.

Sertic Peric, M., C. Jolidon, U. Uehlinger & C.T. Robinson 2015. Long-term ecological patterns of alpine streams: An imprint of glacial legacies. *Limnology and Oceanography* 60: 992–1007. Doi: 10/1002/lno.10069

Tockner, K., F. Malard, P. Burgherr, C.T. Robinson, U. Uehlinger, R. Zah & J.V. Ward 1997. Physico–chemical characterization of channel types in a glacial floodplain ecosystem (Val Roseg, Switzerland). *Archiv für Hydrobiologie* 140: 433–463.

Tockner, K., U. Uehlinger & C.T. Robinson (eds.) 2009. *Rivers of Europe*. 1st edition.

Vogler, H. 2018. *Long-term trends in the ecohydrology of the Macun Lakes system*. Msc. Thesis, ETH Zürich.

Webb, B.W. & F. Nobilis 2007. Long-term changes in river temperature and the influence of climatic and hydrological factors. *Hydrological Sciences Journal* 52: 74–85.

Woodward, G., N. Bonada, L.E. Brown, R.G. Death, I. Durance, C. Gray, S. Hladyz, M.E. Ledger, A.M. Milner, S.J. Ormerod, R.M. Thompson & S. Pawar 2016. The effects of climatic fluctuations and extreme events on running water ecosystems. *Philosophical Transactions Royal Society B* 371: 20150274.

Zarrineh, N., K.C. Abbaspour & A. Holzkämper 2020. Integrated assessment of climate change impacts on multiple ecosystem services in Western Switzerland. *Science of the Total Environment* 708: 135212. Doi: 10.1016/j.scitotenv.2019.135212

Zick, W. 1996. Bewegungsmessungen 1965–1994 am Blockgletscher Macun I (Unterengadin/Schweiz) - neue Ergebnisse. *Zeitschrift für Geomorphologie* N.F., Suppl.-Bd. 104: 59–71.

Authors

Christopher T. Robinson[1,2]

is a senior research scientist at Eawag/ETHZ specializing the the ecology of running waters.

Christa Jolidon[1]

is a research assistant/technician at Eawag and assisted in the field collection and processing of samples.

Gabriele Consoli[1,2]

is a doctoral student at the Eawag/ETHZ in the group Robinson.

Simon Bloem[3]

is a specialist in the Sensor Lab at Eawag and instrumental in installing and maintenance of the Exosonde.

Christian Ebi[3]

is a specialist in the Sensor Lab at Eawag and was instrumental in the installation and maintenance of the Exosonde.

[1] Department of Aquatic Ecology, Swiss Federal Institute of Aquatic Science and Technology (Eawag), 8600 Duebendorf, Switzerland

[2] Institute of Integrative Biology, ETH-Zurich, 8092 Zürich, Switzerland

[3] Department of Urban Water Management, Sensor Lab, Swiss Federal Institute of Aquatic Science and Technology, 8600 Duebendorf, Switzerland

eco.mont – Volume 14, Number 2, July 2022
ISSN 2073-106X print version – ISSN 2073-1558 online version: http://epub.oeaw.ac.at/eco.mont
https://dx.doi.org/10.1553/eco.mont-14-2s24

The effects of landforms and climate on NDVI in Artvin, Turkey

Hilal Turgut & Bülent Turgut

Keywords: NDVI, GIS, drought, regression, interpolation

Abstract

Artvin, located in the Caucasus ecological region, is a unique area due to its high mountains, climatic characteristics, terrestrial and aquatic ecosystems, and high biodiversity. Thus, it is a suitable area for examining the effects of landforms and climate on vegetation dynamics. Vegetation changes over a three-year period (2018 to 2020) were investigated by examining the trends in the Normalized Difference Vegetation Index (NDVI) across the study area. First, the relationships between mean temperature, total precipitation and landforms (elevation, slope, aspect and distance from the sea) were determined by regression analysis, and their interpolated maps were created. In the second stage, the effects of the same landform characteristics and climatic factors, such as total precipitation and mean temperature, on NDVI were analysed. Regression analysis showed that the relationships between precipitation and distance from the sea, and between temperature and elevation were statistically significant. They were therefore used for prediction modelling. Changes in temperature and precipitation affected the NDVI values, but precipitation was found to be more significant than temperature. Landform differences were also responsible for changes in the NDVI values; distance from the sea was the most significant factor. The study also shows that in the drier period (2018), the elevation range where NDVI decreases is lower than during the other periods (2018 and 2020). We therefore conclude that the alpine zone can be more affected during drought periods.

Profile

Protected areas

Kackar Mountain National Park (NP), Hatila Valley NP, Karagöl Sahara NP, Camili Biosphere Reserve, 8 regional protection areas

Mountain range

Artvin mountain, Turkey

Introduction

Sustainable landscape management requires knowledge of abiotic ecosystem components, such as climate and topography, and needs to be able to analyse the interactions between them. Correlations between non-living environmental components (such as landforms and climate) and vegetation constitute an important basis for the creation of sustainable management strategies in today's world, where the effects of climate change are evident.

Temperature and precipitation are key climatic factors that alter the Normalized Difference Vegetation Index (NDVI) (Sanz et al. 2021), which is an indicator of the development of vegetation in terrestrial ecosystems (Myneni & Williams 1994; Xu et al. 2017; Chu et al. 2019). Like all organisms, plants need an optimum temperature range for maximum growth (Kimmins 2004). If the temperature exceeds this optimum range, it adversely affects plant growth due to decreased photosynthetic activity, and water and nutrient availability. Total annual precipitation and its distribution over the vegetation period are the main controls on vegetation structure, composition and distribution. Thus, precipitation greatly impacts the amount of vegetation (Zhang et al. 2013). Researchers have reported that drought due to climate change negatively alters vegetation growth (Gao et al. 2014; Pang et al. 2017; Nanzad et al. 2019; Li et al. 2021; Zhe & Zhang 2021), and that there is a close correlation between vegetation cover changes and climate factors, such as temperature and rainfall (Hou et al. 2015; Liu et al. 2018).

Landforms such as elevation, aspect and slope correlate significantly with vegetation and soil patterns at meso- and microscales (El-Keblawy et al. 2015; Flores et al. 2019). This is because landform controls the intensity of the key factors important to plants and to the soils that develop with them (Jiang et al. 2021; Peilin et al. 2020; Li et al. 2020; Liu et al. 2019). Erosion, for example, restricts plant growth by decreasing soil depth and water efficiency in sloping terrain. Landforms can also affect the large-scale spatial distribution and patterns of vegetation by creating microclimates (Panigrahi et al. 2021).

The NDVI is defined as a measure of surface reflectance; it provides a quantitative estimation of vegetation growth and biomass (Wu et al. 2016). This index varies between −1 and +1, in which values of less than zero during the growing season indicate no vegetation cover (e.g. in areas of desert or bare earth), while values greater than zero in the gowning season describe vegetation cover (Choubin et al. 2019). The NDVI value is associated with the intensity of photosynthetic activity in the vegetation observed (Piao et al. 2006; Wu et al. 2015). NDVI can accurately reflect the metabolic intensity and annual variation of vitality in vegetation; it indicates vegetation growth, and changes in temperature, precipitation and other climatic factors in the absence of human activities and natural disasters (Ghebrezgabher et al. 2020; Jiang et al. 2021; Liu

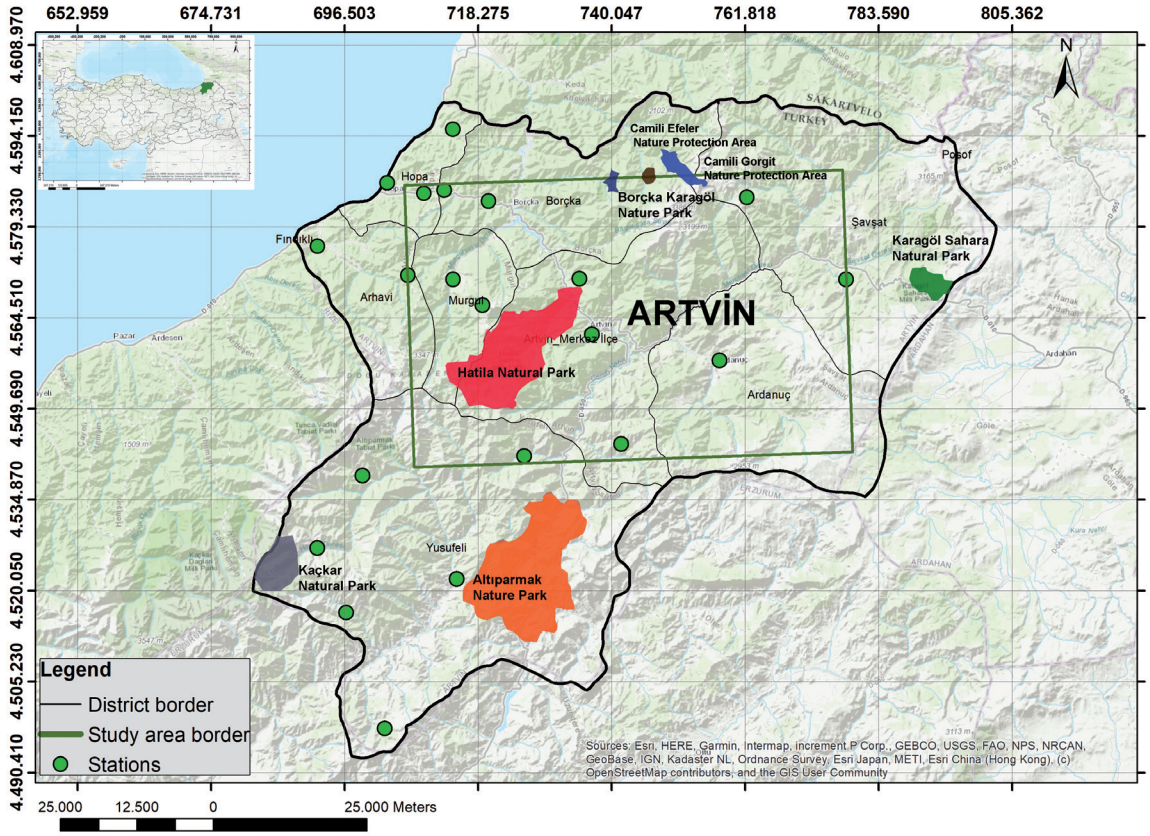

Figure 1 – Location of the study area and of the meteorological observation stations.

et al. 2019; Poll et al. 2009). Thus, NDVI has been widely used to monitor vegetation dynamics and determine the effect of climate variations such as cooling and warming on vegetation in the global (Nemani et al. 2003; Zhu et al. 2016) and regional (Piao et al. 2006; Wu et al. 2015) scale.

Its particular geographical location and topography make Artvin both a special region for climatic variation, and Turkey's richest region in terms of biodiversity (Eminağaoğlu et al. 2015). Within the borders of Artvin, there are three National Parks (NP) (Kaçkar Mountains NP, Hatila Valley NP, Karagöl-Sahara NP), three Nature Protection Areas (NPA) (Camili-Efeler NPA, Camili-Gorgit NPA, Çamburnu NPA), five Natural Parks (NaP) (Altiparmak Mountains NaP, Balıklı-Güneşli Waterfalls NaP, Borcka-Karagöl NaP, Cehennem Deresi Canyon NaP, Tavşan Hill NaP), and Camilli Biosphere Reserve. Due to the variability in topography, climate and vegetation, even over short distances, Artvin is a suitable study area for observing the effects of climatic and topographical factors on the temporal and spatial variability of vegetation. Nowadays, the effects of climate change on ecosystems are observed across the globe. For this reason, new tools and methods are necessary to understand ecosystem components and predict possible changes. By using NDVI, the effects of changes in the abiotic environment on the ecosystem can be determined. The aim of this study was to identify the effects of climatic parameters (such as precipitation and temperature), and landforms (such as elevation, aspect, slope and distance from the sea) on the NDVI during the three years 2018, 2019 and 2020. The results of this study will be useful for practitioners in estimating the possible consequences of climate change and managing sites accordingly.

Materials and Methods

Study area

The study area located in Artvin province is bounded by 455230527235 N and 4585102-4539220 E according to UTM WGS 1984 coordinate system (Figure 1). Topographically, it is defined by deep

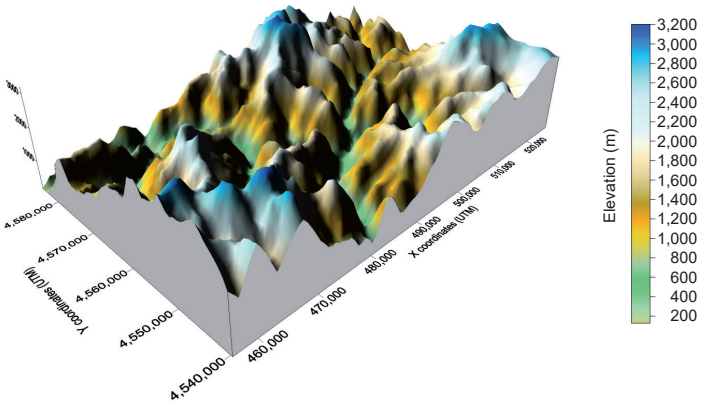

Figure 2 – The surface of the study area in 3D.

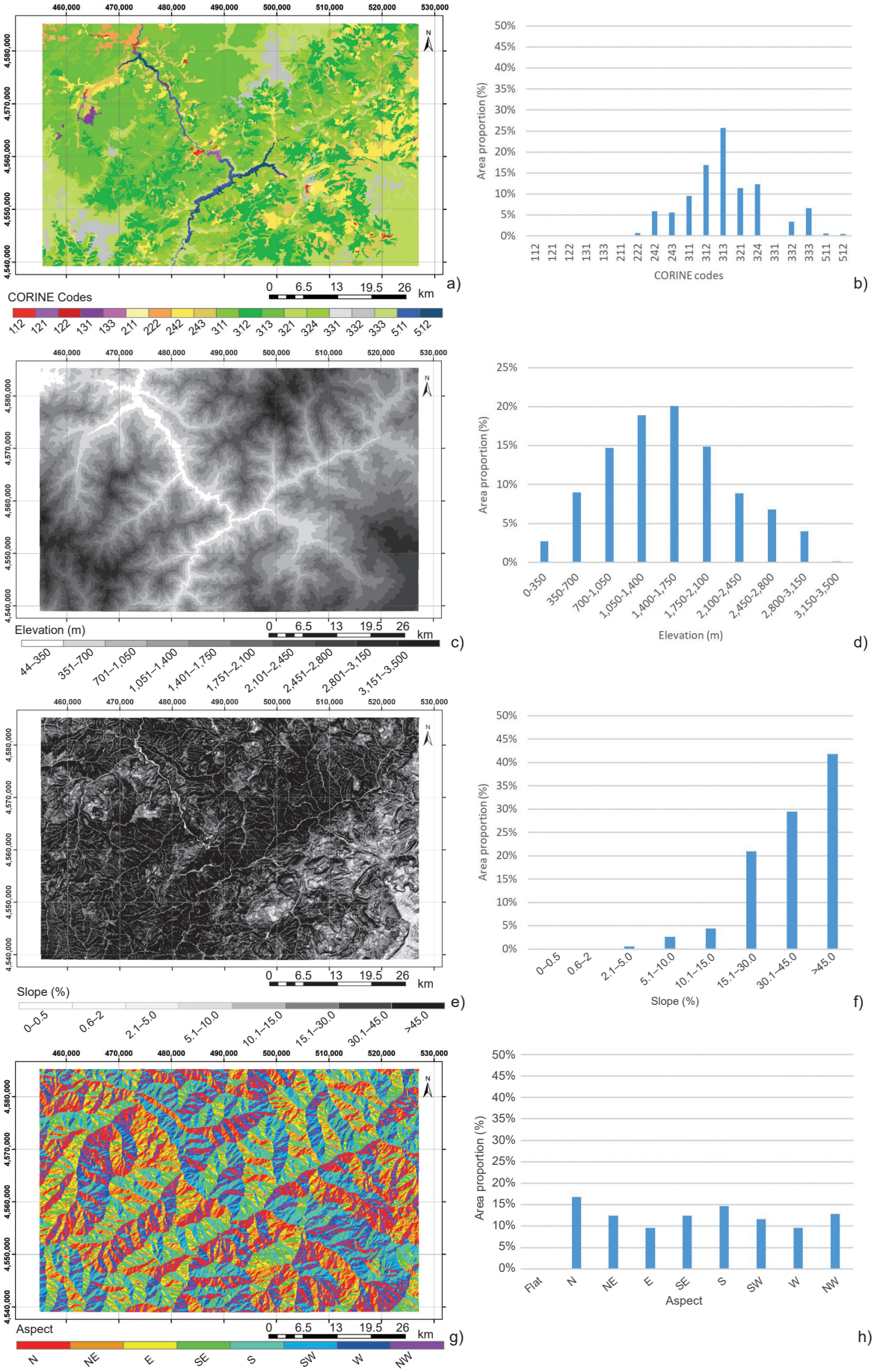

Figure 3 – (a) Corine land use map and (b) the area proportion of the Corine classes; (c) elevation map of the study area and (d) the area proportion of the elevation classes; (e) slope map of the study area and (f) area proportion of the slope classes; (g) aspect map of the study area and (h) area proportion of the aspects.

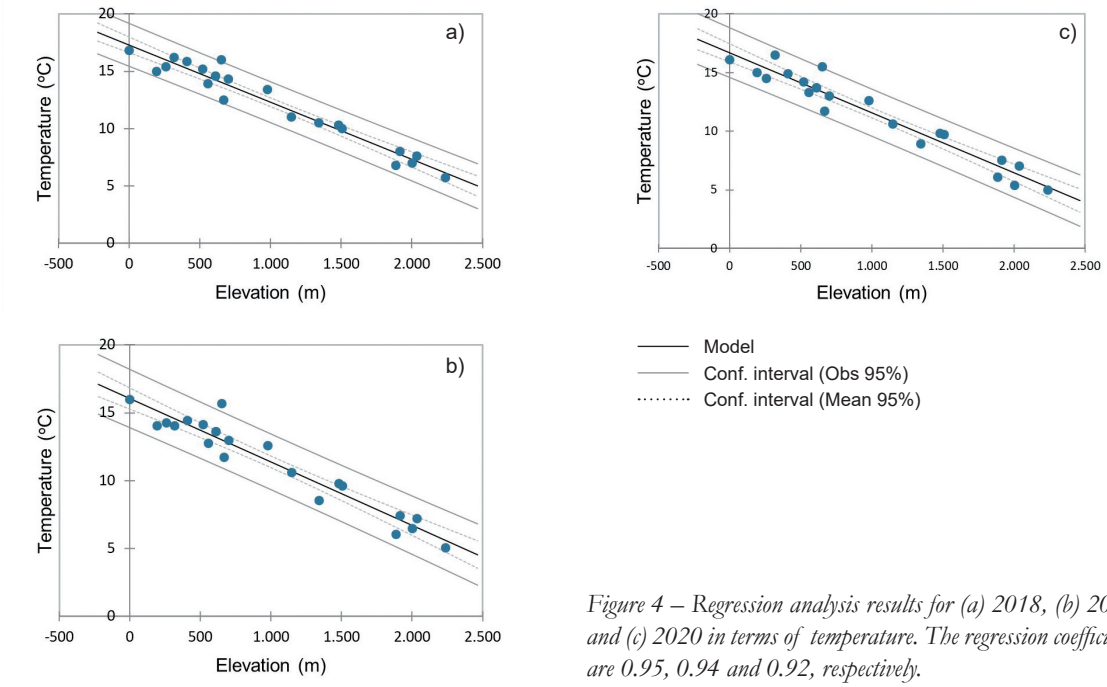

Figure 4 – Regression analysis results for (a) 2018, (b) 2019, and (c) 2020 in terms of temperature. The regression coefficients are 0.95, 0.94 and 0.92, respectively.

valleys and high mountains, so there are considerable variations in elevation and slope, even over short distances (Figure 2). There are four dams in the study area (the Muratlı, Borçka, Deriner and Artvin Dams), built on the Çoruh River to generate hydroelectric power. According to the CORINE land-cover classes, the area comprises 19 different land-use cases (Figure 3a), and forest and seminatural areas cover 86% of study area (Figure 3b). In terms of its flora, Artvin is the richest province in Turkey, with a total of 2,727 plant taxa belonging to 137 families and 761 genera (Eminağaoğlu et al. 2015). According to the Thornthwaite climate classification system, the study area includes six classes: wet (A), humid (B1, B2, B3, B4), and semi-humid (C2) (Turkish State Meteorological Services 2021; https://www.mgm.gov.tr/iklim/iklim-siniflandirmalari.aspx).

The elevation is the lowest in the Coruh riverbed, but reaches 3,400 m in the mountains (Figure 3c). We divided the elevation range into 350 m bands. The range 1,400–1,750 m, accounting for 20.1% of the study area, is the single most extensive altitude class. The least extensive is 3,150–3,500 m (Figure 3d). Steep terrain is common (Figure 3e): in 42% of the study area, the slope is >45% (Figure 3f). Since the mountains in the area extend east-west, the predominant aspects are north- and south-facing (Figure 3g), with north-facing being the most common (16.82%) (Figure 3h).

Data and analysis methods

Mapping landforms

A digital elevation model, slope, distance from the sea and aspect were computed for the study area using the *Spatial analyst* tool in ArcGIS software and Alos Palsar satellite imagery with a resolution of 12.5 m (ASF DAAC 2015). Due to the large size of the study area, maps were created by combining images taken on various cloudless days in 2019, using ArcGIS *image analysis* tools. The slope map created used the classification system recommended by the FAO (2021).

Obtaining climate data and creating interpolated maps

The results of the statistical analyses showed that the years 2018, 2019 and 2020 had significant differences in terms of temperature and precipitation. For this reason, data from these three years were evaluated in the study. The choice of consecutive years minimizes the effects of other factors, such as anthropogenic ones, which may have an impact on NDVI. Meteorological data for 2018, 2019 and 2020, including annual total precipitation and annual mean temperature, were collected from 22 meteorological observation stations of the Turkish State Meteorological Service in Artvin (Figure 1). Their geographical coordinates and elevation were obtained, and their distances from the sea were determined using the ArcGIS software. The fol-

Table 1 – Prediction models determined using regression analysis.

Years	Temperature	Precipitation
2018	17.29 – (0.00499*Elevation)	[0.0000005*(Distance to sea)2]-(0.0589*Distance from sea) + 2,202.4
2019	16.70 – (0.00512*Elevation)	[0.0000006*(Distance to sea)2]-(0.0676*Distance from sea) + 2,148.1
2020	16.04 – (0.00467*Elevation)	[0.0000006*(Distance to sea)2]-(0.0677*Distance from sea) + 2,450.5

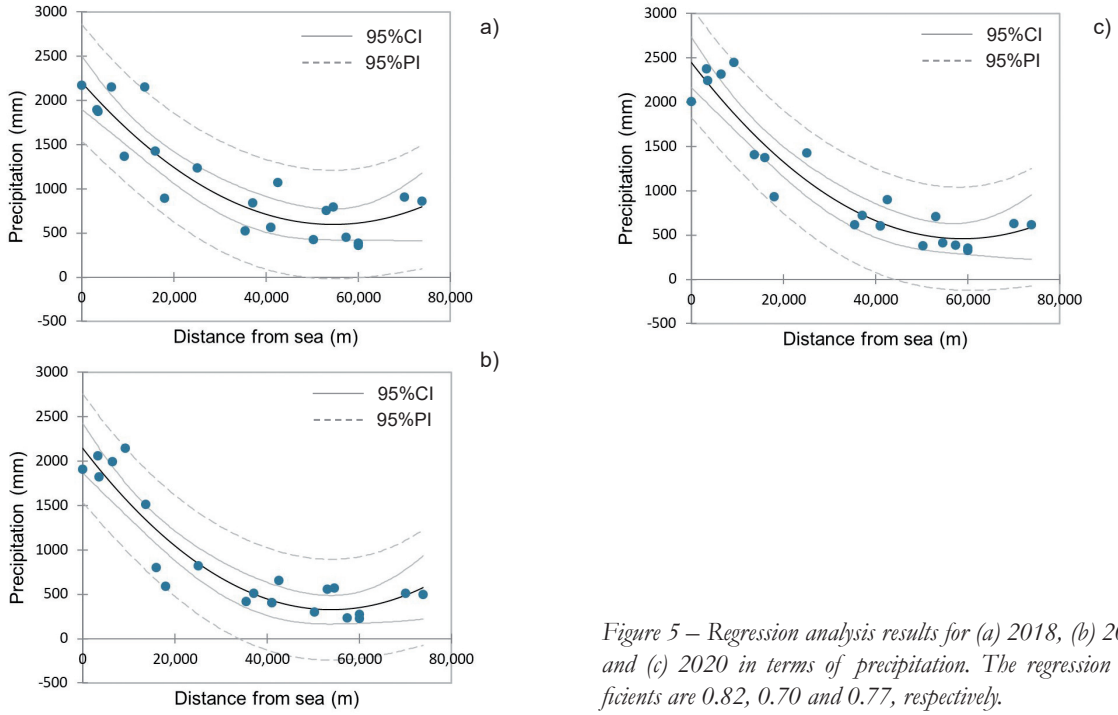

Figure 5 – Regression analysis results for (a) 2018, (b) 2019, and (c) 2020 in terms of precipitation. The regression coefficients are 0.82, 0.70 and 0.77, respectively.

lowing steps were followed in creating interpolated maps for the annual mean temperature and annual total precipitation:

a. Formulating prediction models of mean temperature and total precipitation: Regression analysis was used to determine the relationships between: i. the annual mean temperature and altitude; ii. the annual mean temperature and distance from the sea; iii. the annual total precipitation and altitude; and iv. the annual total precipitation and distance from the sea. It was found that there is a linear relationship between the annual mean temperature and elevation (Figure 4), and an exponential relationship between the annual precipitation and distance from the sea (Figure 5). The prediction models obtained from regression formulae are presented in Table 1.
b. Generating average temperatures and total precipitation values for virtual stations: 2,500 points (50×50 squares) were created within the boundaries of the study area using the ArcGIS *Fishnet* tool (Figure 6). The mean temperature and total precipitation values for 2018, 2019 and 2020 were then interpolated for the same points using the ArcGIS *Raster Calculator* tool, using estimation models. Creating 2,500 virtual stations increased the reliability of the interpolated maps for precipitation and temperature by representing as many elevation and distance-from-sea points as possible. The annual mean temperature and total precipitation data were calculated using prediction models for virtual stations.
c. Mapping for mean temperature and total precipitation: The interpolated maps for mean temperature and total precipitation for each year were created using the Inverse Distance Weighting method, which has a low root mean square error value; the ArcGIS *Interpolation* tool was used.

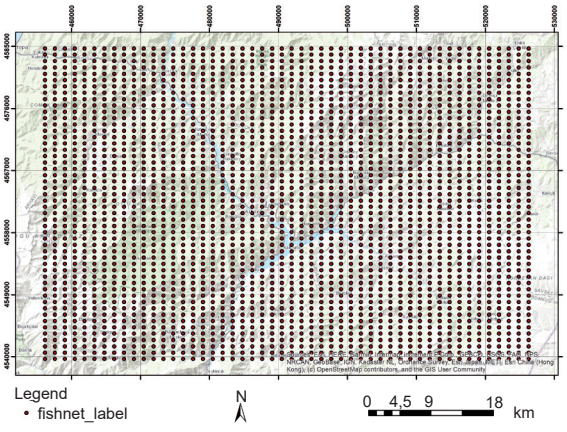

Figure 6 – Distribution of virtual stations in the study area.

Determining the NDVI values of the study area

To calculate the NDVI, band 4 (red) and band 5 (near-infrared) of Landsat 8 OLI/TIRS C2 Level 2 images, with a ground spatial resolution of 30 m, downloaded from United States Geological Survey (USGS) web services (https://earthexplorer.usgs.gov) were used (Li et al. 2013). The ArcGIS *Raster calculator* was used for calculations (Eq 1) based on satellite images dated August 2018, August 2019 and August 2020.

$$NDVI = (p_{NIR} - p_{red}) / (p_{NIR} + p_{red}) \quad \text{Eq 1.}$$

NDVI ... Normalized Difference Vegetation Index
p_{NIR} ... Near-infrar-red band
p_{red} ... Red band

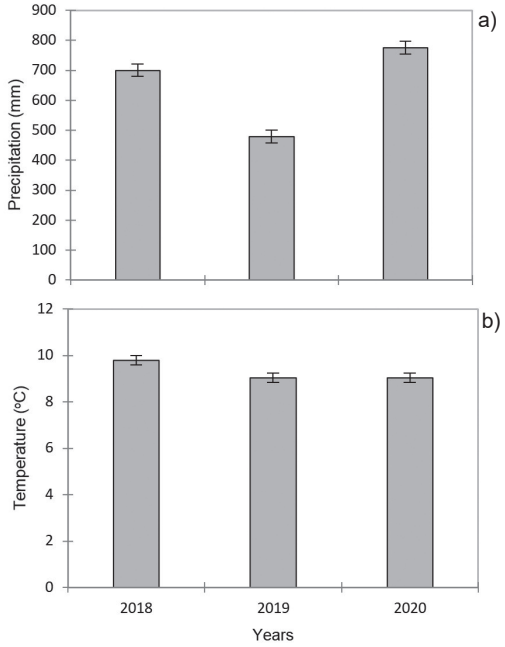

Figure 7 – Variation in (a) annual total precipitation and (b) mean temperature from 2018 to 2020 ($F_{precipitation}$: 483.28; $F_{temperature}$: 48.69; p<.01).

Determining relationships between NDVI and abiotic environment

The following steps were followed to determine the variation of NDVI due to the abiotic environment:

a. Total annual precipitation, mean annual temperature, elevation, aspect, slope and distance-from-sea layers were converted to vector

b. The water surfaces were masked

c. NDVI variation was determined from the differences in abiotic environment using ArcGIS *Zonal statistics as table* tools.

Statistical analysis

Analysis of variance (ANOVA) was used to determine the differences among years, elevation and distance from sea in terms of average temperature, total precipitation and NDVI; the Tukey comparison test was used to determine the differences among means. Regression analysis was performed to determine the relationships between the climatic parameters and landforms. XLSTAT software was used for statistical analysis.

Results and Discussion

Spatiotemporal changes in precipitation and temperature

The total precipitation varied in 2018, 2019 and 2020 (Figure 7a). The highest precipitation occurred in 2020, followed by 2018 and 2019. The differences between the years in terms of precipitation were statistically significant. The average temperature also varied significantly over the years. The highest temperature was in 2018, and the lowest in 2020 (Figure 7b).

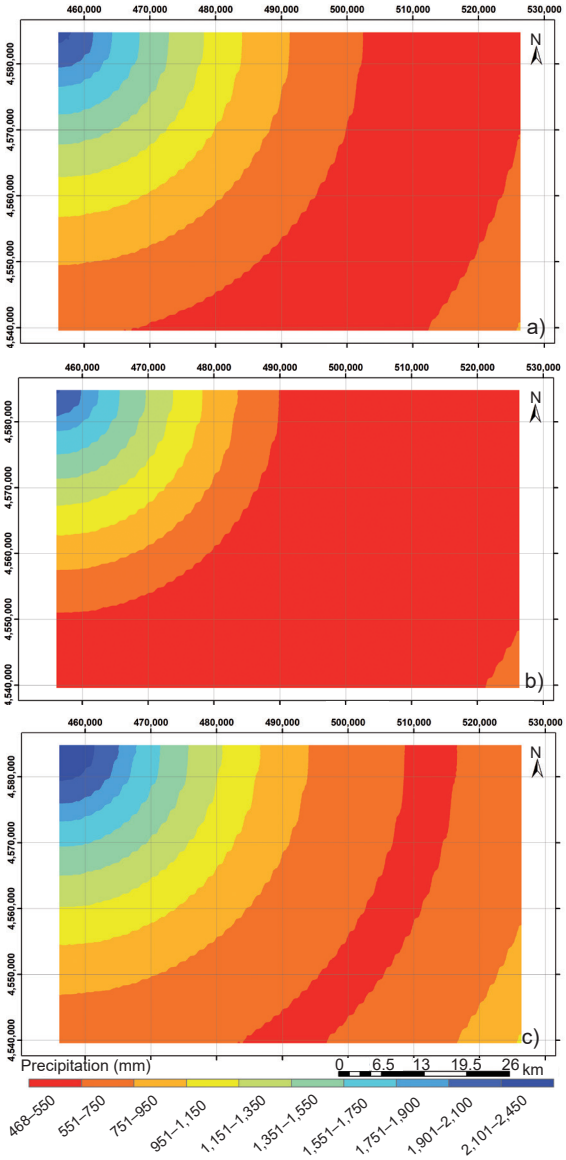

Figure 8 – Spatial variability of precipitation in (a) 2018, (b) 2019, and (c) 2020.

The spatial distributions for annual total precipitation and annual mean temperature are shown in Figures 8 and 9, respectively. The area covered by the lowest precipitation range (< 550 mm) was greater in 2019 than in the other two years. It was the smallest in 2020, which was the most rainy of the three years studied (Figure 8). In line with the results of the variance analysis, the area covered by the highest temperature class (16–17°C) in the distribution map was greater in 2018 than in the other years. It decreased in 2019, and further decreased in 2020 (Figure 9).

The temperature differences among 350 m elevation intervals are statistically significant (Figure 10a). Our results agree with those of previous studies that indicate that mean temperature decreases with increasing elevation (Battey et al. 2019; Poll et al. 2009; Richomme et al. 2010; Yao et al. 2016). The mean temperature also differed significantly depending on the distance from the sea (Figure 10b). However, unlike

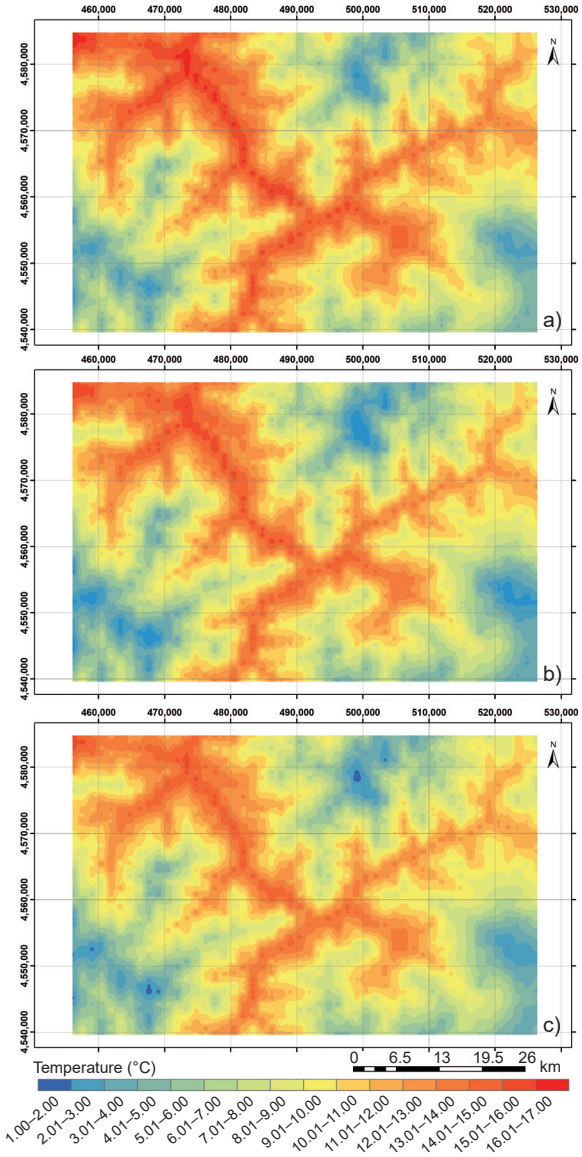

Figure 9 – Spatial variability of temperature in (a) 2018, (b) 2019, and (c) 2020.

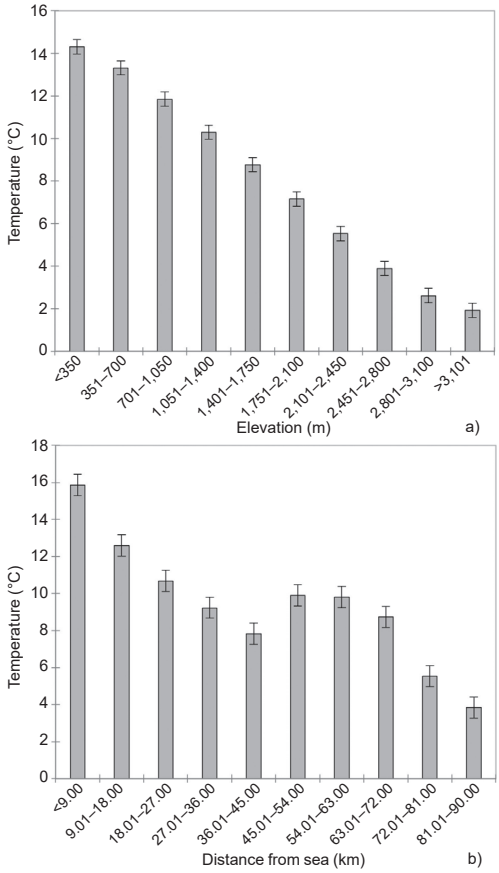

Figure 10 – Variation in average temperature along with (a) elevation and (b) distance from sea ($F_{elevation}$: 758.2; p < .01; $F_{distance\ from\ sea}$: 152.16; p < .01).

the findings for precipitation, the differences did not present a regular trend. They can be explained by the distance from the sea in some parts of the area, but mean temperature was also affected by elevation and aspect, which created higher-temperature microclimates.

The total precipitation differed significantly in relation to elevation (Figure 11a). Researchers have reported a positive linear relationship between elevation and precipitation in arid regions (Yu et al. 2018), while the increase in elevation in humid regions causes a decrease in precipitation (Angelini et al. 2011; Ogino et al. 2016). Further away from the sea, the total annual precipitation changed significantly (Figure 11b). Our findings were consistent with those of other researchers who reported that annual precipitation decreased inland (Bailey 2009; Bao et al. 2021).

Spatiotemporal changes to NDVI

The NDVI values varied over the years. The lowest value was achieved in 2019, followed by 2018 and 2020, respectively (Figure 12): vegetative growth and biomass were lowest in 2019, and highest in 2020. It is noteworthy that the highest NDVI (in 2020) coincided with the highest total annual precipitation. The differences between years in terms of the NDVI were statistically significant: it appears that the changes in temperature and precipitation in 2018, 2019 and 2020 caused a difference in NDVI values in these years (a finding reported by other researchers, see Catorci et al. 2021; Zhe & Zhang 2021), and indeed, that the temperature and precipitation changes are one of the main reasons for the differences in NDVI values in the years we studied. The areas highlighted in green in the NDVI distribution map (Figure 13) represent areas with NDVI values above 0.20. Fretwell et al. (2011) reported that areas with an NDVI value of more than 0.20 can be considered vegetated. The differences in the NDVI distribution maps agree with the results of the ANOVA tests, which compared years. In the NDVI distribution map for 2020, the areas above 0.20 were more extensive than in 2019.

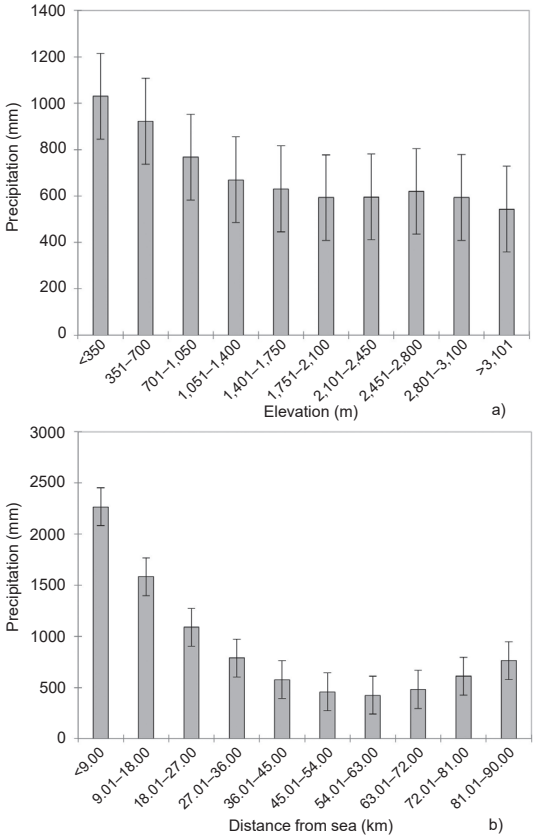

Figure 11 – Variation in average precipitation along with (a) elevation and (b) distance from sea ($F_{elevation}$: 3.289; p < .05; $F_{distance\ from\ sea}$: 44.911; p < .01).

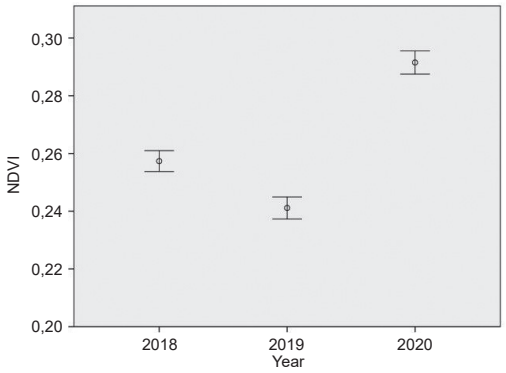

Figure 12 – Variation of the NDVI along with years (F: 74.74; p < .01). Error Bars: +/− 2 SE

Relationships between NDVI and abiotic environment

Variation in NDVI depending on precipitation and temperature

The NDVI increased significantly with increasing precipitation (Figure 14a). A positive correlation between the amount of precipitation and NDVI has been demonstrated in the literature (Fabricante et al. 2009; Wingate et al. 2019). The NDVI differed significantly in relation to temperature (Figure 14b) and was lowest in the coldest temperature. Although it increased with increasing temperature, the trend above

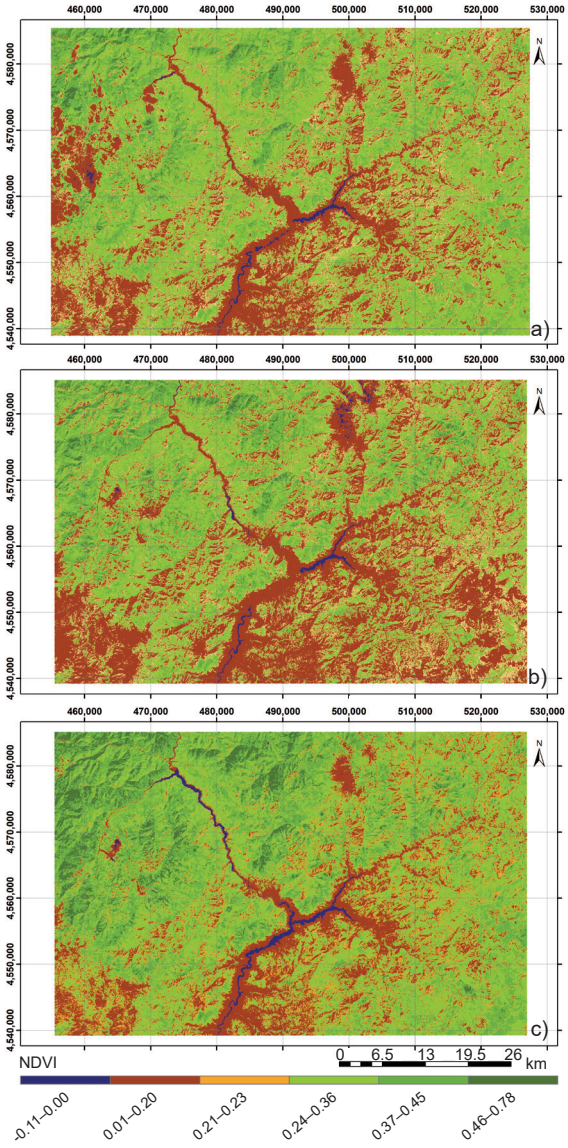

Figure 13 – Spatial variability of NDVI in (a) 2018, (b) 2019, and (c) 2020.

10–11°C was not stable. Low temperatures generally correspond to areas with high elevation, resulting in low vegetation density and, accordingly, low NDVI. The decrease of NDVI at high temperatures may be due to water stress, as researchers have reported that in arid areas the NDVI values decreased as temperature increased (Nse et al. 2020; Rani et al. 2018).

Variation in NDVI depending on elevation

To better interpret the differences in the NDVI caused by the variations in the landforms, both the ANOVA results and the three-year changes in the NDVI are shown in separate graphs. The differences among elevation ranges in terms of NDVI were statistically significant. The lowest NDVI values were found in areas with an altitude above 3,100 m, the highest at 1,050–1,400 m (Figure 15a). The most important information in Figure 15b is that unlike in 2018 and 2020, the altitude range where NDVI started to de-

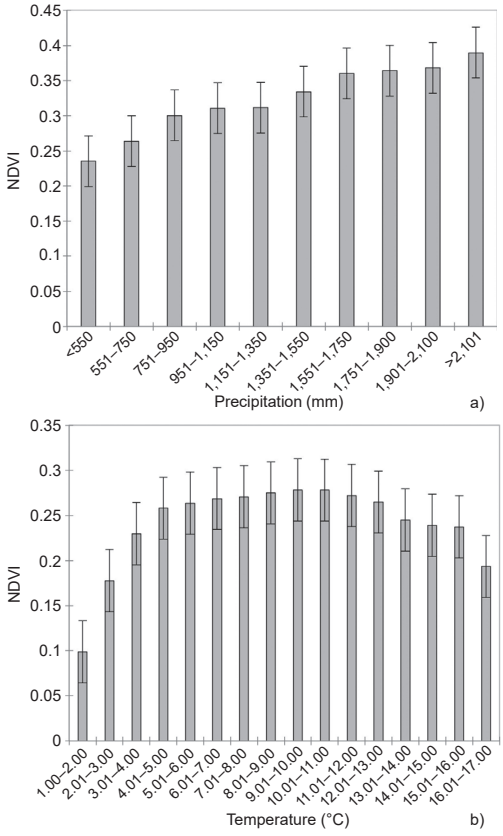

Figure 14 – Variations in average NDVI along with (a) precipitation and (b) temperature ($F_{precipitation}$: 8.042; p < .01; $F_{temperature}$: 8.062; p < .01).

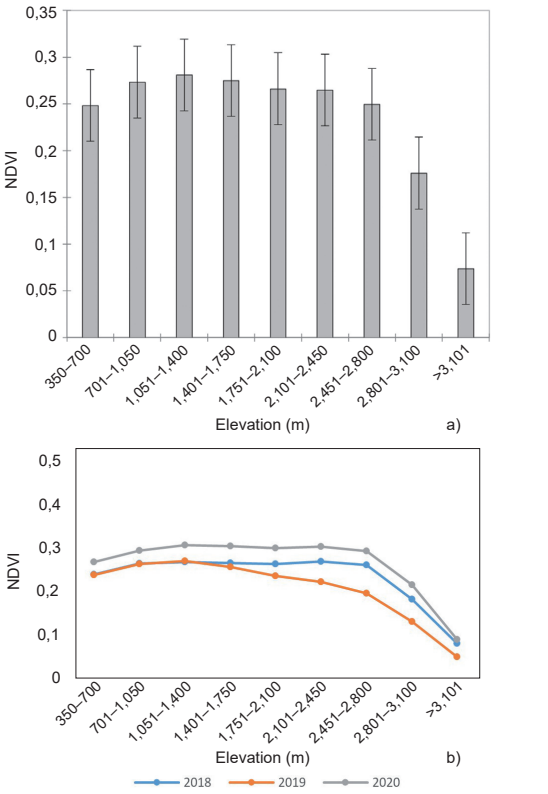

Figure 15 – (a) Variations in average NDVI along with elevation ($F_{elevation}$: 13.818; p < .01); (b) change in NDVI in terms of elevation over time.

crease in 2019 (the driest year) was 1,050–1,400 m. The fact that NDVI values decrease faster in alpine zones during arid periods means that the plants growing in such areas are more affected by dry periods. Researchers have stated that warmer temperatures and changing precipitation patterns due to climate change will increase the relative importance of soil and atmospheric droughts in limiting productivity across different ecosystems, especially fragile ones that are extremely sensitive to environmental changes (Tello-García et al. 2020; Xu et al. 2021). In line with our findings, it has been reported that an increase in temperature decreases the productivity of alpine pastures (Tello-García et al. 2020; Xu et al. 2021).

Variation in NDVI depending on the distance from the sea

The NDVI differed significantly in relation to distance from the sea (Figure 16a). NDVI values were highest on the coastal side of the study area, decreasing with increased distance from the sea, falling to their lowest around 45–54 km inland (the mid-point for distance from the coast), and increasing again from this point. In areas that are more than 45 km from the coast and where precipitation is below 500 mm, the limited increase in precipitation (up to 632 mm) in 2019 did not increase the NDVI. However, an upward trend was observed in these areas in the rainier years of 2018 and 2020 (Figure 16b). The change in NDVI by distance from the sea may be due to variations in precipitation and temperature. Precipitation greatly impacts the amount of vegetation present in any given year (Wingate et al. 2019).

Variation in NDVI depending on aspect

Differences in aspect caused significant changes in the NDVI (Figure 17a). In all three years, the highest NDVI value was in the east, and the lowest in the northwest (Figure 17b). Topographical aspect modifies the amount of solar radiation received by a surface (Geiger, 1965; Oke, 1987; Bennie et al. 2008). In humid regions, vegetation is denser on the east and west sides because of the greater insolation; higher NDVI values were therefore expected on the east-facing slopes of the study area. In agreement with our results, previous studies also reported that vegetation is denser in east- and west-facing areas in humid regions (Jin et al. 2008; Zhan et al. 2012).

Variation in NDVI depending on slope

The change in NDVI depending on the slope was statistically significant (Figure 18a). The study area is predominantly mountainous, and urban areas and agricultural fields are concentrated in regions with gentle slopes. Thus, the NDVI values were the lowest in areas with a slope of 0–0.5%. These increased with increased slope, but then showed a decreasing trend be-

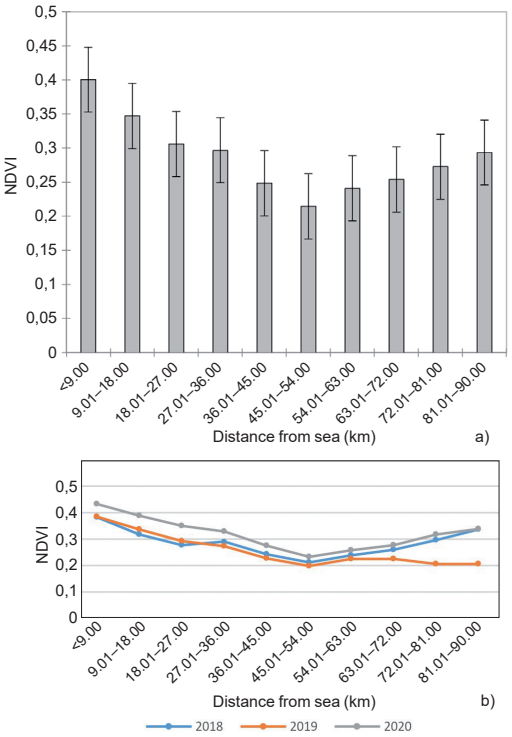

Figure 16 – (a) Variations in average NDVI along with distance from the sea ($F_{distance-from\ sea}$: 5.757; p <.01); (b) change in NDVI in terms of distance from the sea over time.

tween the ranges of 30–45% and > 45% (Figure 18b). The main reason for this is that human activities such as urbanization, tree-felling and agricultural activity are rare on steep terrain. The low NDVI in the steep parts of the study area may be due to shallow soil, low water availability for plants because of very high runoff, and high surface temperatures in sunny aspects. Consistent with our findings, Xiong et al. (2021) reported that the NDVI decreased in areas with a steep gradient.

Conclusion

The NDVI used for qualitative and quantitative estimation of vegetation dynamics is influenced by precipitation, temperature, elevation, distance from sea, aspect and slope. Landform data can be determined from satellite images using geographic information systems. Based on landform data and using regression analysis, patterns in climate dynamics can be predicted. The results showed that in our particular study area located in Artvin: (i) temperature can be predicted by elevation, and precipitation by distance from the sea; (ii) changes in annual mean temperature and annual total precipitation alter the NDVI; (iii) NDVI varies depending on the landform; (iv) the vegetation of alpine zones is more sensitive to dry periods.

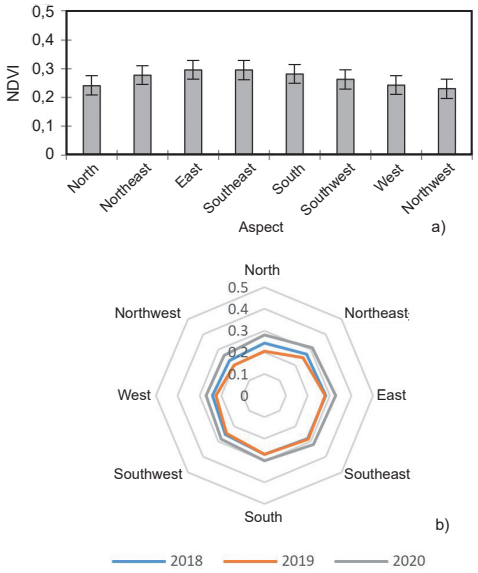

Figure 17 – (a) Variations in NDVI along with aspect (F_{aspect}: 2.679; p <.05); (b) change in NDVI in terms of aspect over time.

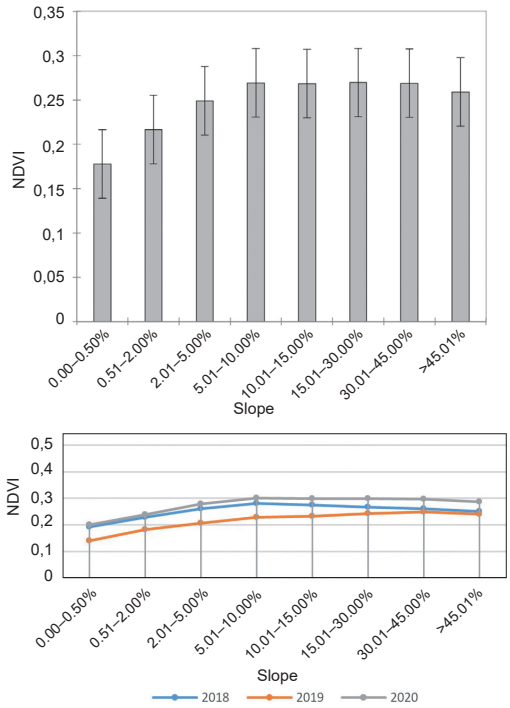

Figure 18 – (a) Variations in NDVI along with slope (Fslope: 3.373; p <.05); (b) change in NDVI in terms of slope over time.

References

Angelini, I. M. Garstang, R. E. Davis, B. Hayden, D.R. Fitzjarrald, D.R. Legates, S. Greco, S. Macko & V. Connors 2011. On the coupling between vegetation and the atmosphere. *Theoretical and Applied Climatology* 105(1): 243–261. Doi: 10.1007/s00704-010-0377-5

ASF DAAC 2015. ALOS PALSAR_Radiometric_Terrain_Corrected_low_res; Includes Material © JAXA/METI 2007. Accessed through ASF DAAC 07.10.2021. Doi: 10.5067/JBYK3J6HFSVF

Bailey, R.G. 2009. Ecosystem Geography: From Ecoregions to Sites. Available at: https://books.google.com.tr/books?id=9wC0Dd5EsJYC

Bao, Z., J. Zhang, G. Wang, T. Guan, J. Jin, Y. Liu, M. Li & T. Ma 2021. The sensitivity of vegetation cover to climate change in multiple climatic zones using machine learning algorithms. *Ecological Indicators* 124: 107443. Doi: 10.1016/j.ecolind.2021.107443

Battey, C.J., L.M. Otero, G.C. Gorman, P.E. Hertz, B.C. Lister, A. García, P.A. Burrowes & R.B. Huey 2019. Why Montane Anolis Lizards are Moving Downhill While Puerto Rico Warms. *BioRxiv* 751941. Doi: 10.1101/751941

Bennie, J., B. Huntley, A. Wiltshire, M.O. Hill & R. Baxter 2008. Slope, aspect and climate: Spatially explicit and implicit models of topographic microclimate in chalk grassland. *Ecological Modelling* 1: 47–59.

Catorci, A., R. Lulli, L. Malatesta, M. Tavoloni & F.M. Tardella 2021. How the interplay between management and interannual climatic variability influences the NDVI variation in a sub-Mediterranean pastoral system: Insight into sustainable grassland use under climate change. *Agriculture. Ecosystems & Environment*: 314: 107372. Doi: 10.1016/j.agee.2021.107372

Choubin, B., F. Soleimani, A. Pirnia, F. Sajedi-Hosseini, H. Alilou, O. Rahmati, A.M. Melesse, V.P. Singh & H. Shahab 2019. Effects of drought on vegetative cover changes: Investigating spatiotemporal patterns. *Extreme Hydrology and Climate Variability*: 213–222. Doi: 10.1016/B978-0-12-815998-9.00017-8

Chu, H.S., S. Venevsky, C. Wu & M.H. Wang 2019. NDVI-based vegetation dynamics and its response to climate changes at Amur-Heilongjiang River Basin from 1982 to 2015. *Science Total Environment* 650: 2051–2062. Doi: 10.1016/j.scitotenv.2018.09.115

El-Keblawy, A., M.A. Abdelfattah & A. Khedr 2015. Relationships between landforms, soil characteristics and dominant xerophytes in the hyper-arid northern United Arab Emirates. *Journal of Arid Environments* 117: 28–36. Doi: 10.1016/j.jaridenv.2015.02.008

Eminağaoğlu, Ö., H. Akyıldırım Beğen & G. Aksu 2015. Artvin'in doğal bitkileri. Promat Basım Yayım. Doi: 10.13140/RG.2.1.4312.3608

Fabricante, I., M. Oesterheld & J.M. Paruelo. 2009. Annual and seasonal variation of NDVI explained by current and previous precipitation across Northern Patagonia. *Journal of Arid Environments* 73(8): 745–753. Doi: 10.1016/j.jaridenv.2009.02.006

FAO 2021. *FAO Soils Portal. Global Terrain Slope and Aspect* Data. Available at: http://www.fao.org/soils-portal/data-hub/soil-maps-and-databases/harmonized-world-soil-database-v12/terrain-data/en/ (accessed: 25/09/2021)

Flores, D., E. Ocaña & A.I. Rodríguez 2019. Relationships between landform properties and vegetation patterns in the Cerro Zonda Mt., Central Precordillera of San Juan. Argentina. *Journal of South American Earth Sciences* 96: 102359. Doi: 10.1016/j.jsames.2019.102359

Fretwell, P.T., P. Convey, A.H. Fleming, H.J. Peat & K.A. Hugles 2011. Detecting and mapping vegetation distribution on the Antarctic Peninsula from remote sensing data. *Polar Biology* 34: 273–281.

Gao, J.G., Y.L. Zhang, L.S. Liu & Z.F. Wang 2014. Climate change as the major driver of alpine grasslands expansion and contraction: A case study in the Mt. Qomolangma (Everest) National Nature Preserve, southern Tibetan, Plateau. *Quaternary International* 336: 108–116.

Geiger, R. 1965. *The Climate Near the Ground*. Cambridge, MA.

Ghebrezgabher, M.G., T. Yang, X Yang & T. Eyassu Serek 2020. Assessment of NDVI variations in responses to climate change in the Horn of Africa. *The Egyptian Journal of Remote Sensing and Space Science* 23(3): 249–261. Doi: 10.1016/j.ejrs.2020.08.003

Hou, W., J. Gao, S. Wu & E. Dai 2015. Interannual variations in growing-season NDVI and its correlation with climate variables in the southwestern karst region of China. *Remote Sensing* 7: 11105–11124.

Jiang, S., X. Chen, K. Smettem & T. Wang 2021. Climate and land use influences on changing spatiotemporal patterns of mountain vegetation cover in southwest China. *Ecological Indicators* 121: 107193. Doi: 10.1016/j.ecolind.2020.107193

Jin, X.M., Y.K. Zhang, M.E. Schaepman, J.G.P.W. Clevers, Z. Su, J. Clevers & M. Schaepman 2008. *Impact of elevation and aspect on the spatial distribution of vegetation in the Gilian mountain area with remote sensing data.* Available at: http://heihe.westgis.ac.cn (accessed: 07/07/2021)

Kimmins, J.P. 2004. *Forest Ecology: A Foundation for Sustainable Forest Management and Environmental Ethics in Forestry. Prentice Hall.* Available at: https://books.google.com.tr/books?id=0LEsAQAAMAAJ

Li, P., L. Jiang & Z. Feng 2013. Cross-comparison of vegetation indices derived from landsat-7 enhanced thematic mapper plus (ETM+) and landsat-8 operational land imager (OLI) sensors. *Remote Sensing* 6(1): 310–329.

Li, P., J. Wang, M. Liu, Z. Xue, A. Bagherzadeh & M. Liu.2021. Spatio-temporal variation characteristics of NDVI and its response to climate on the Loess Plateau from 1985 to 2015. *CATENA* 203: 105331. Doi: 10.1016/j.catena.2021.105331

Li, Q., X. Shi, & Q. Wu. 2020. Exploring suitable topographical factor conditions for vegetation growth in Wanhuigou catchment on the Loess Plateau, Chi-

na: A new perspective for ecological protection and restoration. *Ecological Engineering* 158: 106053. Doi: 10.1016/j.ecoleng.2020.106053

Liu, H., M. Zhang, Z. Lin & X. Xu. 2018. Spatial heterogeneity of the relationship between vegetation dynamics and climate change and their driving forces at multiple time scales in Southwest China. *Agricultural and Forest Meteorology* 256: 10–21.

Liu, L., Y. Wang, Z. Wang, D. Li, Y. Zhang, D. Qin & S. Li 2019. Elevation-dependent decline in vegetation greening rate driven by increasing dryness based on three satellite NDVI datasets on the Tibetan Plateau. *Ecological Indicators* 107: 105569. Doi: 10.1016/j.ecolind.2019.105569

Mokarram, M. & D. Sathyamoorthy 2015. Modeling the relationship between elevation, aspect and spatial distribution of vegetation in the Darab Mountain, Iran using remote sensing data. *Modeling Earth Systems and Environment* 1(4): 1–6. Doi: 10.1007/s40808-015-0038-x

Myneni, R.B. & D.L. Williams 1994. On the relationship between FAPAR and NDVI. *Remote Sensing of Environment* 49: 200–211. Doi: 10.1016/0034-4257(94)90016-7

Nanzad, L., J. Zhang, B. Tuvdendorj, M. Nabil, S. Zhang & Y. Bai 2019. NDVI anomaly for drought monitoring and its correlation with climate factors over Mongolia from 2000 to 2016. *Journal of Arid Environments* 164: 69–77. Doi: 10.1016/j.jaridenv.2019.01.019

Nemani, R.R., C.D. Keeling, H. Hashimoto, W.M. Jolly, S.C. Piper, C.J. Tucker, R.B. Myenni & S.W. Running 2003. Climate-driven increases in global terrestrial net primary production from 1982 to 1999. Science 300(5625): 1560–1563.

Nse, O.U., C.J. Okolie & V.O. Nse 2020. Dynamics of land cover, land surface temperature and NDVI in Uyo City, Nigeria. *Scientific African* 10: e00599. Doi: 10.1016/j.sciaf.2020.e00599

Ogino, S.-Y., M.D.Yamanaka, S. Mori & J. Matsumoto 2016. How Much is the Precipitation Amount over the Tropical Coastal Region? *Journal of Climate* 29(3): 1231–1236. Doi: 10.1175/JCLI-D-15-0484.1

Oke, T.R. 1987. *Boundary Layer Climates* (2nd ed.). London

Pang, G., X. Wang & M. Yang 2017. Using the NDVI to identify variations in, and responses of, vegetation to climate change on the Tibetan Plateau from 1982 to 2012. *Quaternary International* 444: 87–96.

Panigrahi, S., K. Verma & P. Tripathi 2021. Review of MODIS EVI and NDVI data for data mining applications. In: Thwel, T.T. & G.R. Sinha (eds.), *Data Deduplication Approaches*: 231–253. Doi: 10.1016/b978-0-12-823395-5.00018-5

Peilin, L., D. Zhu, Y. Wang & D. Liu 2020. Elevation dependence of drought legacy effects on vegetation greenness over the Tibetan Plateau. *Agricultural and Forest Meteorology* 295: 108190. Doi: 10.1016/j.agrformet.2020.108190

Piao, S., A. Mohammat, J. Fang, Q. Cai & J. Feng 2006. NDVI-based increase in growth of temperate grasslands and its responses to climate changes in China. *Global Environmental Change* 16(4): 340–348. Doi: 10.1016/j.gloenvcha.2006.02.002

Poll, M., B.J. Naylor, J.M. Alexander, P.J. Edwards & H. Dietz 2009. Seedling establishment of Asteraceae forbs along altitudinal gradients: a comparison of transplant experiments in the native and introduced ranges. *Diversity and Distributions* 15(2): 254–265. Doi: 10.1111/j.1472-4642.2008.00540.x

Rani, M., P. Kumar, P.C. Pandey, P.K. Srivastava, B.S. Chaudhary, V. Tomar & V.P. Mandal 2018. Multitemporal NDVI and surface temperature analysis for Urban Heat Island inbuilt surrounding of sub-humid region: A case study of two geographical regions. *Remote Sensing Applications: Society and Environment* 10: 163–172. Doi: 10.1016/j.rsase.2018.03.007

Richomme, C., E. Afonso, V. Tolon, C. Ducrot, L. Halos, A. Alliot, C. Perret, M. Thomas, P. Boireau & E. Gilot-Fromont 2010. Seroprevalence and factors associated with Toxoplasma gondii infection in wild boar (Sus scrofa) in a Mediterranean island. *Epidemiology and Infection* 138(9): 1257–1266. Doi: 10.1017/S0950268810000117

Sanz, E., A. Saa-Requejo, C.H. Díaz-Ambrona, M. Ruiz-Ramos, A.E. RodríguezIglesias, P. Esteve, B. Soriano & A.M. Tarquis 2021. Normalized Difference Vegetation Index Temporal Responses to Temperature and Precipitation in Arid Rangelands. *Remote Sensing* 13, 840. Doi: 10.3390/rs13050840.

Tello-García, E., L. Huber, G. Leitinger, A. Peters, C. Newesely, M.-E. Ringler & E. Tasser 2020. Drought- and heat-induced shifts in vegetation composition impact biomass production and water use of alpine grasslands. *Environmental and Experimental Botany* 169: 103921. Doi: 10.1016/j.envexpbot.2019.103921

Wingate, V.R., S.R. Phinn & N. Kuhn 2019. Mapping precipitation-corrected NDVI trends across Namibia. *Science of the Total Environment* 684: 96–112. Doi: 10.1016/j.scitotenv.2019.05.158

Wu, D., X. Zhao, S. Liang, T. Zhou, K. Huang, B. Tang & W. Zhao 2015. Time-lag effects of global vegetation responses to climate change. *Global Change Biology* 21(9): 3520–3531. Doi: 10.1111/gcb.12945

Wu, Y., W. Li, Q. Wang & S. Yan 2016 Landslide susceptibility assessment using frequency ratio, statistical index and certainty factor models for the Gangu County, China. *Arabian Journal of Geosciences* 9 (2). Doi: 10.1007/s12517-015-2112-0

Xiong, Y., Y. Li, S. Xiong, G. Wu & O. Deng 2021. Multi-scale spatial correlation between vegetation index and terrain attributes in a small watershed of the upper Minjiang River. *Ecological Indicators* 126: 107610. Doi: 10.1016/j.ecolind.2021.107610

Xu, H.J., X.P. Wang & T.B. Yang 2017. Trend shifts in satellite-derived vegetation growth in Central Eurasia, 1982–2013. *Science of the Total Environment* 579: 1658–1674. Doi: 10.1016/j.scitotenv.2016.11.182.

Xu, M., T. Zhang, Y. Zhang, N. Chen, J. Zhu, Y. He, T. Zhao & G. Yu 2021. Drought limits alpine meadow productivity in northern Tibet. *Agricultural and Forest Meteorology* 303: 108371. Doi: 10.1016/j.agrformet.2021.108371

Yang, J., A. El-Kassaby & W. Guan 2020. The effect of slope aspect on vegetation attributes in a mountainous dry valley, Southwest China. *Science report* 10: 16465. Doi: 10.1038/s41598-020-73496-0

Yao, J., Q. Yang, W. Mao, Y. Zhao & X. Xu 2016. Precipitation trend – Elevation relationship in arid regions of China. *Global and Planetary Change* 143: 1–9. Doi: 10.1016/j.gloplacha.2016.05.007

Yu, H., L. Wang, R. Yang, M. Yang & R. Gao 2018. Temporal and spatial variation of precipitation in the Hengduan Mountains region in China and its relationship with elevation and latitude. *Atmospheric Research* 213: 1–16. Doi: 10.1016/j.atmosres.2018.05.025

Zhan, Z.-Z., H.-B. Liu, H.-M. Li, W. Wu & B. Zhong 2012. The Relationship between NDVI and Terrain Factors. A Case Study of Chongqing. *Procedia Environmental Sciences* 12: 765–771. Doi: 10.1016/j.proenv.2012.01.347

Zhang, B., J. Cao, Y. Bai, X. Zhou, Z. Ning, S. Yang & L. Hu 2013. Effects of rainfall amount and frequency on vegetation growth in a Tibetan alpine meadow. *Climatic Change* 118: 197–212

Zhe, M. & X. Zhang 2021. Time-lag effects of NDVI responses to climate change in the Yamzhog Yumco Basin, South Tibet. *Ecological Indicators* 124: 107431. Doi: 10.1016/j.ecolind.2021.107431

Zhu, Z., Y. Fu, C.E. Woodcock, P. Olofsson, C.E. Vogelmann, C. Holden, M. Wang, S. Dai & Y. Yu 2016. Including land cover change in analysis of greenness trends using all available Landsat 5, 7, and 8 images: A case study from Guangzhou, China (2000–2014). *Remote Sensing of Environment* 185: 243–257.

Authors

Hilal Turgut

is an Associate Professor at Karadeniz Technical University, Department of Landscape Architecture. Her main interests are landscape planning, ecosystem services, protected areas and geographic information systems. Karadeniz Technical University Faculty of Forestry, Landscape Architecture Department, 61080 Trabzon, Turkey.

Bülent Turgut

is an Associate Professor at Karadeniz Technical University, Department of Soil and Ecology. His main interests are soil degradation, ecosystem services and geographic information systems. Karadeniz Technical University Faculty of Forestry, Soil and Ecology Department, 61080 Trabzon, Turkey.

eco.mont – Volume 14, Number 2, July 2022
ISSN 2073-106X print version – ISSN 2073-1558 online version: http://epub.oeaw.ac.at/eco.mont
https://dx.doi.org/10.1553/eco.mont-14-2s37

Community structure and diversity of soil nematodes around Lake Paiku in Tibet, China

Huiying Xue, Da Qing Luo*, Bu Duo, Qing Xue, Xing Le Qu & Wen Wen Guo*
*co-first authors

Keywords: biodiversity, soil food web, Mt. Everest, nature reserve

Abstract

The diversity and community structure of soil nematodes around Lake Paiku in Mount Qomolangma (Mt. Everst) National Nature Reserve were investigated, to obtain soil ecosystem information, assess local soil quality, and provide the basis for environmental protection. Twelve plots were selected for typical vegetation communities around the lake. Within each plot, soil samples were collected from depths of 0 to 25 cm. The Baermann tray method was used to extract nematodes. Overall, we acquired 2,272 nematodes belonging to 2 classes, 5 orders, 32 families and 48 genera. The nematode density was 0–413 individuals per 100 g dry soil (average 109). Bacterivores, predators and omnivores were the dominant trophic groups. The individual density and genus numbers of soil nematodes were highest in the northeast and southeast corners of the lake. For most of the area studied, soil nutrients were at a medium level and there was no human disturbance. The energy flow of the soil food web tends to be via fungus decomposition channels. The redundancy analysis shows that soil-available P, pH, alkali-hydrolytic N, and soil-available K have strong effects on the soil nematode community, whereas the soil's total N, organic matter and water content have only minor effects. Soil-available P and pH were negatively correlated with nematode diversity. Soil nematodes showed surface aggregation; the soil food webs tend to have complex structures because of the presence of K-strategist organisms; the lakeshore ecosystem is in the late stage of succession and relatively stable. The increasing amount of soil-available P and increasing pH value corresponded to reduced biodiversity and unstable soil nematode communities. A greater diversity of nematodes were found in the Lake Paiku region in comparison to studies carried out in alpine meadows of the Chang Tang (or Northern Tibet) Grasslands.

Profile

Protected area

Mount Qomolangma (Mt. Everst) National Nature Reserve

Mountain range

Himalaya

Country

China

Introduction

Mount Qomolangma National Nature Reserve (QNNR) is located in the northern ranges of the Himalayas in Tibet, China. Together with the Nepalese Sagamada National Park in the south, it forms a complete and rare alpine forest ecosystem, with an average altitude of 4,200 m, making it the highest nature reserve in the world (Cidanlunzhu et al. 1997). The reserve is characterized by its polar alpine ecosystem, includes the highest peak on earth, and serves as an important model for studying global climate change and biological succession (Olson et al. 1998; Sun et al. 2012). Among seven core reserve zones in QNNR, Qomolangma-Shishapangma is the largest and is typical of the semi-arid plateau shrub and grassland ecosystem in the northern ranges of the Himalayas (Ministry of Ecology and Environment PRC 2018). The core zones of a nature reserve not only typify the natural zones, but are also the *background* that determines the ecological quality of the reserve and its adjacent areas, and their development. They are also a source of species resources in a region, providing the research base for saving and protecting rare and endangered species, and for exploring the sustainable use of biological resources.

In the zoogeographical regionalization of the world, QNNR is located on the dividing line between the palearctic and Oriental regions. The great range of its vertical elevation gradients and the diversity of unique species in the region have attracted the attention of scholars from home and abroad. Since QNNR was established nearly 30 years ago, ecological investigation and research have focused predominantly on aboveground ecosystems such as glaciers (Immerzeel et al. 2013; Nie et al. 2017; Nie et al. 2012), climate (Wang et al. 2018; Dunzhu 2009), vegetation (Shi et al. 2012; Shi et al. 2012; Nie et al. 2012; Zhang et al. 2006), and megafauna (Chen et al. 2017; Li et al. 2013; Pan et al. 2013; Qian et al. 1974). Less research has been done on underground ecosystems and in the lake region (Wang et al. 2018; Wang et al. 2006). So far, no research has looked at soil nematodes.

As global climate change continues to intensify and population growth puts pressure on sustainable development, the Qomolangma region is facing urgent ecological challenges. Due to the region's high altitude,

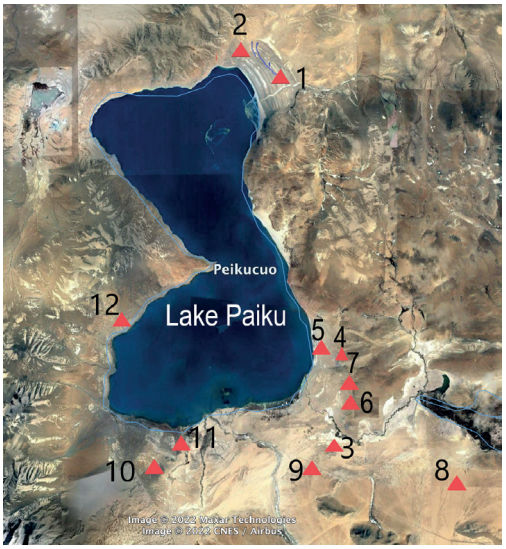

Figure1 – Location of each sample plot (see Table 1) and the surrounding terrain. © 2022 Maxar Tecnologies, 2022 CNES / Airbus. 28°57'45.20" N, 85°28'47.43' E, elev. 4.872m.

cold dry climate, and slow plant growth, it is difficult for the ecosystem to recover if it is degraded. From 2016 to 2018, field investigations were carried out in the Lake Paiku area (in the Qomolangma-Shishapangma core zone of the QNNR) with a focus on fauna and flora resources and environmental quality. Lake Paiku is the largest lake in the core reserve; its surrounding area consists mainly of sensitive semi-arid shrubs and grasslands, which need to be protected urgently. The investigations involved both above-ground ecosystems and soil-dwelling nematodes, aiming to provide scientific support for biodiversity and environmental conservation, and resource exploitation in QNNR and its adjacent areas.

Nematodes are abundant and their assemblages diverse. Their species composition is a bio-indicator of substrate texture, climate, biogeography, organic inputs, and both natural and anthropic disturbances (Yeates 1984). Nematodes interact with other organisms in the soil food web, contributing to the stability of the soil ecosystem, and promoting energy flow and material circulation.

Climate change is one of the most serious threats to lake ecosystems generally, and Lake Paiku specifically has attracted remarkable scientific interest in recent decades. Dekey et al. (2016) and Dai et al. (2013) pointed out that the area and water level of Lake Paiku have fluctuated greatly, with a general decreasing trend, in the last 40 years. These retreating water tables occurred mainly in the northeast, southeast and southwest corners. An earlier study (Zhao 2019) showed that the plant communities in the lake area vary significantly in composition and quantity; species diversity has decreased from the middle of the lake shore towards the south and north sides.

The present study focuses on the structure and diversity of the soil nematode community in QNNR, aiming to answer the following questions: (1) Is the soil nematode diversity in line with that of plant species in the lake area? (2) What is the condition of the soil ecosystem under minor disturbance, as measured by the functional index of the soil nematode community? (3) Is the rate of the biotransformation of soil nutrients increasing or decreasing under protected conditions?

Materials and method

Study site

Lake Paiku is a brackish lake located in Qomolangma-Shishapangma core zone, QNNR, at the northern

Table 1 – Geographical location and plant community composition of each sample plot.

Plots	Survey method	Longitude (E)	Latitude (N)	Altitude (m)	Edificators of plant community	Cover degree (%)	Species quantity
1	50 m line transect	85°38'25.86''	29°1'5.77''	4,631	*Iris loczyi* Kanitz+ *Achnatherum splendens* (Trin.) Nevski	60	5
2	50 m line transect	85°37'1.73''	29°2'13''	4,665	*Festuca ovina* + *Artemisia younghusbandii*	70	11
3	50 m line transect	85°40'58.92''	28°45'47.26''	4,621	*Astragalus strictus* + *Elymus tangutorum*	75	11
4	10 m×10 m quadrat	85°41'7.05''	28°50'10.29''	4,645	*Caragana versicolor* Benth. + *Artemisia wellbyi*	30	4
5	10 m×10 m quadrat	85°41'7.06''	28°50'11.45''	4,645	*Caragana versicolor* Benth. + *Artemisia wellbyi*	40	6
6	50 m line transect	85°41'59.84''	28°48'18.47''	4,659	*Thermopsis lanceolata* + *Artemisia younghusbandii*	75	4
7	50 m line transect	85°41'59.59''	28°48'18.47''	4,659	*Poa tibetica* + *Carex moorcroftii*	90	11
8	50 m line transect	85°47'20.79''	28°44'19.47''	4,676	*Astragalus strictus* + *Carex angustifructus* + *Stipa purpurea*	35	11
9	50 m line transect	85°39'48.55''	28°45'22.43''	4,647	*Astragalus tibetanus* + *Roegneria aristiglumis*	70	6
10	10 m×10 m quadrat	85°32'34.37''	28°45'44.39''	4,614	*Caragana* Fabr. + *Orinus* Hitchc.	65	8
11	1 m×10 m quadrat	85°34'15.49''	28°46'20.56''	4,589	*Carex moorcroftii*	95	10
12	10 m×10 m quadrat	85°31'25.89''	28°51'7.73''	4,633	*Ceratocarpus latens* + *Artemisia younghusbandii*	35	5

foot of Mt. Shishapangma, in Nyalam County, Xigaze City, Tibet Autonomous Region, PR China. The geographical coordinates of the lake are N 28° 20' to N 26° 65', and E 85° 20' to E 86° 50' (see Figure 1). The lake surface is 4,594 m above sea level; the area of the watershed that falls within the reserve covers approximately 2,397 km^2, of which glaciers and Lake Paiku account for 5.6% and 11.3%, respectively. Precipitation and glacial meltwater are the main replenishment sources of Lake Paiku (Chinese Academy of Sciences 1983; Lei et al. 2014).

The Lake Paiku region is a plateau with a temperate monsoon and semi-arid climate; it has typical cold and continental climate characteristics, sufficient sunshine (2,723.5 hours annually), and an obvious distinction between wet and dry seasons (The Meteorological Bureau of the Tibet Climate Center 2013). The area is located in the shrubby sub-region of alpine steppe in southern Tibet, according to the Vegetation Regionalization of China. The local grasslands are characterized by *Stipa purpurea*; grasslands dominated by *Artemisia*, *Carex* spp. and *Caragana versicolor* Benth were also observed in this region.

Soil sampling and testing

At the end of August 2017, 12 sample plots measuring 50 m×50 m were selected to include representative plant communities and different topography (different slope directions in an area that is relatively flat) around Lake Paiku's riparian zone. (See Table 1 for details.) Bulk soil samples were obtained by pooling 5 subsamples from depths of 0–5 cm, 5–10 cm, 10–15 cm, 15–20 cm, and 20–25 cm; soil cores measured 7 cm in diameter.

Soil samples were taken from at least 5 points, randomly, in each plot, giving a total of 60 bulk soil samples. These were packed in polyethylene bags, labelled, refrigerated, and stored in an insulated box with ice bags. The oven-drying method was used to calculate soil moisture content. Approximately 10 grams of fresh soil with a scale of 1/10,000 were weighed, and dried to a constant weight at 105°C (about 4 hours). The water content was then calculated (as a %), using the following formula:
(Fresh soil sample weight – dried soil sample weight) ×100 / fresh soil sample weight = soil moisture content (%)

Soil chemical properties were examined:
- the pH value was measured using the glass electrode method, in a 1:2.5 (soil:water) suspension;
- organic matter was measured using the potassium dichromate oxidation titration-external heating method;
- total phosphorus content was measured using the NaOH fusion-Molybdenum blue colorimetric method;
- total potassium was measured by NaOH fusion-flame photometer;
- available phosphorus was measured by the NaHCO$_3$–Molybdenum blue colorimetric method;
- alkali hydrolysis nitrogen was measured using diffusion.

Identification of soil nematodes

Nematodes were extracted from 30 g soil samples using a Baermann tray, kept at room temperature for 48 h (Oostenbrink 1960), and subsequently sieved using a 45 μm mesh. There can be up to several thousand nematodes in 100 g soil, especially soil samples with high humus content. For the sake of uniformity and for accurate counting, the sample weight was set at 30.0 g. The nematodes collected were fixed in 5% formaldehyde solution and mounted as temporary slides under a dissecting microscope. The nematode density was converted into number of individuals per 100 g of dry soil. Genus-level identifications were made using Olympus CX23 (Japan) according to available references (Bongers 1988; Yin 1998; Xie 2005). Dominant genera are those which represent more than 10% of the total; those accounting for 1% to 10%, and less than 1% were considered common and rare genera respectively.

Analyses of the diversity of the soil nematode communities

Shannon-Weiner diversity index:
$H' = -n_i / N \times \ln (n_i / N)$
Pielou evenness index: $J' = H' / \ln S$
Simpson dominance index: $\lambda = \Sigma(n_i / N)^2$
Margelef abundance index: $SR = (S - 1) / \ln N$

S ... number of groups
n_i ... number of individuals in group i
N ... total number of individuals of all groups in the community

Analyses of the functional groups of soil nematodes

Maturity Index, herbivore nematodes excluded (Bongers 1990): $MI = \Sigma c(i) \times p_i$
Plant Parasite Index (Bongers 1990): $PPI = \Sigma c(i) \times p_i$
Nematode Channel Ratio: $NCR = Ba / (Ba + Fu)$

p_i ... ratio of the non-plant parasitic soil nematode group i to the total number of individuals in the community (MI), or the ratio of the plant parasitic nematode group i to the total number of individuals in the community (PPI)
Ba and Fu ... the number of bacterivores and fungivores respectively
c(i) ... colonizer-persister value of the group i of non-plant-parasitic (or plant-parasitic) soil nematodes

Enrichment Index and Structure Index (Ferris et al. 2001)

The Enrichment Index (EI), based on the abundance of enrichment-opportunistic nematodes, can

be used as an indicator of the bacteria-mediated rapid decomposition of organic matter:
$EI = 100 \times (e / (e + b + s))$

The Structure index (SI), a weighted measure of the proportion of sensitive predator and omnivore nematodes, can be used as a sensitive indicator of soil food-web complexity:
$SI = 100 \times (s / (e + b + s))$

e, b and s ... enriched, basic and structural components respectively
$e = 3.2 \times Ba_1 + 0.8 \times Fu_2$
$b = 0.8 \times (Ba_2 + Fu_2)$
$s = Ba_n \times W_n + Fu_n \times W_n + Om_n \times W_n + Ca_n \times W_n$
$n = 3–5$
$W_3 = 1.8$
$W_4 = 3.2$
$W_5 = 5.0$

W ... weight coefficient
Om ... abundance of omnivorous nematodes
Ca ... abundance of predatory nematodes, and the subscript number
n ... c-p value of a nematode
c-p value ... colonizer-persister value

The higher the SI value is, plus the longer the food chain and the stronger the connectivity, plus the higher the EI value on the one hand, the more nutrients were input to the soil on the other. The particular distribution of the EI and SI results combined in the four quadrants (A, B, C, D) reflects the different succession states of the soil food webs.

When organic matter in soil is abundant and easily decomposed, the energy flow of the soil food web is more inclined to the bacterial decomposition channel; when organic matter in soil is scarce and difficult to decompose, the energy flow is more inclined to the fungal decomposition channel (Ingwersen et al. 2008).

Statistical analysis

A normality test was performed on the results of the soil's physical and chemical properties, and for nematode abundance. The data are normally distributed. Duncan's multiple comparative one-way ANOVA ($p < .05$) and Pearson's relevance analysis between multi-factors were conducted using IBM SPSS statistical 22.0 software to test the effects of different soil layers and soil physical and chemical properties on the structure of the soil nematode community. Redundancy analysis (RDA) and the visualization as graphs of correlations between soil traits and the structure of soil nematode communities were carried out using CANOCO 4.5.

Results

Plant community and soil properties

Twelve representative sample plots were selected covering various plant communities around Lake Paiku. The coordinates of each plot and its basic plant community are shown in Table 1.

Plots 1 and 2 were located in the northeast corner, 3–9 in the southeast corner, 10–12 near the southwest corner, and plot 12 near the central part of the lake's west bank. Sample plot 8 is the farthest from the lake.

Soil properties (pH, water content, total nitrogen, total potassium, available potassium and alkali-hydrolyzed nitrogen) were similar along the vertical profiles of the soil samples, while significant differences were observed among sample plots (Table 2). In terms of element content level, the soil along the bank of Lake Paiku has generally low fertility.

Structure of soil nematode communities

In total, 2,272 nematodes were acquired from soil samples taken from the 12 plots. The nematodes were identified as belonging to 48 genera, 32 families, 5 orders and 2 classes. The soil nematode density ranged from 0 to 413 individuals per 100 g dry soil (average 109 individuals); variations among plots were found to be significant ($F = 6.246$, $p < .001$). Specifically, the density of plots 5, 6 and 12 was lower than average while plots 2, 3, 7, 8 and 9 had relatively higher density. Soil nematode density in the 0–10 cm soil layer was significantly higher than that in the 10–25 cm layer ($F = 3.951$, $p = .008$). *Helicotylenchus* and *Cephalobus* were the two dominant genera in the soil nematode community.

The number of genera recovered ranged from 6 to 30 genera per plot, and inter-plot variations were found to be significant ($F = 14.189$, $p < .001$). Further variance analysis (Duncan) suggested that the 12 sam-

Table 2 – Physical and chemical properties of soil along the shore of Lake Paiku (mean values ± SD), and comparisons for them between sample plots and soil layers (ANOVA).

		pH	Soil		Total			Soil available		Alkali-hydrolyzable nitrogen (mg/kg)
			water content (g/kg)	organic matter (g/kg)	nitrogen (g/kg)	phosphorus (mg/kg)	potassium (%)	phosphorus (mg/kg)	potassium (mg/kg)	
		8.86±0.51	112.4±86.7	131.5±85.2	0.70±0.45	6.38±1.14	0.19±0.02	2.67±2.63	59.64±32.89	40.03±21.80
Plot	F	16.430	30.305	4.703	9.068	19.82	55.441	1.045	3.238	4.298
	Sig.	.000	.000	.003	.000	<.001	.000	.445	.016	.004
Clay	F	1.747	0.136	0.551	0.964	0.109	0.028	3.150	2.529	0.178
	Sig.	.203	.873	.586	.400	.979	.998	.067	.108	.838

Table 3 – Mean relative abundance (%) and c-p value of nematode genera in the sample plots.

Genus	c-p value	Sample plots											
		1	2	3	4	5	6	7	8	9	10	11	12
Fungivores													
Aphelenchus	2	0.5	10.2	3.1	2.2	0.0	15.3	0.6	5.1	2.5	0.8	1.0	0.0
Aphelenchoides	2	0.0	0.0	0.9	0.0	0.0	0.0	0.0	0.0	0.0	0.8	0.0	0.0
Diphtherophora	3	0.0	0.0	0.3	0.0	0.0	0.0	0.0	0.0	0.0	0.0	0.0	0.0
Ditylenchus	2	3.8	2.3	1.9	9.9	3.1	4.2	4.9	0.7	6.8	3.0	11.2	0.0
Filenchus	2	4.9	0.2	3.1	2.2	3.1	0.0	0.9	6.4	7.2	0.0	6.1	17.4
Leptonchus	4	0.5	0.2	2.5	4.4	6.3	0.0	0.3	1.7	1.7	1.5	0.0	0.0
Paraphelenchus	2	0.0	1.6	0.3	0.0	0.0	0.0	0.9	0.3	0.0	0.8	0.0	0.0
Tylencholaimellus	4	0.0	0.2	0.0	2.2	0.0	0.0	0.0	1.4	1.3	6.1	0.0	0.0
Tylencholaimus	4	6.5	4.3	4.4	3.3	0.0	0.0	0.9	5.4	14.8	12.1	0.0	0.0
Plant-parasites													
Coslenchus	2	0.0	0.0	15.9	0.0	0.0	0.0	0.0	0.3	0.0	0.0	0.0	0.0
Dorylaimellus	5	12.5	18.6	10.6	2.2	3.1	0.0	0.3	2.4	5.9	18.9	14.3	0.0
Helicotylenchus	3	0.5	8.6	7.5	0.0	6.3	0.0	38.5	4.7	17.8	0.8	0.0	0.0
Hemicriconemoides	3	0.0	0.0	0.0	0.0	0.0	0.0	0.0	0.0	0.0	0.0	1.0	0.0
Longidorella	4	0.0	0.2	0.0	0.0	0.0	0.0	0.0	0.3	0.0	0.0	0.0	0.0
Malenchus	2	0.5	0.0	0.0	0.0	0.0	0.0	0.0	0.0	0.0	0.0	0.0	0.0
Merlinius	2	10.9	0.0	1.9	1.1	0.0	0.0	2.0	0.0	0.4	0.0	0.0	0.0
Meloidogyne	3	0.0	0.0	0.0	0.0	0.0	0.0	0.3	0.0	0.0	0.0	0.0	0.0
Miculenchus	2	0.0	0.0	0.0	0.0	0.0	0.0	0.0	0.0	0.0	0.0	0.0	0.0
Neothoda	2	0.0	0.7	0.0	0.0	0.0	0.0	0.0	0.0	0.4	0.0	0.0	0.0
Paratylenchus	2	0.0	2.1	7.2	0.0	0.0	0.0	0.0	0.0	0.0	0.0	0.0	0.0
Tylenchorhynchus	3	0.5	5.9	7.5	0.0	0.0	0.0	0.0	22.9	0.0	0.0	1.0	0.0
Xiphinema	5	0.0	0.0	0.6	0.0	0.0	0.0	0.0	0.0	0.0	0.0	0.0	0.0
Bacterivores													
Acrobeles	2	1.6	2.5	3.8	6.6	0.0	2.8	0.6	9.8	6.4	0.0	0.0	0.0
Acrobeloides	2	0.0	2.7	5.0	5.5	0.0	12.5	0.0	2.7	0.9	0.8	0.0	4.3
Alaimus	4	1.1	0.0	0.0	0.0	0.0	4.2	0.0	1.0	0.0	0.0	0.0	0.0
Cephalobus	2	4.9	13.2	2.8	2.2	0.0	31.9	21.6	5.1	1.3	4.6	11.2	8.7
Cervidellus	2	4.4	7.7	7.2	1.1	6.3	5.6	10.1	5.1	6.4	20.5	5.1	0.0
Chiloplacus	2	4.4	0.0	0.0	0.0	0.0	4.2	1.4	0.0	0.0	0.0	0.0	0.0
Cylindrolaimus	3	6.0	0.5	2.2	2.2	0.0	0.0	0.0	3.0	3.0	0.0	0.0	0.0
Eucephalobus	2	0.0	0.0	0.0	0.0	6.3	13.9	8.1	0.0	0.0	0.0	0.0	4.3
Eumonhystera	1	0.0	0.0	0.0	0.0	0.0	0.0	0.0	0.0	0.0	0.0	1.0	0.0
Mesorhabditis	1	0.0	0.0	0.0	0.0	0.0	0.0	0.0	7.4	0.0	0.0	0.0	60.9
Plectus	2	0.0	0.2	0.0	0.0	0.0	0.0	0.0	0.0	0.0	0.0	5.1	0.0
Prismatolainus	3	1.1	0.0	0.3	2.2	6.3	0.0	0.0	0.3	0.0	0.0	0.0	4.3
Rhabdolaimus	3	0.0	0.0	0.0	0.0	0.0	0.0	0.0	3.0	0.0	0.0	0.0	0.0
Wilsonema	2	0.5	0.0	0.6	0.0	0.0	0.0	0.0	0.0	1.3	0.0	0.0	0.0
Omnivores – predators													
Aetholaimus	5	0.0	0.0	0.3	0.0	0.0	0.0	0.0	0.3	0.0	0.0	0.0	0.0
Aporcelaimellus	5	5.4	0.2	4.7	12.1	15.6	4.2	0.3	3.4	3.0	3.0	0.0	0.0
Aporcelaimus	5	0.0	4.1	0.0	0.0	0.0	0.0	0.0	0.0	0.4	5.3	2.0	0.0
Campydora	4	6.5	2.7	0.6	1.1	0.0	0.0	0.0	1.0	1.7	0.0	0.0	0.0
Carcharolaimus	5	0.0	0.0	0.6	0.0	0.0	0.0	0.0	0.0	0.0	0.0	0.0	0.0
Clavicaudoides	5	0.0	0.2	0.0	1.1	0.0	0.0	0.0	0.0	0.4	3.0	0.0	0.0
Discolaimus	5	6.0	0.9	1.6	5.5	0.0	0.0	0.0	1.4	8.5	3.0	1.0	0.0
Dorydorella	4	0.0	0.0	0.0	0.0	0.0	0.0	0.0	0.3	0.0	0.0	0.0	0.0
Ecumenicus	4	9.2	5.5	1.6	29.7	31.3	1.4	8.6	1.0	6.8	14.4	31.6	0.0
Enchodelus	4	6.0	2.5	0.6	0.0	6.3	0.0	0.0	2.0	0.9	0.8	8.2	0.0
Microdorylaimus	4	0.0	0.5	0.0	0.0	0.0	0.0	0.0	0.3	0.0	0.0	0.0	0.0
Paravulvus	5	1.6	1.4	0.3	3.3	6.3	0.0	0.0	1.4	0.4	0.0	0.0	0.0
Total	ΣG		24	28	30	20	12	11	17	30	24	18	14

ple plots could be divided into 4 groups according to the differences in the number of genera (group 1: 12, 5, 6, 4, 11, 10, 1; group 2: 4, 11, 10, 1, 9; group 3: 11, 10, 1, 9, 8; group 4: 9, 2, 3, 7). Sample plots 1, 11, 10, 9 and 4 appeared more frequently in the four groups; the number of genera found in these plots (14–24) was representative in the region.

The composition of the nematode communities in different plots is shown in Table 3. Bacterivores dominated most plots, accounting for 30.27% of indi-

*Table 4 – Ecological indices of each sample plot (Means± SD), and comparisons between sample plots and soil layers to understand the spatial variation indicated by the ecological indices of nematode communities. *: p < .05, **: p < .01. H' = Shannon-Weiner diversity index; J' = Pielou evenness index; λ = Simpson dominance index; SR = Margelef abundance index; MI = Maturity Index; PPI = Plant Parasite Index; NCR = Nematode Channel Ratio.*

Plots		Ecological indices						
		H'	*J'*	*λ*	SR	MI	PPI	NCR
1		2.27±0.13a	0.93±0.02a	0.12±0.02a	3.07±0.33ab**	3.63±0.25a	2.13±0.22ab	0.61±0.10ab
2		2.19±0.18ab	0.88±0.05a	0.14±0.02a	3.03±0.39ab**	3.09±0.45abc	2.68±0.09a	0.60±0.15ab
3		2.55±0.17a	0.88±0.04a	0.10±0.02a	4.17±0.59c	3.22±0.41ab	2.46±0.33ab	0.56±0.11ab
4		1.63±0.82bc*	0.90±0.08a	0.29±0.20ab	2.45±1.18bd**	3.47±0.35ab	0.40±0.89c**	0.62±0.28ab
5		1.14±0.68c**	0.94±0.02a	0.41±0.33b**	1.86±0.28de**	3.42±0.90ab	1.20±1.64bc	0.70±0.27bc
6		1.21±0.72c**	0.93±0.07a	0.40±0.34b*	1.86±0.38de**	2.21±0.27de**	0.00±0.00c**	0.83±0.18bc
7		1.59±0.30c*	0.78±0.10a	0.27±0.11ab	1.61±0.36def**	2.44±0.0.27cde**	2.96±0.06a	0.86±0.11bc
8		2.44±0.17a	0.88±0.08a	0.12±0.03a	4.13±0.50c	2.79±0.54bcd*	2.97±0.06a	0.64±0.13ab
9		2.35±0.31a	0.89±0.07a	0.13±0.06a	3.49±0.60ac	3.40±0.20ab	2.34±1.31ab	0.32±0.10a*
10		1.58±0.57c*	0.86±0.06a	0.28±0.16ab	2.05±0.69de**	3.70±0.55a	0.60±1.34c*	0.52±0.38ab
11		1.32±0.61c**	0.85±0.13a	0.36±0.22ab*	1.55±0.75ef**	3.45±0.39ab	1.20±1.64bc	0.60±0.39ab
12		0.44±0.44d**	0.30±0.38b**	0.76±0.25c**	0.92±0.28f**	2.04±0.94e**	0.00±0.00c**	1.00±0.00c*
Plot	F	9.626	7.828	4.758	15.612	5.504	7.543	2.475
	P	0.000	0.000	0.000	0.000	0.000	0.000	0.017
Clay	F	4.197	0.396	3.104	2.795	0.157	1.662	0.526
	P	0.006	0.811	0.025	0.039	0.959	0.177	0.717

viduals; predators / omnivores accounted for 28.46%; plant-parasites were less abundant (just 19.09%). More specifically, plots 6, 7, 8 and 12 were dominated by bacterivores; plot 3 was associated with plant-parasites; plots 1, 2, 4, 5, 10 and 11 had more predators / omnivores (the percentage is the largest in the community). Plot 9 stands out as the only one dominated by fungivores.

Ecological indices of the soil nematode community

The *H'*, *J'*, *λ* and SR indices were calculated to characterize the diversity of the nematode communities around Lake Paiku.

According to the results of the Duncan test, the H' values of sample plots 1, 2, 3, 8 and 9 were significantly higher than those of other plots (p 4,7,10 < .05; p 5,6,11,12 < .01; $n = 5$). The SR value was generally consistent with that of *H'*. The values of plots 1, 2, 3, 8 and 9 (especially 3, 8 and 9) were significantly higher than those of the other plots (p 1,2 < .01; p 4,5,6,7,10,11,12 < .01; $n = 5$). The *J'* index for plot 12 was significantly lower than for the other plots ($p < .01$). The *λ* index for plots 5, 6, 11 and 12 was significantly higher than for the other plots (p 6,11 < .05; p 5,12 < .01).

The maturity index MI, plant-parasitic nematode index PPI, and nematode channel index NCR were calculated to describe the functional and structural characteristics of the soil nematode community. MI and PPI values of the 12 sample plots were 1.13–4.42 and 2.00–3.02 respectively. It should be noted that plant-parasites were absent from 40% (24 out of 60) of the soil samples. The PPI values of less than 2 (see Table 4) are the result of including PPI values of 0 (plant-parasites were absent).

According to the Duncan test results, the MI values of plots 6, 7, 8 and 12 were significantly lower than those of other plots (p 6,7,12 < .01, p 8 < .05). The PPI values of plots 4, 6, 10 and 12 were significantly lower than those of other samples (p 10 < .05, p 4,6,12 < .01). For the NCR values, only plot 9 was less than 0.5.

The *H'*, *λ* and SR values differed significantly for different soil layers. Notably, *H'* reached an extremely significant level ($p < .01$).

EI and SI give indications of the structure and function of the soil food web. Figure 2 shows the distribution of the 12 sample plots in the four quadrants. The order of plots along the EI axis is 12 > 8 > 11 > 9 > 4 > 1 > 2 > 5 > 3 > 6 > 10 > 7. The order of plots along the SI axis is 5 > 1 >10 > 4 > 9 > 11 > 2 > 3 > 8 > 7 > 6 > 12.

Relationship between soil nematode communities and soil properties

The RDA analysis results (see Figure 3 and Table 5) showed that the chemical properties of the soil were related to the soil nematode community. Seven environmental variables (soil pH, total N, available P, alkali-hydrolytic N, available K, organic matter, water content) accounted for 77.7% of the total data difference. The contributions to the variance of the first and second axes are 24.1% and 0.0% respectively. The correlation coefficients of the species-environment fac-

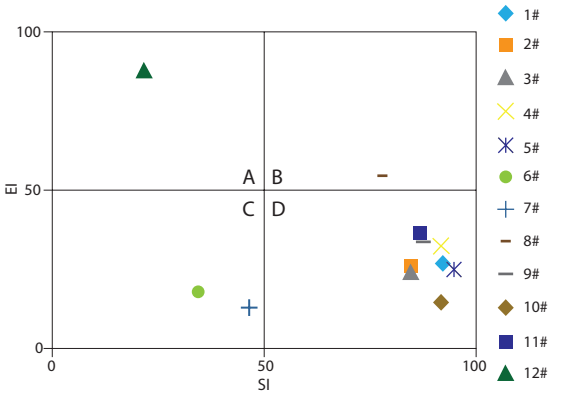

Figure 2 – Enrichment index (EI) and structure index (SI) of soil nematode community. The combination of EI and SI can be used to indicate the succession status of soil food web: A quadrant, high disturbance degree, good nutrient enrichment, organic matter degradation channel is dominated by bacteria, low C/N, food web is disturbed to A certain extent. B quadrant, low to medium disturbance, good nutrient enrichment, relatively balanced organic matter degradation channels, low C/N, mature food web. C quadrant, no disturbance, medium nutrient enrichment, fungal degradation channels, medium to high C/N, structured food web. D quadrant, the highest disturbance, poor nutrient enrichment, degradation channels mainly fungi, high C/N, food web degradation.

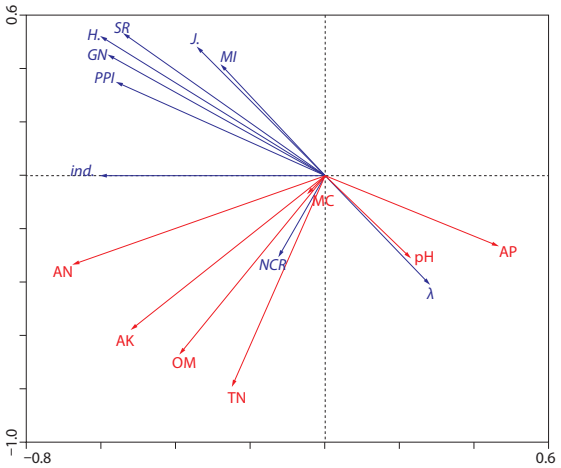

Figure 3 – Redundancy analysis (RDA) summary of the soil nematode community with soil properties. The blue lines represent ecological indicators; the red lines represent soil properties. The soil property and ecological indicators are as follows: MC: moisture content; TN: total nitrogen; AK: available potassium; AN: alkali-hydrolyzed nitrogen; OM: organic matter; AP: available phosphorus; GN: number of genera; ind.: nematode individual density.

Table 5 – Redundancy analysis (RDA) summary.

Ordination Summary	Axis 1	Axis 2	Axis 3
Eigenvalue	0.38	0.366	0.031
Species-environment correlation coefficient	0.616	0.606	0.672
Cumulative percentage variance of species data (%)	38.0	38.0	38.0

tor sequencing axis were 0.616 and 0.606 for the first and second axes respectively. The cumulative percentage of species-environment relationships was 100%, indicating that the species-environment correlation coefficient for the first ordination axis was high, and 100% of the total variance of species and environment was explained. The two-dimensional distribution figure (Figure 3) reflects well the relationship between the soil's nematode community and its physical and chemical properties.

Based on the RDA ranking results, soil-available P, pH, alkali-hydrolytic N and available K are key factors that have strong effects on the soil nematode community, whereas the total soil N, organic matter and water content have minor effects.

Various community characteristics correlate differently with soil properties. The density of nematodes (as opposed to the number of genera present) was more affected by the soil's physical and chemical properties. There was a strong correlation between nematode density and alkali-hydrolytic N content. Available P correlated negatively with several community characteristics. pH had a significant effect on α diversity of the nematode community. The redundancy analysis results (above) and the results of the Pearson correlation test (below) illustrate the consistency of the statistical results obtained by the two methods.

The Pearson results were as follows:
$r_{ins/AN} = 0.420^*, p = .021, N = 30$; [1]
$r_{GN/AP} = -0.401^*, p = .028$;
$r_{NCR/AK} = 0.394^*, p = .074$;
$r_{H'/AP} = -0.454^*, p = .012$;
$r_{J'/TN} = -0.529^{**}, p = .003$;
$r_{J'/AP} = -0.495^{**}, p = .005$;
$r_{SR/AP} = -0.458^*, p = .011$;
$r_{MI/AP} = -0.565^{**}, p = .001$;
$r_{PPI/pH} = -0.498^{**}, p = .005$.

Discussion

Structure of nematode communities

Our study in the Lake Paiku region recovered greater nematode diversity in comparison to studies carried out in the alpine meadows of the Northern Tibet Grasslands. For the years 2013, 2014 and 2015, at a similar altitude (4,596 m), we found 34, 42 and 39 genera respectively (Xue et al. 2017).

In a lower altitude zone in the eastern Qinghai-Tibet Plateau grasslands, Hu et al. (2016) found 42 gen-

[1] $r_{ins/AN}$ ... correlation coefficient between the individual number of nematodes and the amount of alkali-hydrolyzed nitrogen in the soil.

era. Furthermore, our figures exceeded the 31 genera reported by Vinciguerra (1988) from grasslands in the Alps, and the 33 genera reported by Gerber in Austria (Gerber 1991). With respect to nematode density, our study found a less abundant community (0–413 individuals per 100 g dry soil) in this region compared to other available studies: >500 individuals per 100 g^{-1} dry soil (Xue et al. 2017), and 1,033 individuals per 100 g dry soil (Hu et al. 2016).

In our study, the density of individuals and species diversity of the soil nematode community increased from the middle of the lake shore towards the south and north banks, which contrasted with the results of Zhao et al. (2019). According to RDA testing, total soil N, organic matter, available K and alkali-hydrolytic N contents were all at low levels, which would limit the numbers of nematodes and result in a low density. At the same time, the study showed that higher above-ground plant diversity may promote higher underground biodiversity (Zhang et al. 2006); lower density of nematodes may be related to the species composition and coverage of plant communities (see Table 1). Plants provide soil organic matter, and the distribution and quantity of roots affect the species diversity and total numbers of the soil nematode community through the presence of rhizosphere microorganisms and plant-parasite nematodes (Wardle et al. 2004).

Although the nematode density in plot 7 was the highest, its species diversity (genus number and the *H'*, SR, etc. indices) was significantly lower than for plots 1, 2, 3, 8 and 9. Genus Helicotylenchus was far more abundant in plot 7, accounting for 38.51% of the total nematodes and contributing to the high population density. This shows that the positive correlation between species diversity and individual density is not inevitable.

Nutritional structure of soil nematode communities

Our study reports a rare occurrence: only 2 of the 12 plots were dominated by plant-parasitic nematodes, and their percentage was relatively low (0–41%) in comparison to 69%–81% in the *Stipa grandis* steppe soil of Inner Mongolia (Ruan et al. 2007), 62%–66% in the Romanian steppe (Popovici et al. 2000), and 32%–42% in the alpine meadows of northern Tibet (Xue et al. 2013).

This might be related to sparse vegetation cover around the lake. The species present and number of plant-parasitic nematodes relate closely to plant biomass, including above-ground biomass and underground root biomass (Wardle et al. 2004).

Omnivores and predators are key trophic groups in determining the complexity of the soil food web (Polis et al. 1996). In the present study, half of the sample plots (plots 1, 2, 4, 5, 10 and 11) were dominated by these two trophic groups. As they are extremely sensitive to environmental disturbance, the prevalence of the omnivores and predators indicates that the region studied is in the stable later stage of succession, and the ecosystem has remained undisturbed. Soil environmental factors under the influence of plant communities, such as soil temperature and humidity, as well as pH, form and content of nutrient elements, organic matter content and soil type, explain the differences in nematode community composition between different sites, but no one of these factors can be said to be more important than the others (Zhan et al. 2019; Háněl 2017; Siemann et al. 1998).

Ecological function of soil nematode communities

MI and PPI values reflect the stability of the ecosystem and the degree of human disturbance. The higher the MI value and the higher the maturity of the ecosystem, the better the stability (Liu 2010); ecosystems are degraded by disturbance (Shao et al. 2007). The PPI value is positively correlated with the frequency of disturbance (Liu 2010). However, the MI values of plots 6, 7 and 12 in this investigation are lower, indicating that the stability of these three plots is lower than for other plots. The PPI value of plot 7 is the highest, indicating that this plot was most affected by disturbance.

Functional group-based EI indicates the outside-in nutrient inputs; SI indicates connectivity and the length of the food chains found within the soil food web (Ferris et al. 2001).

The results of the EI and SI showed that the soil nutrients were at a medium level without human disturbance, and the energy flow of the soil food web in most areas around the lake tended to be via fungus decomposition channels. The soil food webs were structured: the results of this study showed that most of the areas along the lake shore were more inclined to the fungal decomposition channel (the exceptions were plots 12 and 8, whose soil food webs were dominated by the bacteria decomposition channel); the food webs dominated by fungi channels, in comparison to bacterial decomposition channels, were more conducive to the preservation of soil nutrients.

Examples of degraded underground food webs also exist in the regions investigated. Plot 12 (the only plot in quadrant A) had the largest input of nutrients, but the connectivity was weak, the length of the food chain was very short, and environmental disturbance has led to serious degradation of the food chain. Plot 8 (in quadrant B) is similar. In plots 6 and 7, the nutrient input was lower, resulting in poor nutrient accumulation, and the high intensity of environmental disturbance resulted in significant degradation of the food web.

The NCR value also reflects the energy flow of the soil food web (Ingwersen et al. 2008). According to the NCR value, plot 9 was characterized by a fungal degradation channel, while the other sample plots all had bacterial degradation channels. This result is quite different from that indicated by the combination of

EI and SI, which use different calculation methods. The NCR value is calculated for all bacterial- and fungal-feeding nematodes combined, while EI and SI give different weights to different functional groups. They are therefore more sensitive to the energy flow of the soil food web.

Relationship between soil nematode community and soil properties

The RDA results showed the relationships between soil nematode communities and soil properties. Soil-available phosphorus (AP), pH and alkali solution nitrogen (AN) influence the soil nematode community significantly. An increase of the AN content and of the AP will increase the density of nematodes. In particular, increased AN caused an increase in the relative number of bacterivores (NCR increases), which was consistent with the conclusions of both EI and SI.

AP was negatively correlated with several community characteristics; the increase of AP would reduce the biodiversity and stability of the soil nematode community. Soil total nutrients, organic matter and water content were relatively unimportant, and Pearson correlation analysis also showed that there was no significant correlation between soil water content and any characteristic factors of the soil nematode community.

What deserves special attention is the AP, which has a significant negative correlation with some community characteristics, such as the number of genera, diversity index *H'*, richness index SR, and maturity index MI. Studies in other regions and under different environmental conditions also showed that the number of fauna species in soil and the density of individuals were significantly negatively correlated with soil P content (Li et al. 2017; Wang 2015).

However, each soil property factor (except water content) is at a poor or extremely poor level for fertility, so why does available phosphorus show a stronger correlation than other factors? This remains to be further studied.

Conclusion

Soil nematodes showed surface aggregation (mainly distributed in the 0–10 cm soil layer) for both individual density and biodiversity. The soil nematode community around Lake Paiku was rich in diversity but low in population density. The individual density of nematodes was more affected by the soil's physical and chemical properties than was the number of genera. Soil-available phosphorus, pH and alkali-hydrolytic nitrogen (AN) had significant effects on the soil nematode community. Total nutrients, organic matter and soil moisture content are less important. The soil AP content around Lake Paiku is at a low level (mean 2.67 mg / kg); low soil AP content is a limiting factor for plant growth, and affects nematode communities via plant biomass.

The soil food web in the Lake Paiku area was more complex, less disturbed by human activities, in the late stage of succession, and relatively stable. The results of the EI and SI based on functional groups showed that in most areas around the lake, the soil nutrients were at a medium level without human disturbance, the soil food web was structured, and the energy flow was dominated by the fungus energy channel. The energy flow of the soil food web given by the EI and SI is more sensitive and reliable than that of the NCR.

The individual density of soil nematodes was highest in the northeast and southeast corners of the lake; the genus numbers had the same distribution. The results of the diversity index *H'* support this distribution pattern.

Funding

This study was funded by the National Natural Science Foundation of China (No. 31660155) and the Plateau Ecological Project of the Collaborative Innovation Centre for Research and Development on Characteristic Tibetan Agricultural and Animal Husbandry Resources.

References

Bongers, T. 1988. *De Nematoden van Nederland*. Utrecht: Stichting Uitgeverij Koninklijke Nederlandse Natuurhistorische Vereniging.

Bongers, T. 1990. The maturity index: An ecological measure of environmental disturbance based on nematode species composition. *Oecologia* 83: 14–19.

Chen, P.J., Y.F. Gao, J. Wang, Q. Pu, C. Lhaba, H.J. Hu, J. Xu & K. Shi 2017. Status and conservation of the Endangered snow leopard *Panthera uncia* in Qomolangma National Nature Reserve, Tibet. *Oryx* 51(4): 590–593.

Chinese Academy of Sciences, the Tibetan plateau integrated research team 1983. Tibetan landscape. Beijing: *Science Press* 166-191: 224–229.

Cidanlunzhu 1997. Overview of Qomolangma National Nature Preserve. *China Tibetology* 21(1): 3–22.

Dai, Y.F., Y. Gao, G.Q. Zhang & Y. Xiang 2013. Water volume change of the Paiku Co in the southern Tibetan Plateau and its response to climate change in 2003–2011. *Journal of Glaciology and Geocryology* 35(3): 723–732.

Dekey Y.Z., D.M. Lhaba, Lhaba, K. Nima & T. Chen 2016. Lake area variation of Peiku Tao (lake) in 1975–2013 and its influential factors. *Journal of Lake Sciences* 28(6): 1338–1347.

Dunzhu, T. 2009. Mount Everest region suffered a significant climate warming. *Tibet Science and Technology* 1: 63–64.

Ferris, H., T. Bongers & R.G.M. de Goede 2001. A framework for soil food web diagnostics: extension of the nematode faunal analysis concept. *Applied Soil Ecology* 18(1): 13–29.

Gerber, K. 1991. Einige Nematoden aus Alpinen Böden in den Hohen Tauern (Österreich) [Some nematodes of alpine soils in the Hohen Tauern (Austria)]. *Linzer biologische Beiträge* 23(2): 661–700.

Háněl, L. 2017. Soil nematodes in alpine meadows of the Tatra National Park (Slovak Republic). *Helminthologia* 54(1): 48–67.

Hu, J., G.Y. He, J. Yan, H. Chen, X. Yin, L. Li & G. Du 2016. Effect of Grazing on Soil Nematode in Alpine Meadow on East Edge of the Tibetan Plateau and Its Mechanism. *Acta Pedologica Sinica* 53(6): 1506–1516. Doi: 10.11766/trxb201512190508

Immerzeel, W.W., F. Pellicciotti & M.F.P. Bierkens 2013. Rising river flows throughout the twenty-first century in two Himalayan glacierized watersheds. *National Geoscience* 6: 742–745. Doi: 10.1038/ngeo1896

Ingwersen, J., C. Poll, T. Streck & E. Kandeler 2008. Micro-scale modelling of carbon turnover driven by microbial succession at a biogeochemical interface. *Soil Biology and Biochemistry* 40(4): 864–878.

Lei, Y., K. Yang, B. Wang, Y.W. Sheng, B.W. Bird, G.Q. Zhang & L. Tian 2014. Response of inland lake dynamics over the Tibetan Plateau to climate change. *Climatic Change* 125(2): 281–290.

Li, J.J., L.X. Han, H.F. Cao, Y. Tian, B.-Y. Peng, B. Wang & H.-J. Hu 2013. The fauna and vertical distribution of birds in Mount Qomolangma National Nature Reserve. *Zoological Research* 34(6): 531–548.

Li, Y.F., J.X. Xu, Q.P. Sun, B.S. Liu, J. Li & J.J. Li 2017. Effects of biogas residue application on soil nematode community structure. *Journal of China Agricultural University* 22(8): 64–73.

Liu, Y.J. 2010. *Structure characteristics of soil nematodes in greenhouse*. Harbin.

Meteorological Bureau of the Tibet Climate Centre 2013. *Tibet's climate change monitoring bulletin.*

Ministry of Ecology and Environment, PRC 2018. *The area and scope of 10 national nature reserves including Liaoning Wuhua Ding*. Available at: http://www.Mee.Gov.cn/gkml/sthjbgw/sthjbh/201807/t20180730_447470.htm.

Nie, Y., L.S. Liu, Y.L. Zhang, M.J. Ding 2012. NDVI Change Analysis in the Mount Qomolangma (Everest) National Nature Preserve during 1982–2009. *Progress In Geography* 31(7): 895–903.

Nie, Y., Y.W. Sheng, Q. Liu, L. Liu, S. Liu, Y. Zhang & C. Song 2017. A regional-scale assessment of Himalayan glacial lake changes using satellite observations from 1990 to 2015. *Remote Sensing of Environment* 189: 1–13.

Olson, D.M. & E. Dinerstein 1998. The global 200: a representation approach to conserving the earth's most biologically valuable eco-regions. *Conservation Biology* 12(3): 502–515.

Oostenbrink, M. 1960. Estimating nematode populations by some selected methods. *Nematologica* 6: 85–102.

Pan, H.J., D.D. Yang, H.H. Qin, L. Zhang, K. Jiang & H.J. Hu 2013. Herpetofauna of Mount Qomolangma National Nature Reserve in Tibet, China. *Biodiversity Science* 21(5): 610–615. Doi: 10.3724/SP.J.1003.2013.06045

Polis, G.A. & D.R. Strong 1996. Food web complexity and community dynamics. *American Naturalist* 147: 813–846.

Popovici, I. & M. Ciobanu 2000. Diversity and distribution of nematode communities in grassland from Romania in relation to vegetation and soil characteristics. *Applied Soil Ecology* 14(1): 27–36.

Qian, Y.W., Z.J. Feng & L.L. Ma 1974. *Survey of birds and mammals fauna in the Everest region. Scientific investigation report of Mount Everest. Biology and mountain physiology 1966–1968*. Beijing.

Ruan, W.B., J.B. Wu, X. Zhang, et al. 2007. Soil nematode diversity in *Stipa grandis* community in the mid-east of Inner Mongolia. *Chinese Journal of Applied and Environmental Biology* 13(3): 333–337.

Shao, Y.H., S.L. Fu 2007. The diversity and functions of soil nematodes. *Biodiversity Science* 15(2): 116–123.

Shi, S.L, P.H. Peng, J.J. Li, W.D. Chen & Z.Y. Gao 2012. Study on the Pteridophyte Flora of Qomolangma National Nature Reserve. *Acta Botanica Boreali-Occidentalia Sinica* 32(7): 1459–1465.

Shi, S.L., J. Wang, J.J. Li, P.H. Peng & Z.Y. Gao 2012. Biodiversity of Orchidaceae of Qomolangma National Nature Reserve. *Acta Botanica Boreali-Occidentalia Sinica* 32(9): 1897–1902.

Sun, H.L., D. Zheng, T.D. Yao & Y.L. Zhang 2012. Protection and Construction of the National Ecological Security Shelter Zone on Tibetan Plateau. *Acta Geographica Sinica* 67(1): 3–12.

Siemann, E., D. Tilman & J.H.M. Haarstad 1998. Experimental tests of the dependence of arthropod diversity on plant diversity. *The American Naturalist* 152: 738–750.

Wang, S.J. 2015. *Study on ecological characteristics and function of soil faunal community in the Wuyi Mountains*. Shanghai Jiao Tong press (China): 58–62.

Wang, X.P., Y.D. Yao & Z.Y. Cong 2006. Polycyclic aromatic hydrocarbons content in soil and vegetation and elevation gradient distribution in Mount Everest region. *Chinese Science Bulletin* 51(21): 2517–2525.

Wang, Y., J.J. Li & Z.J. Han 2018. The dynamics of lakes in Mount Qomolangma Nature Reserve and their responses to regional climate change. *Journal of Glaciology and Geocryology* 40(2): 378–387.

Wardle, D.A., R.D. Bardgett, J.N. Klironomos, H. Setälä, W.H. van der Putten & D.H. Wall 2004. Ecological linkages between aboveground and belowground biota. *Science* 304(5677): 1629–1633. Doi: 10.1126/science.1094875

Wardle, D.A. & G.W. Yeates 1993. The dual importance of competition and predation as regulatory forces in terrestrial ecosystems: evidence from decomposer food-webs. *Oecologia* 93(2): 303–306.

Xie, H. 2005. *Taxonomy of plant nematodes*. 2nd ed. Beijing.

Xue, H.Y., F. Hu & D.Q. Luo 2013. Effects of alpine meadow plant communities on soil nematode functional structure in Northern Tibet, China. *Acta Ecologica Sinica* 33(5): 1482–1494.

Xue, H.Y, D.Q. Luo, H.Y. Wang & X. Qu 2017. Effects of Free Grazing or Enclosure on Soil Nematodes in Alpine Meadows in North Tibet, China. *Acta Pedologica Sinica* 54(2): 480–492.

Yeates, G.W. 1984. Variation in soil nematode diversity under pasture with soil and year. *Soil Biology Biochemistry* 16: 95–102.

Yeates, G.W., T. Bonges, R.G.M. de Goede, D.W. Freckman & S.S. Georgieva 1993. Feeding habits in soil nematode families and genera. An outline for soil ecologists. *Journal of Nematology* 25: 315–331.

Yin, W.Y. 1988. *Pictorial keys to soil animals of China*. Beijing.

Zhan, T.Y., G. Hou, M. Liu, J. Sun & S. Fu 2019. Different characteristics of vegetation and soil properties along degraded gradients of alpine grasslands in the Qinghai-Tibet Plateau. *Pratacultural Science* 36(4): 1010–1021.

Zhang, W., Y.L. Zhang & Z.F. Wang 2006. Analysis of vegetation change in Mt. Qomolangma Natural Reserve. *Progress in Geography* 25(3): 12–21.

Zhao, J.Y., X.L. Qu, H.Y. Xue & D.Q. Luo 2019. Research on plant community classification and species diversity of Peiku Tso in Tibet. *Acta Agrestia Sinica* 27(4): 969–976.

Authors

Huiying Xue – corresponding author

has a Doctorate in ecology, and is a Professor of environmental science. She is engaged in the teaching of environmental science and research into soil ecology at the College of Resources and the Environment, Tibet University of Agriculture and Animal Husbandry. E-mail: xhytibetan@xza.edu.cn

Da Qing Luo

is a Professor of ecology. He is engaged in particular in research into the ecology of forest communities on the Qinghai-Tibet Plateau. He works at the Institute of Tibet Plateau Ecology, Tibet Agriculture & Animal Husbandry University. E-mail: dqluo0894@163.com

Bu Duo

is a Professor of environmental Science. He is mainly engaged in environmental science research on the Qinghai-Tibet Plateau. He is based at the college of science, Tibet University.

Qing Xue

is an Associate Professor of nematology. His main research interests are plant nematology. He works at the College of Plant Protection, Key Laboratory of Integrated Management of Crop Diseases and Pests, Ministry of Education, Nanjing Agricultural University.

Xing Le Qu

has a PhD in ecology. His principal area is plant taxonomy, at the Institute of Tibet Plateau Ecology, Tibet Agriculture & Animal Husbandry University.

Wen Wen Guo

holds a Master's in ecology. He works at the Tibet Agriculture & Animal Husbandry University, where his main research interest is ecological restoration.

eco.mont – Volume 14, Number 2, July 2022
ISSN 2073-106X print version – ISSN 2073-1558 online version: http://epub.oeaw.ac.at/eco.mont
https://dx.doi.org/10.1553/eco.mont-14-2s48

Long-term monitoring of high-elevation terrestrial and aquatic ecosystems in the Alps – a five-year synthesis

Christian Körner, Ulrike-Gabriele Berninger, Andreas Daim, Thomas Eberl, Fernando Fernández Mendoza, Leopold Füreder, Martin Grube, Elisabeth Hainzer, Roland Kaiser, Erwin Meyer, Christian Newesely, Georg Niedrist, Georg H. Niedrist, Jana S. Petermann, Julia Seeber, Ulrike Tappeiner & Stephen Wickham

Keywords: Alpine belt, arthropods, biodiversity, catchment, climate, conservation, lakes, LTER, microbes, plants, plankton, productivity, snow, soil and wildlife

Abstract

Whether and how alpine organismic communities respond to ongoing environmental changes is difficult to assess quantitatively, given their intrinsically slow responses, remote locations and limited data. Here we provide a synthesis of the first five years of a multidisciplinary, highly standardized, long-term monitoring programme of terrestrial and aquatic ecosystems in the Austrian Hohe Tauern National Park and companion sites in northern Italy and the central Swiss Alps. The programme aims at evidencing the ecological state and trends in largely late-successional, high-elevation ecosystems. We present the conceptual framework, the study design and first results. Replicated over five regions, different sites and a multitude of permanent plots, the abiotic (microclimate, physics and chemistry of soils and water bodies), biodiversity (plants, animals, microbes), and productivity data (alpine grassland, lakes, streams) provide a representative reference for future re-assessments. The wide spectrum of biological baseline data presented and their spatial and temporal variation also illustrate the degree of uncertainty associated with smaller-scale and short-term studies and the role of stochasticity in long-term biological monitoring.

Introduction

The alpine life zone above the climatic treeline often represents the last wilderness at continental scale, where organismic assemblages reflect the outcome of evolutionary selection and the requirements of the abiotic environment. Biological communities are nature's long-term answer to climatic and geochemical conditions; they also reflect natural biotic interactions (i. e. when there is no or hardly any human influence). If conditions change, the assemblages of organisms are expected to change as well. These changes are often slow, subtle and not obvious to an observer, unless long time series of standardized observations are available. Here we report on a broad, interdisciplinary, long-term monitoring programme of terrestrial and aquatic alpine biota in the Alps, with the intention of providing a reference point for future re-assessments. We present the conceptual framework and a summary of the initial years' findings for both terrestrial and associated aquatic ecosystems.

Long-term monitoring

It has long been noted that assessing environmental influences on biota requires long-term data series in analogy to meteorology, where day-to-day weather reveals climatic trends only once decades of standardized observations are available (for a high-elevation application of climatic trends in ecology, see e. g. Kittel et al. 2015). Standardization requires tools and procedures agreed upon initially by the research teams involved, as well as continuous recordings at a given location. These ideas stimulated the foundation of Long-Term Ecosystem Research (LTER) in North America in the 1980s, which was developed into an international platform in 1993 (iLTER), with European (eLTER) networks launched in 2003 (Mirtl et al. 2018). Pioneer long-term monitoring projects at high elevation are those for aquatic systems (Miller and McKnight 2015) and terrestrial systems (Williams et al. 2015) in the Niwot Ridge region in the Rocky Mountains. The international GLORIA programme (Global Observation Research Initiative in Alpine environments) is a successful worldwide initiative that monitors summit floras and is best exemplified by the work carried out to date in Europe (Pauli et al. 2007; Gottfried et al. 2012; Lamprecht et al. 2018).

Data collection of all LTER-related activities rests on the permanent plot concept (Bakker et al. 1996; Blonder et al. 2018). A permanent plot can be a defined piece of land, a lake, part of a river system, or a specific ocean area. Once such permanent plots have been established, long-term observations or experiments help understand long-term ecological responses. A famous example is the ongoing Rothamsted Park Grass experiment, which started in 1856 in the UK. Its immense archive of stored samples became a treasure for modern analytical procedures (Silvertown et al. 2006). Snow manipulation experiments have a long tradition in alpine settings (Williams et al. 1998; Walker et al. 1999; Mark et al. 2015). Decades of observation (up to 52 years) of both experimental (Wipf & Rixen 2010) and natural observations (Freppaz et al. 2012) are available for snowmelt gradients, for simulating effects of climatic warming (Hansen et al. 2006), and for monitoring grazing effects on alpine plant communities (Virtanen et al. 1997; Mayer & Erschbamer 2017).

Some observations can become *long-term* post-hoc, by using natural archives such as dendrochronology or sediment cores of lakes, which may permit reconstructing life conditions and biota over millennia (e.g. Lotter et al. 2006 for alpine chronologies). Another type of post-hoc *monitoring* is revisiting locations for which very old but credible observation data are available, although the critical issue here is identifying of the original location. Here, we present examples from mountains. By identifying the original plots, a grassland experiment in the Swiss Alps could be re-visited 60 years after its foundation, and the fingerprints of past fertilizer treatments could be identified half a century later (Hegg et al. 1992). Thanks to their obvious geographical identity, very high and precipitous mountain peaks offer a unique opportunity for re-assessing inventories of plant species a hundred years later, with clear evidence for a rise in the number of species over the 20th century (Pauli et al. 2001; Stöckli et al. 2011; Wipf et al. 2013). Inevitably, summit research is confined to exposed habitats, often dominated by raw substrates and pioneer species that spread well, and yield rapid responses to climatic warming (early *warning*). In late successional vegetation on mature soils, such responses will be slower and not so easy to identify, given the dominance of long-lived clonal plant species (Vittoz et al. 2009). Clonal plants do not depend on regular sexual reproduction, and their genets may become thousands of years old (Steinger et al. 1996; de Witte & Stöcklin 2010; de Witte et al 2012). However, their vigour and spreading, but also their mortality, depend on micro-environmental conditions.

So, why monitor? If we were to ask meteorologists, they would be perplexed by that question, because it seems obvious that society needs information about ongoing weather patterns, and only long time series of data will allow climatic trends and the magnitudes of extreme events to be revealed in a historical context. However, the justification seems less obvious when it comes to monitoring biotic communities. Some reasons to carry out biological long-term monitoring are incontrovertible (e.g. Franklin et al. 1990; Silvertown et al. 2010; Fischer et al. 2010): (1) Changes in organismic assemblages cannot be traced by our senses, because the changes are often too subtle or too slow (exceptions are the disappearance or arrival of large animals or obvious neobiota). Hence, monitoring the state of such assemblages will allow the visualization of changes for both science and society. (2) If monitoring includes potential drivers of change, we may be able to explain the changes. (3) Such changes can have conservation implications (e.g. the local disappearance of rare species). (4) If associated with specific drivers of global change, such changes allow the identification of nature's responses, and thus provide information on the long-term consequences of the environmental changes (e.g. the response of Chironomids to palaeotemperature, Ilyashuk et al. 2011). (5) Stochastic phenomena, such as extreme drought (Craine et al. 2012), freezing or extreme snow-cover scenarios, all of which potentially exert lasting effects, are not adequately captured by long-term means or single site visits. (6) When documented in a protected area, evidencing such changes helps the respective protecting agency to estimate conservation implications.

Why monitor mountain ecosystems?

In addition to the general motives listed above, others relate to mountains more specifically. At low elevation, almost all land has undergone some anthropogenic transformation, most dramatically in the temperate and subtropical zones, making it hard to distinguish between consequences of ever-changing land use and changing atmospheric conditions. This applies even more to aquatic systems, which are typically very dynamic. Remote mountainous regions are exceptional, often hosting the last remaining wilderness areas in a wider subcontinental or even continental range. Representing c. 12% of the terrestrial surface outside Antarctica (Körner et al. 2011), mountains also host a disproportionate fraction of global biodiversity, because they stretch across contrasting climates over short geographical distances. At low latitude, the elevational stratification of mountain biota can include humid tropical forests and glacial forelands, all closely tied to the elevation-specific temperature regime. Roughly a third of all terrestrial protected areas are associated with mountains (Körner & Ohsawa 2005).

Within sufficiently high mountains, the alpine belt is defined as the land above the climatic treeline; it covers c. 2.6% of the global land surface outside Antarctica. Its plant species richness was estimated to be as high as 4% of the global total (Körner 1995) – almost double what is expected by area only, in particular when one takes into account that much of the area consists of bare rock and ice. In mountainous countries such as Austria and Switzerland, the alpine land area may reach 20% of the total land area, with even higher species richness. The high biodiversity in what is commonly considered a harsh environment reflects the diversity of microhabitats across short distances (Körner 2004, 2021). Above the climatic treeline, life conditions are defined by topography and plant stature, rather than elevation (Körner & Hiltbrunner 2021). The mean temperature of the growing season across such alpine (or arctic) mosaics of thermal habitats was found to differ by more than 8 K over a few tens of metres (Scherrer & Körner 2009). In addition to exposure and topographic shelter, plant stature is key, because a dense, low plant canopy traps solar heat, with plant and topsoil temperatures often approaching those found 1,000 to 2,000 m lower. In other words, above the treeline, the actual life conditions for terrestrial biota can be substantially warmer than assumed from measured air temperature; they cannot therefore be deduced from weather service data, but must be measured in situ. These strongly varying life conditions at very small spatial scales result in alpine biota

in general being rather robust against climatic change (Körner & Hiltbrunner 2021). However, if one captures the micro-scale transitions from one microhabitat to the next, these mosaics of alpine life also provide extremely sensitive indicators of change over short distances (Smith et al. 2012; Körner 2021).

Alpine aquatic systems may be substantially cooler than local air temperature during snow- or ice-melting and early in the growing season, but may warm up more and store heat during clear weather in summer, depending on wind and lake characteristics such as water depth, lake size and fetch, and discharge from and into streams. But, compared to terrestrial systems, aquatic systems are thermally far more buffered, and life conditions are often dominated by the nutrients provided by the surrounding terrestrial ecosystems and the lithography. As such, small alpine lakes and small rivers serve as signal integrators of the terrestrial conditions in the catchments from which they drain (Füreder 2010; Williams et al. 2011). Because of their integrating role, such aquatic systems, streams in particular, also have the potential for up-stream genetic diversity to be assessed using novel molecular tools (e.g. Deiner et al. 2016).

Because of the often cm-scale differences of life conditions, the terrestrial alpine world provides unrivalled opportunities to study effects of temperature on life in what might be seen as *experiments by nature*. The current distribution patterns of terrestrial alpine species in a varied topography reflect long-term selective pressures, with ranges and range limits of species across microclimatic gradients reflecting these conditions. Over very short distances, soils bear a location-specific *memory* of millennia of topography-biota interactions. In contrast, biota of aquatic systems are likely to track year-to-year variations in water quality and weather. The planktonic basis of the food web can change within a few days, or benthic biofilms in stream habitats may change in weeks, whereas the annual biomass production is buffered to some degree in terrestrial systems by the large below-ground biomass and reserves. In both systems, multi-year data are required in order to achieve an acceptable signal-to-noise ratio and elaborate a reference database that is not biased by stochasticity (see the stochasticity section). The initial phase of such long-term monitoring must be continued until robust means are established. A time span that will cover the range of year-to-year signal variation will be somewhere between 5 and 10 years, as a minimum. Thereafter, a longer interval between monitoring periods may be appropriate, with any later reassessment again requiring multiple years of continuous monitoring. The change in species' range limits, of clonal plant species in particular, may yield trustworthy evidence only over census intervals of several years. Yet, even 21 years of monitoring of plant communities in contrasting habitat types on Niwot Ridge, in the Rocky Mountains, revealed considerable non-directional scatter, causing the authors to urge for fine-scale observations along defined environmental gradients (as explored here for that reason) in order to cope with the intrinsic heterogeneity of alpine vegetation (Spasojevic et al. 2013).

What should be monitored?

In an ecosystem approach, a number of abiotic and biotic conditions and parameters need to be monitored for several reasons. First, it is not *a priori* clear how responsive different organisms are; second, a mechanistic explanation needs to build on cause-and-effect relationships; and third, no monitoring should be conducted that does not meet basic scientific standards, which means collecting information beyond its mere documentary value, in order to advance the theory of ecosystem functioning. Various environmental drivers may exert interactive effects. For instance, snow cover, lake ice and the dynamics of both may interact with atmospheric nitrogen deposition or the nutrient cycle in general (Baron & Cambell 1997; Williams et al. 1998). Species identity may matter for entire-community responses. Hence, knowing traits of organisms and the functions of these traits can guide towards understanding and explaining whole-system responses (see e.g. Matteodo et al. 2013).

The environmental parameters and organismic groups to be included in long-term monitoring are likely to exert different responses at different time scales. Soil physics, soil chemistry and certain aquatic parameters (pH, bedrock chemistry) can be characterized by a single initial assessment and are unlikely to change over decades. Plant species' ranges or abundance may vary significantly over 5 to 10 years only (Spasojevic et al. 2013; Mayer & Erschbamer 2017); aquatic and terrestrial productivity and associated biogeochemical cycles (nutrients, carbon) will differ from year to year. The species composition of soil arthropods and soil microbiota may be rather stable, but the relative abundance of certain taxa may vary over very short periods. Influences other than weather data need to be recorded, such as wild or domestic ungulate presence. In addition, the actual micro-environmental conditions need to be recorded at sub-diurnal (e.g. hourly) resolution, because it is the frequency distribution of these conditions rather than their long-term mean that matters for life (e.g. temperature in the most active soil layer or water in aquatic systems, presence / absence of snow cover or ice on water etc.).

Because the spatial variation can be so large, replication at regional and larger scales is required to arrive at a representative picture, even when similar types of ecosystems are selected. At each site, replicated permanent plots are required, best aligned with a series of typical and well-documented local life conditions (e.g. topographic snowmelt gradient). Combining subject-specific temporal and spatial replication can cause such monitoring to become logistically overwhelming. Deciding on a certain sampling / observation design and census frequency, one has to take into account the

long-term nature of the proposed monitoring. What might seem feasible to accomplish in one or two years could be beyond the realms of what can be done over multiple years in a consistent manner.

Stochasticity and disturbance

There are periods or entire years with exceptional conditions. Embedded in a continuous series of observations, such events can help to test theory, but they are unsuitable as a reference point for long-term monitoring. This is a problem with re-visitations of sites dominated by short-lived pioneer plant species, where the stochasticity of weather conditions can affect both the historical reference records and the new data, making it hard to identify trends. Perennial flowering plants from later-succession habitats that are likely to persist over a couple of years under varying weather conditions would be more robust in this respect. Further, it is hard to account for shifts in species-specific range limits, because species that have arrived at a new location may still be operating far from their outer limits (niche boundary), and may have moved in over large distances (Körner 2011) during once-in-a-century climatic events. In contrast to re-visitations, long-term monitoring reveals fine-grain temporal responses, permitting a separation of long-term trends from noise (year-to-year variation). Continuous monitoring will thus cover and evidence short-term variability that must not be confused with long-term trends (Walker et al. 1994; Körner 2018a; Dai et al. 2019).

One of the biggest problems of ecosystem monitoring is natural and anthropogenic disturbances. Major natural disturbances are erosion, rock fall, flooding, avalanches, fire, dust storms or rodent invasions, and major anthropogenic disturbances are related to pastoralism, tourism, hydroelectric installations, road, hiking trail, powerline, cable car construction, or the introduction of fish into remote lakes (Körner & Ohsawa 2005; Körner 2014). The natural hazards can be minimized by careful site selection. Further, publicly protected areas provide a certain safeguard against anthropogenic disturbance that private land ownership cannot guarantee. National parks offer the highest level of protection. In addition, they are designed to be institutionally stable over the long term. They therefore offer the greatest likelihood that observations will be repeatable in a century's time, making them the preferred hosts for long-term monitoring. Research institutions, but also other public institutions, are inherently unstable, depending on political *weather conditions*, changes in personnel and shifts in interest. However, national parks need external research partners who agree on and document a high degree of standardization in their approaches, so that a change in research staff does not put the long-term task of monitoring at risk of inconsistency.

The current monitoring programme

The programme was initiated and is coordinated by the Austrian Hohe Tauern National Park (NPHT; see also Körner 2014; Körner et al. 2020). It uses sites in three regions of the NPHT (Innergschlöss, IN; Seebachtal, SE; Untersulzbachtal, UN), and terrestrial partner sites in Northern Italy (South Tyrol; Oberettes, OB) and Switzerland (Furka pass, FU). The programme is carried out by researchers associated with the universities in Graz, Innsbruck, Salzburg and Vienna, and a private lab in Salzburg. The partners for South Tyrol are from Eurac research, Bozen; those for Switzerland are from the University of Basel (Table 1, Figure 1).

This coordinated long-term monitoring programme aims at producing a baseline for future reassessments of the state of typical alpine ecosystems in the central Alps at 260 to 400 m above the regional mean elevation of the current climatic treeline (Table 1). The programme started in 2016, with the first data becoming available in 2017. Our aim is to provide a summary of the abiotic site conditions as a reference for future thematic publications. Further, we will synthesize the evidence that is currently available in the biotic inventory (and the methods employed) for these sites, including plant species diversity and productivity, soil meso-fauna, soil microbiome, lake zooplankton diversity, and benthic fauna of streams in micro-catchments. Documentation of the initial monitoring phase has been produced by the NPHT and is available online (Körner et al. 2020; in German).

In what follows, we will explain the design of the programme, which aims to optimize spatial and temporal replication, cover key organismic groups and habitat types, and discuss feasibility (methods, logistics, personnel).

Methods: study design, sites and techniques employed

Five test sites were selected on siliceous bedrock only, in the regions listed in Table 1. The sites cover different weather regimes ranging from more frontal NW weather (Salzburg), more southern or mixed weather regimes (Carinthia, Swiss site), and more continental inner Alps weather (East Tyrol, South Tyrol). In East and South Tyrol, the weather combines with the climatic *mass elevation effect*. The programme as a whole thus covers a great deal of variation along the main divide of the Alps, over a geographical distance of 360 km, at roughly 47° N, in a cool temperate climate that is under the pronounced influence of the Gulf Stream (for its latitude, Europe has a comparatively warm climate). The terrestrial site in Salzburg (UN) belongs to a wilderness region that was never under human land use; the sites in Carinthia (SE), East Tyrol (IN) and the Swiss Furka pass (FU) show marginal land use (episodic sheep, minor tourism); the site in South Tyrol (OB) is not only by far the highest, but

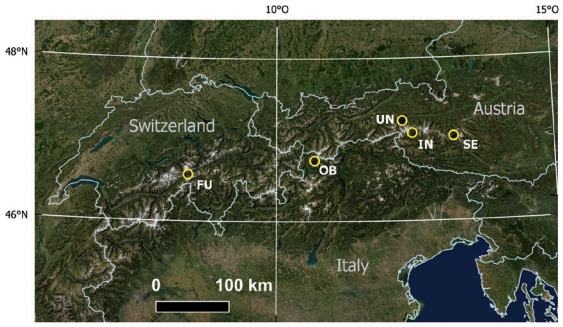

Figure 1 – Location of the long-term monitoring sites in the Alps. Yellow circles: Terrestrial site locations: IN = Innergschlöss, SE = Seebachtal, UN = Untersulzbachtal, FU = Furka pass, OB = Oberettes). Basemap source: Esri, Maxar, GeoEye, Earthstar Geographics, CNES/Airbus DS, USDA, USGS, AeroGRID, IGN, and the GIS User Community

also the only site under heavy, traditional grazing pressure from sheep.

The terrestrial data originate from five regions (three in NPHT, plus OB and FU), specifically from monitoring sites in the alpine grassland belt dominated by *Carex curvula* and *Nardus stricta*. In each of the five terrestrial test sites, a transect approach is employed (Körner 2018b) (see below for explanation). The aquatic data are based on six small alpine lakes for each of the three NPHT regions within 8 km of IN, UN and SE (total of 18 lakes), and streams discharging from each of these three terrestrial sites. Since no lakes exist at UN itself, the 6 lakes for that region were chosen from the adjacent Obersulzbachtal.

Terrestrial sites

As mentioned earlier, environmental gradients that are tied to topographic features represent a sort of long-term experiment by nature itself, because topography does not change over time scales that are relevant for monitoring purposes. The biota associated with such gradients can be assumed to reflect long-term selective pressure – that is, nature's response to the life conditions along the gradients. Among the ecologically most powerful gradients are snowmelt gradients, which impose similar yearly spatial melting patterns on biota (related to topography) but with variable timing (Friedel 1961; Körner 2018b, 2021). Along a snowpack gradient, microhabitats vary from those least affected by snow at exposed edges or ridges (longest growing season) to the most affected microhabitats (snowbeds) which are released from snow only late in the season (shortest growing season). For the terrestrial part of the current monitoring programme, we selected 3–6 gradients per site, the gradients ranging from the locally highest to the locally lowest in terms of plant biomass production over a distance of 7–10 m. We address these season-length gradients as transects and in what follows will frequently refer to H (top), M (middle) and L (bottom) sections along the transects (Figure 2).

Each of the transects is composed of three adjacent, 1-m wide strips that go from the bottom to the top of the snowmelt gradient. The central strip is reserved for non-destructive assessments; the other two are used for sampling biological material in a way that prevents resampling the same location for the next 6 to 8 years (Figure 3). Strips are divided into a grid of 1 m² quadrats (*plots*), each subdivided into 4 smaller quadrats of 50 cm x 50 cm (*subplots*), the identity of which is recorded during each sampling. Transects are georeferenced, marked with pegs and permanent metal geo-reference points at either end. Since alpine terrain is never homogeneous, a list of criteria was developed for subplots to be included or excluded from sampling. For instance, bare ground, stones or rock, isolated massive tussocks, and areas that are bare because of the activity of mice are excluded (see Figure 3). In total, the terrestrial teams are surveying 22 transects, each with 18–27 permanent quadrats (depending on transect length), yielding a total of c. 500 permanent quadrats (1 m grid cells) and c. 2000 subplots (0.5 m x 0.5 m), two thirds of which are available for invasive sampling. While sampling is strictly confined to individual permanent plots, the plots were assembled post-hoc into the three

Table 1 – Terrestrial site locations and their macro-climate. Treeline elevation is presented as a bioclimatological reference. On-site seasonal mean air temperatures are calculated for two slightly differing summer periods for a total of three years (2017–2019) and show that the atmospheric conditions are very similar across the sites. Aquatic sites are located within a few km (alpine lakes) or <0.5 km (riverine sites) of the terrestrial sites. NPHT = Hohe Tauern National Park.*

Location name (code)	Region (country)	Geographical coordinates	Site elev. (m)	Mean treeline elev. (m)	Maximal treeline elev. (m)	Seasonal mean T (°C) 16/6–15/9	Seasonal mean T (°C) 1/7–30/9
Innergschlöss (IN)	East-Tyrol (A), NPHT	47°06′40.1″N, 12°25′35.5″E	2,350	2,020	2,070	8.65	8.01
Seebachtal (SE)	Carinthia (A), NPHT	47°02′21.9″N, 13°10′58.1″E	2,303	2,040	2,160	8.15	7.84
Untersulzbachtal (UN)	Salzburg (A), NPHT	47°09′58.2″N, 12°19′51.1″E	2,380	1,980	2,050	8.19	7.72
Furka pass (FU)	Switzerland (CH)	46°34′40″N, 08°25′12″E	2,467	2,080	2,150	8.26	7.52
Oberettes (OB)	South-Tyrol (I)	46°45′59.9″N, 10°42′38.2″E	2,700	2,320	2,360	8.38	7.59

** These google-earth-based elevations are provided for an estimated mean elevation (repeatedly recorded treeline position within 5 km of the site), while maxima refer to the position of the uppermost groups of trees >2 m in height in the same region in the early 21st century.*

sections: bottom (least productive, L), middle (M), and top (most productive, H). Although high in number, and although grid positions resemble a random initial selection along the climatic gradient, repeated sampling of these permanent plots and subplots cannot be randomized. The reason is that each year certain additional *blind areas* are defined by the previous year's sampling. Hence sampling-locations require a plan that will ensure that the entire subplot provides enough space for new sampling to take place until traces of past sampling have faded (this takes a few years in alpine grasslands such as those in our study areas). Each subplot is potentially suitable for 4 plant biomass harvests on a 20 cm x 20 cm sampling area, yielding theoretically c. 5,000 locations for an annual plant biomass harvest of 132 samples (6 samples for each of the 22 transects). The variable alpine topography did not allow wider or longer transects without including terrain that does not match our definition of a consistent L-M-H snowmelt gradient (Körner 2018b).

Aquatic sites

The lakes team chose 18 small natural lakes. The maximum depths of the lakes vary from 1 to 42 m (with most in the 5–10 m range); the areas of the lakes range between 0.03 and 15 ha (with most measuring around 1 ha). Measurements and samples were taken from the entire depth profile in a stratified manner. In the larger lakes, a small inflatable boat was used. Except for the few periglacial lakes, each lake is surrounded along at least half of its shoreline by alpine vegetation. It was expected that these lakes would continue to exist for many years. They were chosen for being as close to the terrestrial sites as possible and at different alpine elevations within each valley. Logistical constraints also played a role in site selection (e.g. location within hiking distance from a road or hut). In three of the 18 lakes, we noticed fish (Seebachsee, Löbbensee and its adjacent lake); all other lakes are currently fish-free, to the best of our knowledge.

For each terrestrial site, the stream team selected a small stream that drained from adjacent land (< 200 m away). The stream at SE dried up almost completely under summer heat-wave conditions (2018, 2019). All abiotic conditions were assessed upstream and downstream of a reference location within 100 m of the source at IN, UN and SE. Streams are < 2 m wide, have a sandy or rocky bed, and are surrounded by closed-cover alpine vegetation; none of the streams originates directly from a retreating glacier or permanent snowfield.

Sampling concept: what, how often, for how long?

For the *terrestrial* systems, it was decided to monitor snow dynamics and the temperature of the topsoil, and to cover different organismic groups that typically occur across snowmelt gradients: assemblages of flowering plants and their biomass production, soil

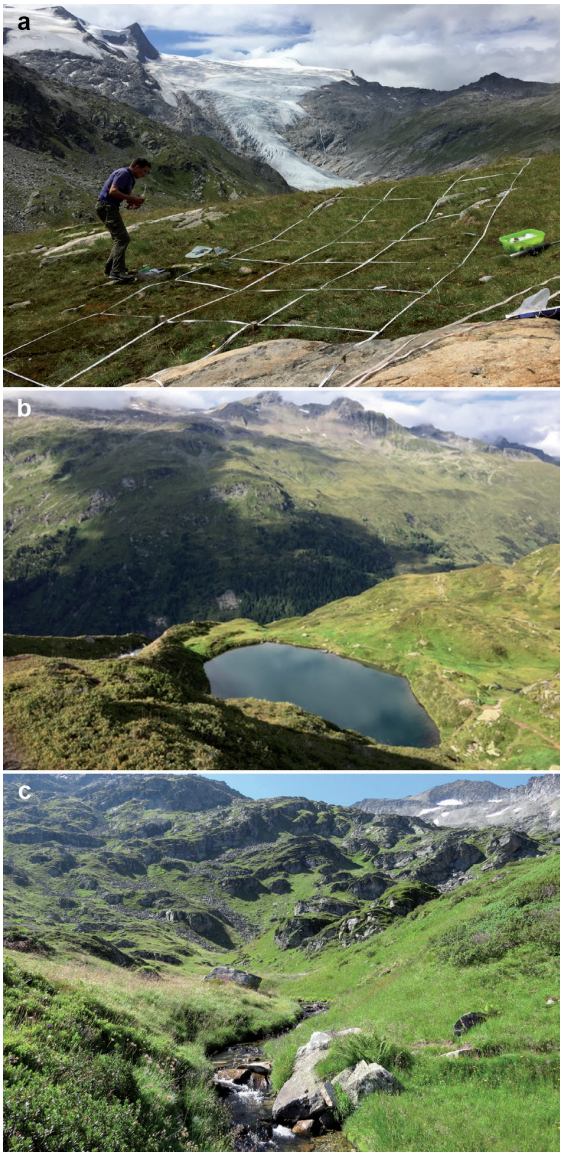

Figure 2 – Examples of study sites. a) Terrestrial snowmelt gradients with a grid of permanent plots in Innergschlöss (IN) with the 3,700 m Venediger massif in the background); b) example of an alpine lake (Salzbodensee, IN); c) micro-catchment with a stream explored in East Tyrol (IN). © C. Körner

mesofauna, and soil microbiome (bacteria and fungi). A detailed physical and chemical characterization of soils across the transects is an obvious starting point.

In the *aquatic systems* monitored, the lake team assessed the water's chemical characteristics and temperature (including ice dynamics), phytoplankton biomass (via chlorophyll-a estimated from *in situ* algal fluorescence), as well as zooplankton abundance and species richness. The stream team monitored water chemistry, pH, water temperature, flow rate, biofilms and benthic invertebrate communities.

Different abiotic and biotic parameters require different sampling and observation intervals. Among the abiotic conditions, most aspects of soil physics (density, porosity, grain-size spectra, water-holding capacity) require only a single initial assessment, because such

Figure 3 – Fieldwork at the terrestrial and aquatic sites. a) 20 cm × 20 cm plot after peak season biomass harvest; b) measurement of reference air temperature (here at Untersulzbachtal); c) soil coring for physical soil data, microbiome and soil-mesofauna; d automatic monitoring of large herbivores; e) digital imaging device; f) sampling at an alpine stream (Innergschlöss); g) filtering scraped and washed biofilm; h) plankton sampling at defined depth at Seebachtal. © a–d) C. Körner, e) R. Kaiser, f–g) G.H. Niedrist, h) E. Hainzer

characteristics are not going to change. This also holds for basic chemical characteristics of soil such as buffer capacity, pH, concentration of soil organic matter, and total and available cations and anions. Cations and anions may require re-assessments after a few decades. In contrast, temperature and snow or ice cover require records at a resolution of 1–3 h for as long as other observations are continued. Such data need to account for microclimatology (upper soil-layer temperature across the snowmelt gradient *versus* air temperature on terrestrial sites, water depth in lakes, in situ records in streams).

Some of the biological assessments are comparatively simple (harvesting above-ground plant biomass, collecting lake or stream water), while others are extremely laborious (e. g. identifying and counting collembola and mites in soil samples). The data reported in this paper also reflect such pragmatic criteria. The presence of organismic groups and species (or operational taxonomic units [OTUs], in the case of microbes) is unlikely to change over a couple of years (plants, for instance, are sessile). However, individual abundance or biomass of entire communities or certain taxa (or OTUs) may change rapidly (from year to year, for instance, depending on the weather). This means that inventory data (presence / absence) need to be collected repeatedly over longer periods. Annual data are required for the abundance of key organismic groups, plant biomass, lake plankton and stream biota.

For how long? As in meteorology, data have to be collected continuously over a long enough period, so that short-term variability (or *noise*) is recorded with sufficient detail while permitting longer-term trends to be distilled (this is when *weather* becomes *climate* in meteorology). Since it is not clear *a-priori* how large the intrinsic variability is, one of the results of the initial period of long-term monitoring is to identify variance with at least 95% confidence. For some of the biological indicators, we can provide initial guidance for year-to-year variance, and we recommend that variance assessments are repeated so that the duration of the initial phase can be planned. Earlier attempts to assess time series of grassland productivity in the Rocky Mountains and on the Tibetan plateau (Walker et al. 1994; Dai et al. 2019) suggest a minimum duration of 7–10 years for the initial recording phase.

For the synthesis we present here, the specific methods applied by the various teams will be presented as succinctly as possible, together with the first findings. A detailed description of the methods used will be provided in the individual thematic publications to come, and can be found in the online manual of methods (Ecosystem Monitoring Team 2021).

Results

Abiotic conditions

Macro-climate

Using waterproof, single-channel data loggers in standard radiation screens, we obtained year-round air temperature data, illustrating that we were successful in selecting locations that were thermally fairly similar (Table 1). Data gathered over three years revealed that, for the period 15 June to 15 September, which covers most of the growing season at the top

of each transect (position H), the air temperature differed by only 0.4 K across the five sites (0.5 K for July to September). Hence the differences in site elevation account for regional climate in such a way that the mean air temperatures during the growing season are almost identical. The warmest month is commonly July. At FU, for example, the mean air temperature in July varied from 6.6°C (2014) to 11.0°C (2015), and the July mean over 8 years (2013–2020) was 8.9°C. From precipitation data recorded at regional weather stations, all five sites can be characterized as humid, receiving > 1,000 mm precipitation annually: the on-site annual mean for FU is 1,140 mm for 2013–2020, with a range of 1,020–1,280 (of which 240–500 mm fell from June-August); for OB we estimated precipitation from data collected at the nearby village of Match at 2,000 m asl using a 30 mm / 100 m rise as elevation lapse rate, arriving at a mean of 1,080 mm at 2,750 m asl (the driest of all sites).

All sites may experience moderate drought during midsummer, which may cause small streams to dry up, as was shown for SE in 2018 (see abiotic conditions in streams). Although snow may fall on any day during the year, snowmelt outside snowbeds commonly occurs in mid-June (see microclimate), with substantial year-to-year variations and local variations between early May and mid-July. The season ends with vegetation browning in mid- to late September, resulting in a growing season of 8–12 weeks (shorter in snowbeds).

Terrestrial microclimate

For 25 to 75 days from snowmelt (variable date) until 31 August, and for day-time hours (09–18h) only, the mean temperature 3 cm below the soil surface was 3–5 K warmer than the air temperature at 2 m (Figure 4). A depth of 3 cm was chosen because this is roughly where apical shoots, basal leaf meristems of the dominant graminoids, rhizomes, and peak microbial activity are found.

Remarkably, there are no significant differences in temperature between the bottom (L) and top (H) of the transects, indicating that the differentiation in life conditions reflected so obviously in vegetation composition and seasonal productivity (see biological results below) largely rests on the length of the season. Season length ranges from 49 to 122 days across sites, years and positions along transects. Averaged across years and sites, the length of the growing season is roughly 3 months at H, and 20 days shorter, on average, at L (Table 2).

These mean temperature differences between topsoil and air correspond to a difference in air temperature over a change in elevation of c. 700 m (applying a mean atmospheric temperature lapse rate of 0.55 K per 100 m). Importantly, these means include all types of weather conditions. The main driver of topsoil (and bottom canopy) warming is solar radiation (Figure 4) modulated by wind speed. On bright days, the topsoil-air difference exceeds 10 K, reflecting a substantial decoupling of microclimate and macroclimate. If we compare temperatures for H and L positions for such bright days only, we still do not see a thermal differentiation during daylight hours. However, soils cool faster (become more similar to air temperature) at L during the night, presumably as a result of the lower plant cover at L, and thus greater radiative and convective heat loss.

Water temperature was recorded every 6 hours at a depth of c. 40 cm using two data loggers installed in each lake. The mean temperature of the ice-free period across all lakes was 8.8°C, which was surprisingly similar to the seasonal mean air temperature (Ta-

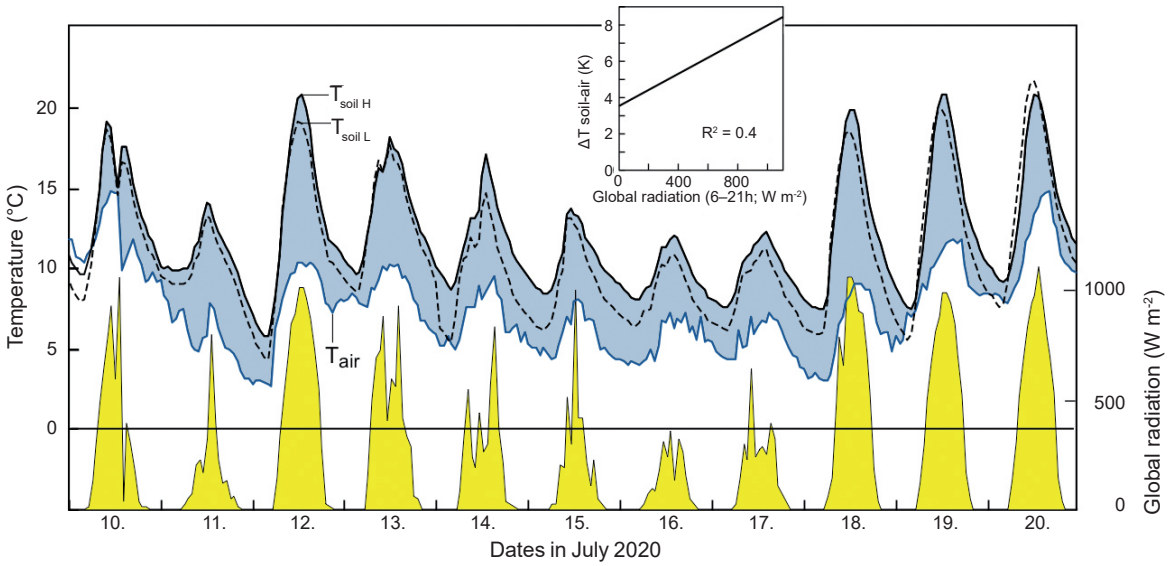

Figure 4 – A comparison of topsoil and air temperature at positions bottom (L) and top (H) across the five snowmelt gradients at Furka pass (FU) during a typical summer period, including both clear sky (12, 18–20 July) and overcast conditions (16, 17 July). Note the effect of solar radiation (regressed for H during daytime; inset diagram). L and H differed little, but a little more at night under cloudy skies, when soils lose less of the stored heat by radiative cooling at H, presumably because of higher plant cover.

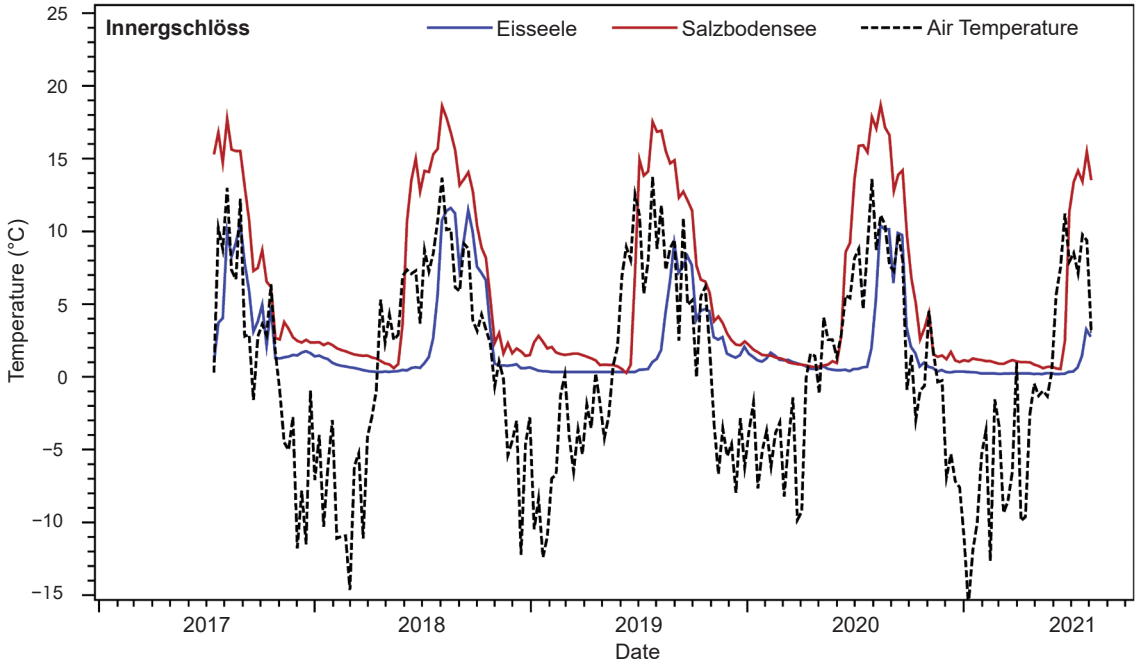

Figure 5 – Air (2 m) and water temperatures (at 40 cm depth) in two lakes in Innergschlöss (IN): Eisseele (2,550 m) and Salzbodensee (2,138 m; horizontal distance 2.2 km). 6-hourly data for the lakes, and 6 h means for air temperature at 2,350 m (IN, Table 1), with lines smoothed by loess fits. Note the sharp rise of lake temperature at melt-out.

ble 1). However, the ice-free period and temperatures varied substantially among and within lakes. For instance, we recorded seasonal means of 5.4°C in Sulzsee (Obersulzbachtal valley, next to UN) *vs.* 12.5°C in Salzbodensee (IN), which can be partly explained by differences in lake size, elevation and exposure. Lake Eisseele has a much shorter ice-free period (the ice-out occurs almost two months later than on Sulzsee and Salzbodensee), and also has a much cooler mean temperature during the ice-free period (8°C) than Salzbodensee from the same region (Figure 5). As would be expected, water temperature differences in winter are small, irrespective of elevation; in this respect, lakes are similar to terrestrial ecosystems under snow. The lakes investigated were all well oxygenated (68–81% saturation, averaged over all measured depths) and nutrient-poor, with nitrate levels of 0.2–1.1 mg NO_3-N L^{-1} (P data are not yet available). The highest nutrient levels were found in the hypolimnion of stratified lakes, particularly those with a deep chlorophyll maximum (DCM) in this zone. The pH range in the lakes was narrow (pH 6.7–8.2, again averaged over depth).

Table 2 – Effective season length (days) across sites (a year effect) and across years (b site effect) for the L (bottom) vs H (top) positions at Seebachtal (SE), Untersulzbachtal (UN), Innergschlöss (IN), Oberettes (OB) and Furka pass (FU). Means for 5 years (4 at UN and OB). The season is counted from day of snow melt to 15 September, when communities are commonly senesced.

a)	2017	2018	2019	2020	2021
H	106	109	81	102	84
L	92	89	67	83	68
H-L	14	20	14	19	16

b)	SE	UN	IN	OB	FU
H	104	106	90	104	82
L	101	92	62	84	65
H-L	3*	14	28	20	17

** SE turned out to show minor H-L gradients, with snow drift caused by wind dominating over topographical effects.*

Abiotic conditions in streams

Stream temperatures ranged between 0 and 1.9°C in winter, warming to mean summer temperatures (July, August and September) of between 4.6°C (UN) and 7.8°C (IN) – that is, they were mostly cooler than the concurrent mean air temperatures (Table 1, Figure 6). Higher temperatures were recorded in SE, which are related to very low discharge and dry periods (see gaps in Figure 6). Based on longer time series (2010–2017) of water temperatures from multiple rivers (18) in the NPHT (Niedrist & Füreder 2021), the summers of 2017 and 2018 can be rated as exceptionally warm.

The streams differ in the concentration of transported plant nutrients. The highest mean nitrogen levels (NH_4-N and NO_3-N) were recorded in SE, with 155 ±50 µg L^{-1} (2019–2021, n=12), followed by UN (89 ±19 µg L^{-1}, n=8), and IN with 36 ±7 µg L^{-1} (n=16). Phosphorus concentration was also highest in SE (2.2 ±1.0 µg L^{-1}) and lower in the other streams (1.8 ±1.0 µg L^{-1} in IN and 1.6 ±0.8 µg L^{-1} in UN). Compared to the other sites, IN exported the highest concentrations of dissolved organic carbon (776

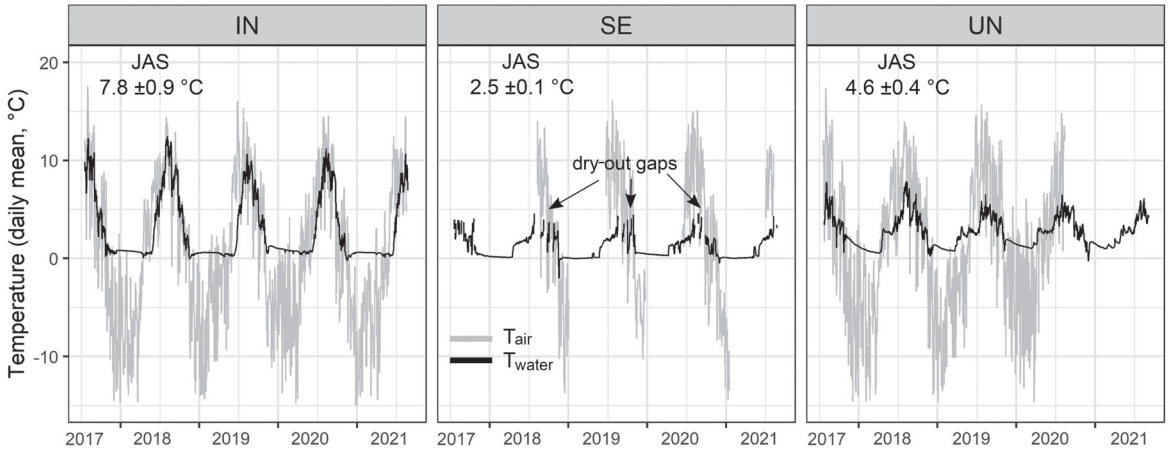

Figure 6 – Daily means of water temperature (based on hourly measurements) in the three study streams (IN = Innergschlöss, SE = Seebachtal, UN = Untersulzbachtal) from July 2017 to July 2021. Mean water temperatures for summer (JAS: July, August, September) ±SD are given for each plot (the data from SE has multiple gaps during summer, when the stream became almost dry).

±230 µg L^{-1}), caused by the well-developed peat bog areas in the catchment. As expected for non-glacial streams, concentration of suspended solids was moderate (highest in UN with 3.9 ±2.3, and lowest in IN with 1.2 ±1.1 mg d.m. L^{-1}) and linked to slope and discharge of the streams.

Soils

Our attempts to avoid as far as possible any confounding variations in soil properties among the sites and transects were successful: for KCl extracts, we arrived at very similar soil pH (3.8) across sites, with very little variation (3.4 the single lowest value in a peat layer at SE). There is one exception to this pattern: of the five transects at FU, one showed a pH of 5 and 6 at positions M and L, due to an unexpected, small pocket of carbonate-rich glacier deposits. The overall low pH reflects both the acidic bedrock and the high soil organic matter (SOM), across transect means, for topsoil 8–13% dry matter (d.m.) (FU, UN and IN); 23–25% (OB and SE). Soils contain on average c. 8% and 4% d.m. soil organic carbon (SOC) at depths of 0–5 and 5–10 cm respectively, with a consistent topsoil (0–5 cm) C / N ratio of around 15 across sites (at 5–10 cm; values are consistently lower, at around 12). With a mean soil density of 1 g cm^{-3}, the soil pore volume is substantial (c. 50% vol.: c. 60% top 5 cm, c. 40% 5–10 cm). With a mean plant wilting point reached at 15% vol. soil water content, a maximum of c. 35% of the soil water content is available to plants in the top 10 cm (35 mm over a 10 cm soil profile). Assuming a typical mean daily evapotranspiration of 3 mm under bright weather conditions, these reserves would last for 12 days only. Hence rooted profiles must be substantially deeper (as they commonly are) to cope with longer dry periods, as during the 2018 heatwave. Given the well-known decline in SOM along snowmelt gradients (from 20 to 10% d.m. from H to L in FU, IN, UN), local summer drought effects are more likely to impact L-biota. The gradients are reversed at OB, where there is an accumulation of fines at L as a result of up-slope trampling by sheep (erosion). At SE the mineral soil fraction is very low in some plots at L, with peat (43% SOM) overlaying bare rock.

As an indication of the rate at which nitrogen cycles through soils, we obtained ^{15}N / ^{14}N soil signals (expressed as $\delta^{15}N$). The most abundant N isotope, ^{14}N, is metabolically more active, and thus mineralized more quickly from plant debris, causing the rare, heavier and metabolically discriminated ^{15}N to accumulate in the SOM pool. The more ^{15}N accumulates, the older the recalictrant N-pool in the soil. We found very similar $\delta^{15}N$ signals across all sites, and no difference along snowmelt gradients in topsoil SOM ($\delta^{15}N$ of 3.4, 3.7 and 3.2‰ for H, M and L across all sites; $\delta^{15}N$ is 2–5, mostly 3, across H, M, L sites, with s.d. between 0.5 and 1‰). The accumulation of ^{15}N almost doubles in 5–10 cm soil depth, and thus N is older ($\delta^{15}N$ 5.8, 6.4, 5.7‰ for H, M, L across sites; again, the differences are not statistically significant). This indicates that the smaller annual biomass production at L compared to H is in balance with smaller annual recycling, and thus arrives at similar $\delta^{15}N$, with longer residence times of ^{15}N in deeper layers (Yang et al. 2015). For a summary of the physical conditions in the top 5 cm of soil, see Seeber et al. (2021).

As one moves from H to L, soil nutrients (liquid extraction by BaCl for cations) change little when expressed per unit of sieved-soil dry matter (soluble forms of Ca, Na, Mg, K, Fe, Al). There is a small but not significant trend for lower concentrations at L. The only exception, and with surprising consistency, is the decline of Mn^{++} from H to L in the most-active top 5 cm of the profile (not at a depth of 5–10 cm, where extractable concentrations were less than one tenth of those at 0–5 cm). However, the absolute concentrations of Mn^{++} extracted by the BaCl solution vary substantially among sites, reaching 4–6 mmol kg^{-1} at FU and < 0.4 mmol kg^{-1} at IN. We have no explanation for these trends in Mn^{++}, nor is it clear whether

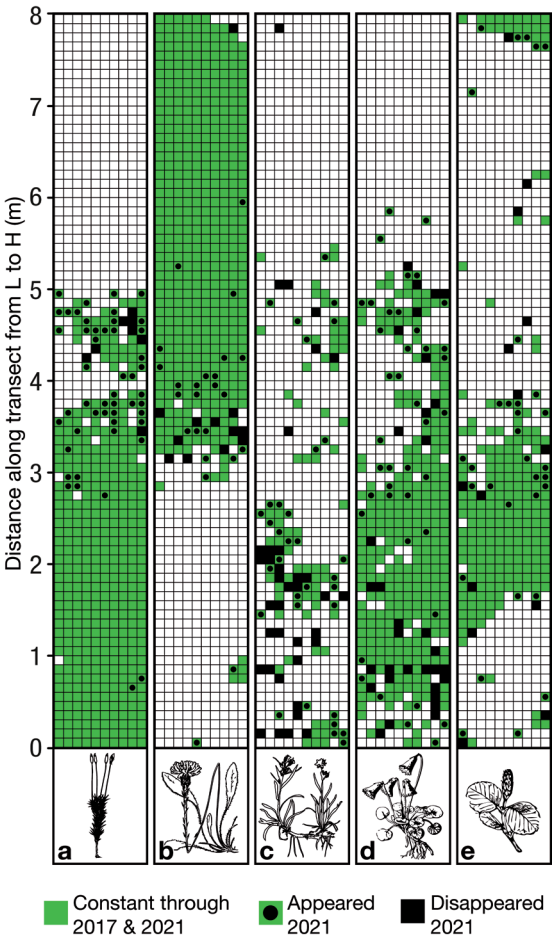

Figure 7 – Examples of species distributions along the bottom (L) to top (H) snowmelt gradients as captured by digital image analysis (H at the top). Note the sharp range limits for a) Polytrichum sexangulare and b) Leontodon helveticus b, and the more diffuse or even bimodal patterns in others (c) Gnaphalium supinum, d) Soldanella pusilla, e) Salix herbacea). Data from transect 4 at site Innergschlöss (IN) for 2017 and 2021 with differences at the 10 cm x 10 cm grid level highlighted by different symbols. Note that turnover tends to be more intense near the range edge.

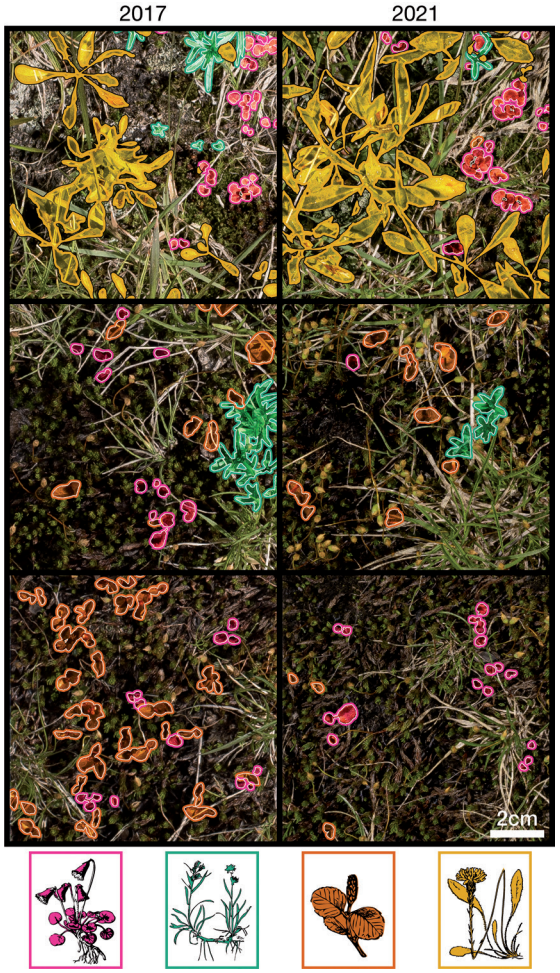

Figure 8 – Examples of 10 cm x 10 cm image pairs from transect 4 at site Innergschlöss (IN) from mid (M) to low (L) position: 4.9–4.8 m, 2.3–2.2 m, 1.2–1.1 m (lowest position = 0 m) for the years 2017 (31 July) and 2021 (11 August, a year with a late season start). Outlined shapes of four selected species as used in the training of machine learning algorithms (for species see Figure 7).

this is of ecological relevance. High concentrations of Mn^{++} are toxic to some species (even more so Fe^{++} and Al^{+++}, neither of which exhibits such a trend). As a reference for future research, we archived (in glass jars) 100–200 cm^3 of air-dried samples from the 2 mm soil fraction from all transects at the Tyrolian Landesmuseum Ferdinandeum, Innsbruck, Austria.

Biological results

Plant species diversity

Vegetation transects were monitored with a close-range image acquisition system that uses standardized illumination (exclusion of daylight). The images provide a resolution of ca. 0.1 mm that not only permits species identification but also facilitates automatic image analysis using machine learning and computer vision algorithms to classify, outline shapes, and count individual plants or plant organs. However, overlapping plant canopies constrain the analysis in dense communities. The strengths of the technique are its high precision, adjustable scale of analysis, reproducibility, and the absence of classical sources of error in fieldwork such as subjectivity, and varying degrees of attention and botanical expertise. In a year-by-year image comparison, individual plants, especially long-lived clonal species and tussock grasses, can literally be *watched growing*. By capturing numbers and sizes of individuals or ramets of clonal plants, population dynamics can be assessed. Since data are digitally archived, it will be possible to re-evaluate them in the future. Conventional photographs and ground-truth species lists are available for all 1 m^2 plots from OB and FU.

The distribution of indicator species reflects the H to L environmental gradient across the 14 transects

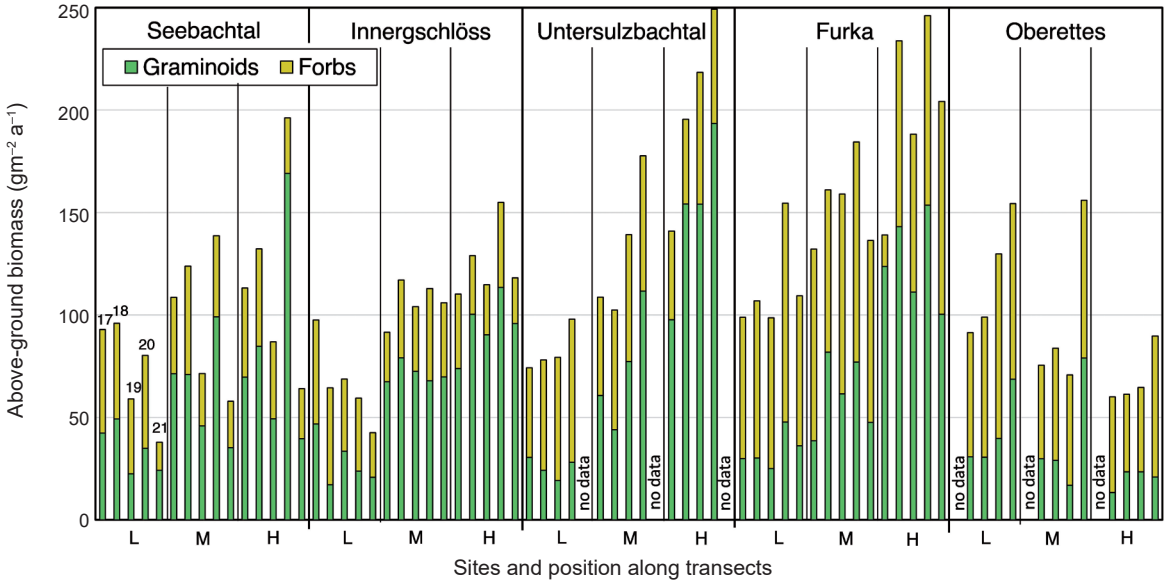

Figure 9 – Seasonal plant biomass production for five years and three positions along snowmelt gradients (L for bottom snowbed, M for middle, H for high, earliest melting; missing data: no site access to Untersulzbachtal in 2021 because road closed by mudslides, and a late start in Oberettes). Means for 3–6 transects per site, separated into graminoids (grasses, sedges and rushes) and forbs. Note that the H-to-L difference comes largely from graminoids, pointing to these as potential indicator species for climate warming.

monitored (Figure 7). A future lengthening of the growing season in a warmer climate would cause a decline in snowbed species and favour grassland species. Moss communities, which are currently important in L, may also lose ground. Our survey so far has encountered 85 species of flowering plants. We have also obtained data for the dominant (i. e. most abundant) moss species (*Polytrichum sexangulare*) and two lichen species that have very high indicator power (*Solorina crocea*) or wide distribution (*Cetraria islandica*) across all sites (*S. crocea* is not found in OB). Of the flowering plant species, 19 were found in all 5 sites; 13 occur in the Hohe Tauern region only (SE, IN, UN). In total, 45 species occurred at one site only (of these, 22 alone at FU, and 10 at OB). Species lists from these sites indicate that the most abundant taxa typically found in either H or L co-occur at all 5 sites: *Helictotrichon versicolor* [=*Avenula versicolor*], *Leontodon helveticus* [=*Scorconeroides helvetica*] in H; *Gnaphalium supinum, Leucanthemopsis alpina*, and *P. sexangulare* in L. The current data suggest that *G. supinum, P. sexangulare, Salix herbacea, Soldanella pusilla,* and *H. versicolor* are the most promising species for identifying climatic warming effects, because these taxa show clear position preferences along the transects and are widely distributed. We also identified a few species with a known preference for warmer locations that are promising candidates for future range expansion (*Anthoxanthum alpinum, L. helveticus,* and *Geum montanum*). Our comparison of the 2017 and the 2021 data in the Hohe Tauern (Figure 8) reveals a down-slope (H to L) shift for *L. helveticus,* signs of grass encroachment in L, and reduced abundance (number of ramets) of *G. supinum* and *S. pusilla* in L. Based on 50 random samples, a pairwise comparison for transect 4 in IN results in mean differences in cover: –25 cm^{-2} (–29% change), –23 cm^{-2} (–33%), –26 cm^{-2} (–29%), and +145 cm^{-2} (+119%) for *Soldanella, Gnaphalium, Salix and Leontodon,* respectively, between the 2017 and 2021 surveys (Figure 8). However, it will require a longer time series to distinguish any such trend from stochastic events and the effects of micro-environmental heterogeneity.

Plant biomass production

Harvested at peak season, live (green), annual, above-ground biomass production varied between 40 and 250 g m^{-2} across all sites, transect positions and years (Figure 9). The date of harvest, commonly around mid-August, was chosen depending on the year-specific snowmelt regime and the phenology, so that communities at H had not yet entered seasonal senescence (leaf browning), while the communities released from snow latest at L had just reached their seasonal peak. We found end of flowering / onset of fruiting (stalk elongation stage) in the typical snowbed species *Gnaphalium supinum* to be the most suitable pheno-marker at L for the compromise in sampling date (repeated site visits were logistically impossible in all sites except FU). Attached dead parts (necromass) and litter were discarded. Bryophytes (mainly tiny *Polytrichum* sp.), fruticose lichens (commonly very small amounts) and earlier years' woody stems (again tiny fractions) were also dismissed, because they cannot be attributed to a given year's productivity. Biomass was sorted into dicots (herbs) and monocots (graminoids).

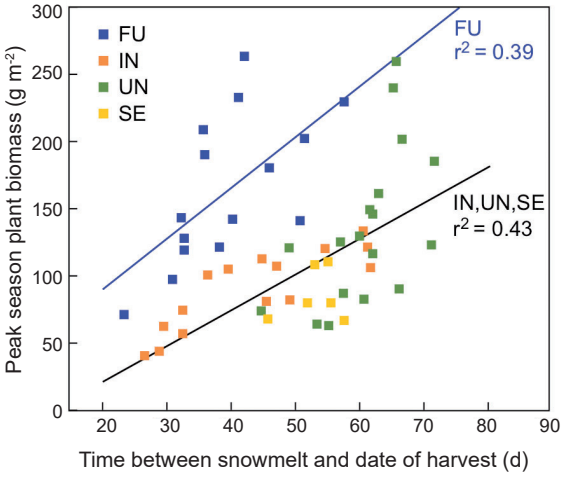

Figure 10 – Mean seasonal peak biomass for 5 years plotted against the 5-year mean of the time between snowmelt and harvest. Given the obvious difference between Furka pass (FU) and the three sites in the Hohe Tauern National Park, we show two regressions. The variance reflects a combination of (a) the 5-year period not yet capturing the long-term mean season length to which communities are adapted, (b) the spatial variation of biomass at the scale of the 20 cm x 20 cm harvest plots.

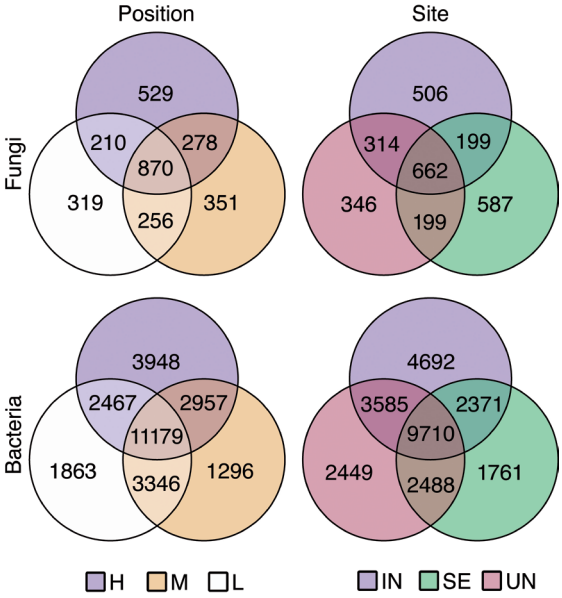

Figure 11 – Operational taxonomic units (OTUs) of the fungal and bacterial communities in top soil separated by site (Innergschlöss, Seebachtal, Untersulzbachtal) and by position (H=top, M=middle, L=low) with the overlaps illustrating commonness. The total number of fungal OTUs is 2,813 and that of bacteria 27,056.

High-intensity traditional grazing at our highest site, at OB, reversed the soil conditions (best in depressions, worst at the top), causing the biomass production to reverse as well, despite caging the harvest plots in the year of harvest. The effect of the soil quality was therefore greater than the effect of the shorter season at L. With means of 100 g m^{-2} at L and 60 g m^{-2} at H, this was also the least productive site, despite the similar growing season temperatures. At all other sites, productivity showed a significant decline from H (mean 160 g m^{-2}; range 120 at SE to around 200 g m^{-2} at UN and FU) to c. 80 g m^{-2} at L, across sites and years (range 70 at SE and IN to 110 g m^{-2} at FU). Year-to-year variation was substantial, and in part also reflected the 20 cm x 20 cm plots that happened to be harvested in a given year at a given site, illustrating the importance of site replication for arriving at a typical mean annual pattern. Across sites and transect positions, productivity rose from 2017 to 2021, with the highest biomass for H at all four sites occurring in 2020 (up to 250 g m^{-2} at UN and FU). This trend was less pronounced at L and even reversed at SE and IN. Productivity rose in the sequence SE, IN, UN, FU, which seems to be unrelated to temperature or snowmelt regimes but rather to reflect the greater soil depth at UN and particularly at FU, with thinner soils overlying glacial cuttings at SE and IN. Overall, annual biomass production correlates with the mean L-M-H-related duration of the growing season across sites (Figure 10).

In a linear multivariant statistical model, year (n=5), site (n=5), and position on transect (n=3; L, M, H) for 22 transects explain 47% of the variance. Excluding OB because of the intense pressure caused by traditional grazing, and transect 2 at site SE which turned out to have neither a snowmelt nor a soil or vegetation gradient, the model explains 56% of the variance, with site (21%) and L-M-H position on transect (29%) showing the largest influences, each with high statistical significance. Year explains only 6% of the variance, because a single year's weather conditions exert little influence on cover in these perennial systems. Much of the above-ground spring growth is produced from *stored growth*, using reserves mobilized from the large below-ground biomass fraction (> 80% of total). This is also why we averaged the time to peak biomass in Figure 10. As the regression in Figure 9 illustrates, the 3 sites in the NPHT (SE, IN, UN) form a cluster distinct from the Swiss site (FU). As mentioned above, the most likely reason for this is deeper soil profiles at FU (the soil chemistry itself does not hold an obvious answer). The remaining unexplained variance is largely associated with the patchiness of biomass at the 20 cm x 20 cm sampling scale.

Soil mesofauna

Vertically stratified samples collected using a split-core sampler were used to evaluate the abundance and diversity of soil microarthropods (mainly collembolans and oribatid mites). These small invertebrates (body size < 2 mm) are abundant and important members of high-alpine soil animal communities and are well adapted to life in cold environments. They can also use the intra-nivean space for moving during snow cover (Hågvar 2010) and prolong their life cycles to compensate for the shorter growing season (e.g. Søvik et al. 2003). Due to these adaptions, micro-scale

distribution and community composition of snowbed microarthropods might be affected above-average by climate warming.

Most individuals (> 95%) were obtained from the litter layer and the upper 5 cm of the soil profile via heat extraction in a Macfadyen high-gradient apparatus. Across all sites and transects, 25 species of collembola and 49 species of oribatid mites were found (see Seeber et al. 2021). Transects at FU harboured the highest mean number of microarthropod individuals (c. 15,660 individuals m^{-2}); SE exhibited the highest species diversity (17 collembolan and 25 oribatid mite species). Most individuals belonged to a few widespread species which occurred in at least three out of the five sites. Consequently, community composition, which was driven mainly by soil organic matter content and soil porosity, showed little variation across the study sites. Mean snowpack duration between bottom and top of the transect generally differed by 1-3 weeks, causing drastic changes in vegetation. However, unlike in other studies (e.g. Green & Slatyer 2019), our currently available data do not reveal any significant effect of snowpack duration on the abundance and species numbers of soil microarthropods. To what extent potential differences in individual longevity contribute to the small abundance gradient from H to L remains unresolved.

Soil microbiome

Culture-independent, high-throughput genome sequencing of soil samples from the terrestrial transects yielded a total of 27,056 bacterial and 2,813 fungal OTUs (note the order of magnitude difference). We observed a general decrease in OTU richness towards the nutritionally poorer, lowest parts of the gradients. Among bacteria, taxa known for their preference for drier habitats dominated the top (H), and taxa affiliated with moister conditions dominated near the bottom (L). Among fungal taxa, such trends were not as pronounced, but first data show a stronger presence of Basidiomycota in snowbeds (L), including ectomycorrhizal and saprobic taxa, while at L, microfungi are more abundant, including AM mycorrhizae. There is a remarkable site and position specificity of OTU communities (Figure 11). For comparison, 10,406 bacterial and 6,291 fungal taxa were recorded across 10 summit sites of the GLORIA programme by Adamczyk et al. (2019). In their study (on much less developed soils), bacterial diversity was positively correlated with increasing (less acidic) soil pH, but negatively with increasing elevation, whereas fungal α-diversity remained more or less the same. Yao et al. (2013) mapped fungal diversity in the rhizosphere of the ectomycorrhizal plant species *Bistorta (syn. Polygonum) vivipara* along ridge-to-snowbed gradients in alpine Norway, and found taxonomic differentiation between ridges (with Sebacinales-relaed OTUs) and snowbeds (harbouring specific *Tomentella* and *Cortinarius* OTUs).

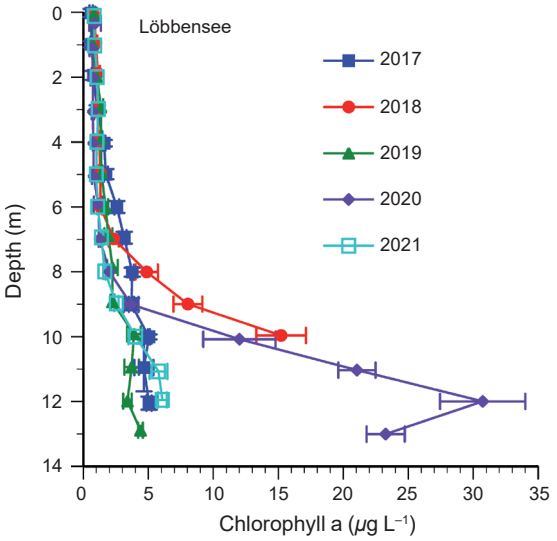

Figure 12 – The 5-year variation in vertical chlorophyll-a concentration exemplified by lake Löbbensee (2,226 m, region Innergschlöss). Note the high chlorophyll maxima very deep in the profile in 2018 and 2020 only.

In addition to the influences of topography, microbial abundance patterns are also affected by seasonality. Lazzaro et al. (2015) found a clearly reduced bacterial abundance in winter (as measured by detected gene copy numbers) and a rise after snowmelt to a summer maximum. In contrast, there was much less seasonality in fungal OTUs, with a trend towards higher abundances in winter. Broadbent et al. (2021) found that bacterial and fungal lineages responded differently to experimental snow-removal in alpine grassland, which corresponds to our H position: among bacteria, Acidobacteria increased and Actinobacteria decreased after snow-removal; among fungi, Geminibasidiales increased and Pleosporales decreased. Shifts included functional ones (assessed by quantifying corresponding genes). Notably, microbial genes associated with N-cycling increased significantly in summer. It is therefore important *when* in the course of a year standardized samples are obtained in long-term monitoring. The timing of snowmelt triggers the composition, abundance and activity of the soil microbiome, but unlike plant and animal activity, microbial activity remains high under snow, explaining why most of the annual net ecosystem production is recycled over winter (Scholz et al. 2017).

Lake biota

Like the abiotic parameters, the vertical chlorophyll-*a* profiles also differ from year to year (Figure 12), with some lakes exhibiting similar patterns, while some neighbouring lakes may differ substantially, underlining the importance of microclimate and replication. Covering a wide range of habitats is key to identifying regionally representative trends in the context of environmental change (e.g. nitrogen deposition; Elser et al. 2020). The monitoring of plankton (30 µm

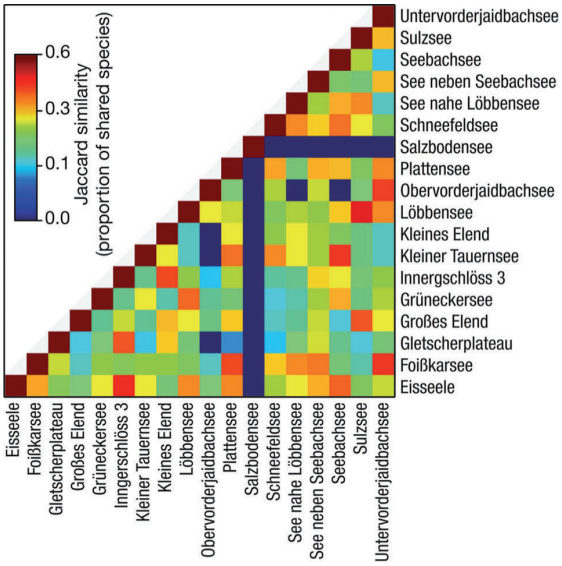

Figure 13 – Jaccard similarity between the zooplankton communities of the 18 sampled lakes. Data for four years (2017–2020). Warmer colours indicate greater similarity. The blue bar for Salzbodensee indicates that this lake has no taxa in common with any other lake (two unique and large omnivorous species).

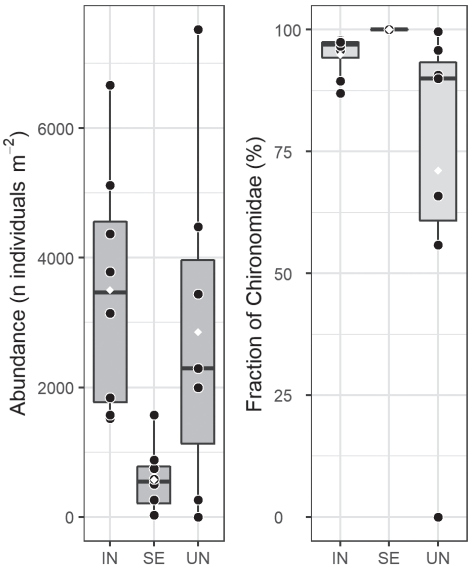

Figure 14 – Abundance of stream invertebrates and the fraction of Chironomidae (non-biting midges) in all samples per site from July 2017. Bold horizontal lines for median; white dots are means. Single dots (=individual samples) indicate the microhabitats along each stream. IN=Innergschlöss, SE=Seebachtal, UN=Untersulzbachtal.

plankton net samples for metazoan zooplankton and large ciliates, whole water samples for phytoplankton and smaller ciliates) has also revealed a wide variety of responses to environmental conditions. Zooplankton alpha diversity differs strongly among lakes (1–11 species per lake). The lakes have remarkably few species in common, and even neighbouring lakes may differ greatly – i. e. beta diversity in zooplankton is high (Figure 13). Only 3 species (two rotifers, *Keratella quadrata* and *Polyarthra dolichoptera*, and one ciliate, *Bursaridium* sp.) were found to be common to at least one third of all lakes. This result is supported by analysis of the total molecular diversity of the lakes (R. Ptacnik, unpublished results). These contrasts can only partly be explained by abiotic differences, but may result also from strong dispersal limitations (Allen et al. 2012) or other factors. Species composition in most lakes has remained stable over the last five years, with few lakes showing establishment of new species. Young lakes (≤ 30 years) that have emerged since the retreat of glaciers are probably still in a colonization phase, and can be expected to become more species-rich in the future (Cauvy-Fraunié & Dangles 2019). There is a positive relationship between phytoplankton and zooplankton biomass, but there are clearly more drivers of zooplankton biomass and diversity than simply primary production. In lakes with fish, for example, there is higher zooplankton diversity, particularly in rotifers, compared with fish-free lakes, where large crustacean zooplankton dominates. The lakes with the lowest zooplankton diversity tend to be young, cold and turbid, indicating that both colonization rates and hostile abiotic conditions contribute to driving zooplankton diversity. The picture we have after five years of data collection is one of unexpectedly high abiotic and biotic diversity among these small alpine lakes. It is still too early to formulate hypotheses for future trends. The data illustrate that the long-term monitoring of alpine lakes requires more than five years of initial data collection to overcome stochastic effects.

Life in streams

The biofilm biomass on stones averaged 0.135 ±0.02 mg cm^{-2} (2017–2018, n=90), with a maximum of 0.43 mg cm^{-2} at UN late in the season. However, seasonal changes were generally small (no increase during the growing period, in contrast to terrestrial plant biomass), except for low-water and dry conditions at SE in August, followed by a green algal bloom when the water flow decreased and then returned. Generally, biofilm biomass increased from upstream to downstream. Biofilms are largely composed of periphytic groups (cyanobacteria, diatoms and green algae) and other bacteria and fungi (these other bacteria and fungi are not studied here), with cyanobacteria contributing 49–55% of the cover in all three streams studied, followed by diatoms (18–42%) and green algae (5–16% only, predominantly after low-water conditions). Cyanobacteria profit from a stable environment and thus are barely present in glacier-fed streams, which benefit diatoms (Niedrist et al. 2018). As alpine streams warm, we expect an increase in cyanobacteria, especially in non-glacial streams (Niedrist & Füreder 2021; Lürling et al. 2018).

Benthic invertebrate abundance was highest during the early alpine summer (July), and declined by more

than 50% later in the season. In July, we recorded densities of 3,503 ±655 individuals m^{-2} at IN, 577 ±180 individuals m^{-2} at SE, and 2857 ±984 individuals m^{-2} at UN (Figure 14); the highest taxa richness was found at IN and UN (48 and 46, respectively; 12 at SE). The low taxa number at SE reflects periodic stream-drying, where only a selection of tolerant organisms can reproduce. As expected, the dipteran family Chironomidae dominates (commonly >80% of all individuals) at all sites (Figure 14), which also corresponds to observations in other rivers of the NPHT (e.g. Niedrist & Füreder 2021), and underlines the adaptation of this family to harsh living conditions (Füreder 1999).

Large herbivores

Since the terrestrial monitoring part of our research aims at identifying changes in plants and associated soil biota and ecosystem processes in response to environmental change (climate change, changes in atmospheric chemistry), it is important to identify all potentially confounding influences, including changes in the abundance and activity of herbivores. We monitored the presence of, and habitat use by, large herbivores and marmot using automatic wildlife camera traps with 10 s photo intervals over a distance of up to 200 m. The cameras were operated at IN, UN and SE each year, at FU (which revealed almost no wild animals) during one season only, and not at all at OB (because of the very intense and high sheep stocking). We documented (in descending frequency) *Rupicapra rupicapra* (chamois), *Marmota marmota* (alpine marmot), *Capreolus capreolus* (roe deer), *Capra ibex* (alpine ibex), *Cervus elaphus* (red deer), and *Ovis gmelini aries* (domestic sheep, at IN and FU). In our image analysis, we distinguished states of grazing, movement or resting, for July, August and September (daytime only). At IN, there are mainly sheep; at UN and SE, mainly chamois. The total land area covered by each camera was used to calculate the overall grazing time per m^2 weighted by the number of animals (Table 3). Animal presence was generally low at IN, UN, SE and FU, but varied substantially among study sites and years. The comparatively low incidence at SE is probably a consequence of the proximity of a popular hiking trail. The decline in presence at IN in 2019 is probably due to the reduction in the sheep-flock size (a yearly random effect). Animal presence may affect the composition of vegetation and ecosystem processes through grazing (e.g. Meier et al. 2017) or dung (e.g. Iravani et al. 2011; Williams & Haynes 1995); it may also affect the actual standing crop of plant biomass. Thus, where sheep are present traditionally (not at UN or SE; low frequency at IN and FU; very high stocking at OB), a given year's targeted micro-plot for plant biomass harvest had to be fenced (IN) or caged (FU, OB) in the early part of the season (i.e. until harvest).

Within an elevational transect from the climatic treeline up to (or slightly above) the permanent plots (SE 1900–2300 m; IN 2080–2350 m; UN 1730–2400 m), 10 regularly spaced cameras documented the general wildlife presence in open terrain in these test regions. Roe deer was documented up to 2,160 m only; chamois and marmot were documented everywhere, but in densities that increased rapidly with elevation. These animals are heat-sensitive and shift to higher (cooler) regions when it gets too warm (which is a likely scenario for the future, leading to habitat shrinkage).

Table 3 – Large herbivore presence at the study sites Innergschlöss (IN), Seebachtal (SE), Untersulzbachtal (UN) (data for the biomass sampling sites only, not for elevation transects) in the Hohe Tauern National Park region. Note: the generally low s m^{-2} mean grazing-time values for the total land area covered by the camera may result from local hotspots of use in otherwise hardly impacted terrain (presence in hours was calculated as presence time × number of animals for a 14.8 h mean of total daylight monitoring time).

Study site	Weighted sum of presence (h)*				Grazing time (s m^{-2})			
	2017	2018	2019	2020	2017	2018	2019	2020
IN	304	306	51	73	0.79	0.78	0.13	0.19
SE	159	38	48	53	0.27	0.06	0.08	0.09
UN	436	143	361	n.d.	0.24	0.20	0.20	n.d.

** Data for FU are available for the first half of the 2017 season only (a total of 92 h of weighted presence of either marmot or sheep, up to 12 August 2020). This represents a low presence when scaled to the entire season.*

Discussion and conclusion

After five years of fieldwork, this interdisciplinary long-term monitoring programme of alpine ecosystems in the central Alps has arrived at a first consolidated database and has established working routines. For both terrestrial and aquatic ecosystems, the teams provide datasets that allow the study sites to be characterized in a comparative way, and the data illustrate the spatial and temporal variability of the parameters monitored. Macroclimatic, water and soil data provide evidence that site selection was successful in terms of achieving the maximum possible standardization of terrestrial sites in an alpine context, or of covering the small-scale spatial variation which is intrinsic to aquatic systems. These are essential pre-requisites to identify effects of environmental changes that act on top of local influences.

For the terrestrial sites, we evidence a surprisingly similar (almost identical) macroclimatic situation, as characterized by a mean air temperature of 8°C during the main growing season. This high temperature for sites at 260–400 m above the treeline reflects late snowmelt and a short growing period, confined to the two warmest months of the year (after the summer solstice). The main finding from microclimate monitoring is that the H vs L contrast along the snowmelt gradients is the duration of the snow-free period as such, whereas differences in temperature after snow melt were negligible. The critical temperatures in the

topsoil, where meristems are nested and most mesofauna and microbial activity occur, are on average 4 K warmer than the air temperature (consistent across sites), with midday peaks exceeding 10K on bright summer days. Lakes and streams, in contrast, show more pronounced spatial variability and sharp influences of the local ice dynamics. Nitrate loading in streams is an order of magnitude lower than in lakes; overall, the concentrations obtained are relatively low, as would be expected for alpine systems, but with exceptions. According to Swiss sources (Kosonen et al. 2019), current rates of total N-deposition (wet plus dry) in the central Alps is close to 7 kg ha^{-1} a^{-1}, with rates at UN likely to be higher than in all other sites (exposed to front range weather). 4–6 kg N m^{-2} a^{-1} were reported by Bowman (1992) and Baron and Campbell (1997) for the Rocky Mountains in Colorado, placing the rates in the central Alps at the high end for temperate alpine sites. Such rates of N-deposition are likely to exceed critical loads for alpine vegetation (i. e. loads to which vegetation responds) (Kosonen et al. 2019).

One major message from the biological data collected annually so far is a pronounced year-to-year variation at all sites (up to a factor of 2), while the spatial differences (both along transects and among sites, as well as across lakes or streams) have largely been conserved over the years. The monitoring has not yet reached a point where we can separate long-term trends from stochasticity. Therefore, we refrain from attributing the steady rise in terrestrial productivity to climatic change. The data captured some exceptionally warm summers (2018–2020); data for further years are clearly needed to arrive at a consolidated mean that can serve as a reference for future re-assessments. Averaged across years, the terrestrial productivity at FU and UN is similar to the 200 g m^{-2} reported in the literature for H-type alpine grasslands (Körner 2021), but is only half as high at SE, IN and OB, suggesting that these sites operate within more limiting growth conditions. At SE and IN, the probable explanation is shallow soil on solid bedrock, while at OB the long-term grazing pressure has reduced the carrying capacity of the system, particularly at H, where trampling appears to have caused fines to become washed out to L.

Digital vegetation surveys open up an arena for fine-scale monitoring of *populations at the edge*. The technique allows the identification of seedlings and clonal expansion or retraction at the mm scale. Our data confirm the power of very detailed assessments of well-defined, small-scale permanent plots for assessing high-alpine vegetation dynamics (Blonder et al. 2018). Most species that have been newly identified by us downslope on the H to L transects belong to the typical grassland flora, suggesting that the recent exceptionally warm years facilitated their establishment. The fact that a quarter of the flowering plant species co-occur at all sites underlines the importance of selecting sites with similar environmental starting conditions, a practice which holds promise for future site comparisons and for identifying species-specific responses to environmental change.

Similar to flowering plants, initial data for soil biota (mesofauna and microbiota) suggest that less than a third of all species or OTUs occur at all sites studied. To date, neither of these assessments reveals clear H to L abundance shifts. Since a large proportion of the mesofauna was found in the litter layer and top mm of soils, high mobility may be one answer. Another reason might be a greater longevity of individuals at the cold end, balancing a potentially reduced rate of reproduction. Among microbiota, there is a shift in the abundance of some fungal taxa from H to L, while among bacteria there is a shift in functional groups, pointing to higher moisture at L. A repeat assessment is urgently needed in order to identify taxonomic groups that can serve as focal organisms for future re-assessments and for validating the initial data.

Thanks to our monitoring of site visits by large herbivores, we can conclude that the grazing pressure by these animals on plant biomass is very low (except in OB) and is unlikely to affect our productivity data as long as the pre-harvest protection of designated sampling plots is ensured (IN, FU). But it is important that land-use effects are accounted for, even for areas where they are expected to be small, and particularly where they can be intrinsic, as in mountain biosphere reserves (Becker et al. 2007). At the whole-mountain scale, thus including montane elevations, the effects of changes in land use are likely to be significantly greater than the effects of climate change (Spehn et al. 2006; Körner 2014; Caro et al. 2022). This also relates to the presence of fish, which can completely restructure the food web in alpine lakes (Manca & Amiraglio 2002; Schabetsberger et al. 2009).

In terms of the further development of this monitoring project, the teams conclude that the following schedule for the completion of the base-line data acquisition is required: (1) soil physics and chemistry: no need for repetition within the next decade; (2) macro- and microclimate, lake and stream chemistry: continue as long as regular field sampling is under way; (3) plant biomass, lake and stream biota: current data suggest an obvious need for more than 5 years to consolidate site-specific means (e. g. up to 2027); (4) soil mesofauna and microbiota: a second survey is urgently needed (2022), and a third one might ideally be conducted around 2027; (5) large herbivore monitoring: reduce to plant biomass sampling sites at IN and UN for as long as these surveys are continued. Given the great impact and stochasticity of mice activity on vegetation, the group suggests expanding the monitoring work to rodents.

The methods and field experience of the various teams will hopefully encourage other researchers or conservation managers to initiate similar programmes elsewhere in comparable alpine habitat types. In this way, an interdisciplinary network of alpine ecosystem

monitoring sites could increase the confidence in ongoing ecological changes at high elevations at even larger geographical scale. The results obtained here for late successional vegetation on well-developed soils complement the outcome of the summit monitoring programme for largely pioneer biota in exposed habitats by the world-wide GLORIA programme (see Introduction). By combining the terrestrial with the aquatic biota, the monitoring programme provides a holistic view of alpine life under change.

Acknowledgements

The concept of this monitoring project was developed by the scientific advisory board of the Hohe Tauern National Park (2012–2016) in cooperation with the park authorities. Funding for the Austrian groups was provided by the Federal Ministry for Climate Action, Environment, Energy, Mobility, Innovation, and Technology (BMK) and the European Union. The Oberettes (OB) site belongs to the LTSER site Matsch / Mazia, which is supported financially by the Autonomous Province of South Tyrol (ITA). Studies at Furka pass (FU) were facilitated by the ALPFOR research station (www.alpfor.ch), which also provided detailed meteorological data. At IN, UN and SE the teams received essential support from National Park staff and the park's infrastructure. The research personnel and laboratory support came from the home institutions of the authors. All teams received help from a great number of people, impossible to list here, particularly during field campaigns. In 2020, the group tragically lost E. Meyer (Innsbruck), who designed and conducted the soil mesofauna project.

References

Adamczyk M., F. Hagedorn, S. Wipf, J. Donhauser, P. Vittoz, C. Rixen, A. Frossard, J.-P. Theurillat & B. Frey 2019. The soil microbiome of Gloria Mountain summits in the Swiss Alps. *Frontiers Microbiology* 10: 1080.

Allen, M.R., R.A. Thum, J.N. Vandyke & C.E. Caceres 2012. Trait sorting in *Daphnia* colonising man-made lakes. *Freshwater Biology* 57: 1813–1822.

Bakker, J.P., H. Olff, J.H. Willems & M. Zobel 1996. Why do we need permanent plots in the study of long-term vegetation dynamics? *Journal of Vegetation Science* 7: 147–156.

Baron, J.S. & D.H. Campbell 1997. Nitrogen fluxes in a high elevation Colorado Rocky Mountain basin. *Hydrological Processes* 11: 783–799.

Becker, A., C. Körner, J.J. Brun, A. Guisan & U. Tappeiner 2007. Ecological and land use studies along elevational gradients. *Mountain Research and Development* 27: 58–65.

Blonder, B., R.E. Kapas, R. Dalton, B. Graae, J. Heiling & O. Opedal 2018. Microenvironment and functional-trait context dependence predict alpine plant community dynamics. *Journal of Ecology* 6: 1323–1337.

Bowman, W.D. 1992. Inputs and storage of nitrogen in winter snowpack in an alpine ecosystem. *Arctic, Antarctic, and Alpine Research* 24: 211–215.

Broadbent, A.A., H.S. Snell, A. Michas, W.J. Pritchard, L. Newbold, I. Cordero, T. Goodall, N. Schallhart, R. Kaufmann, R.I. Griffith, M. Schloter, M. Bahn & R.D. Bardgett 2021. Climate change alters temporal dynamics of alpine soil microbial functioning and biogeochemical cycling via earlier snow melt. *The ISME Journal* 15: 2264–2275.

Caro, T., Z. Rowe, J. Berger, P. Wholey & A. Dobson 2022. An inconvenient misconception: Climate change is not the principal driver of biodiversity loss. *Conservation Letters*: e12868. Doi: 10.1111/conl.12868

Cauvy-Fraunié, S. & O. Dangles 2019. A global synthesis of biodiversity responses to glacier retreat. *Nature Ecology and Evolution* 3: 1675–1685.

Craine, J.M., J.B. Nippert, A.J. Elmore, A.M. Skibbe, S.L. Hutchinson & N.A. Brunsell 2012. Timing of climate variability and grassland productivity. *Proceedings of the National Academy of Sciences of the USA* 109: 3401–3405.

Dai, L., X. Ke, X. Guo, Y. Du, F. Zhang, Y. Li, Q. Li, L. Lin C. Peng, K. Shu & G. Cao 2019. Responses of biomass allocation across two vegetation types to climate fluctuations in the northern Qinghai-Tibet Plateau. *Ecology and Evolution* 9: 6105–6115.

de Witte, L.C., G.F.J. Armbruster, L. Gielly, P. Taberlet & J. Stocklin 2012. AFLP markers reveal high clonal diversity and extreme longevity in four key arctic-alpine species. *Molecular Ecology* 21: 1081–1097.

de Witte, L.C. & J. Stöcklin 2010. Longevity of clonal plants: why it matters and how to measure it. *Annals of Botany* 106: 859–870.

Deiner, K., E.A. Fronhofer, E. Mächler, J.C. Walser & F. Altermatt 2016. Environmental DNA reveals that rivers are conveyer belts of biodiversity information. *Nature Communications* 7: 12544. Doi: 10.1038/ncomms12544

Ecosystem Monitoring Team 2021. *Manual of methods/Methodenhandbuch.* Hohe Tauern National Park - Research (Matrei in East-Tyrol) and Academy of Sciences (Vienna). Available at: https://hohetauern.at/de/forschung/langzeitmonitoring.html (accessed 17/03/2022)

Elser, J.J. et al. 2020. Key rules of life and the fading cryosphere: Impacts in alpine lakes and streams. *Global Change Biology* 26: 6644–6656. Doi: 10.1111/gcb.15362

Fischer, M., O. Bossdorf, S. Gockel, F. Hansel, A. Hemp, D. Hessenmoller, G. Korte, J. Nieschulze, S. Pfeiffer, D. Prati, S. Renner, I. Schoning, U. Schumacher, K. Wells, F. Buscot, E.K.V. Kalko, K.E. Linsenmair, E.D. Schulze & W.W. Weisser 2010. Implementing large-scale and long-term functional biodiversity research: The Biodiversity Exploratories. *Basic and Applied Ecology* 11: 473–485.

Franklin, J.F., C.S. Bledsoe & J.T. Callahan 1990. Contributions of the long-term ecological research program. An expanded network of scientists, sites, and programs can provide crucial comparative analyses. *BioScience* 40: 509–523.

Freppaz, M., M.W. Williams, T. Seasteclt & G. Filippa 2012. Response of soil organic and inorganic nutrients in alpine soils to a 16-year factorial snow and N-fertilization experiment, Colorado Front Range, USA. *Applied Soil Ecology* 62: 131–141.

Friedel, H. 1961. Schneedeckendauer und Vegetationsverteilung im Gelände. *Mitteilungen der Forstlichen Bundesversuchsanstalt Mariabrunn (Vienna)* 59: 317–369.

Füreder, L. 1999. High alpine streams: cold habitats for insect larvae. In: Margesin, R. & F Schinner (eds.), *Cold-Adapted Organisms*: 181–196. Springer, Berlin.

Füreder, L. 2010. Hochalpine Flusslandschaft Rotmoos. In: Koch, E.M. & B. Erschbamer (eds.), *Glaziale und periglaziale Lebensräume im Raum Obergurgl*: 185–202.

Gottfried, M. et al. 2012. Continent-wide response of mountain vegetation to climate change. *Nature Climate Change* 2: 111–115. Doi: 10.1038/nclimate1329

Green, K. & R. Slatyer 2019. Arthropod Community Composition along Snowmelt Gradients in Snowbeds in the Snowy Mountains of South-Eastern Australia. *Austral Ecology* 45: 144–157.

Hågvar, S. 2010. A review of Fennoscandian arthropods living on and in snow. *European Journal of Entomology* 107: 281–298.

Hansen, A.H., S. Jonasson, A. Michelsen & R. Julkunen-Tiitto 2006. Long-term experimental warming, shading and nutrient addition affect the concentration of phenolic compounds in arctic-alpine deciduous and evergreen dwarf shrubs. *Oecologia* 147: 1–11.

Hegg, O., U. Feller, W. Dahler & C. Scherrer 1992. Long term influence of fertilization in a Nardetum. *Vegetatio* 103: 151–158.

Ilyashuk, E.A., K.A. Koinig, O. Heiri, B.P. Ilyashuk & R. Psenner 2011. Holocene temperature variations at a high-altitude site in the Eastern Alps: a chironomid record from Schwarzsee ob Sölden, Austria. *Quaternary Science Reviews* 30: 176–191. Doi: 10.1016/j.quascirev.2010.10.008

Iravani, M., M. Schütz, P. Edwards, A. Risch, Ch. Scheidegger & H. Wagner 2011. Seed dispersal in red deer (*Cervus elaphus* L.) dung and its potential importance for vegetation dynamics in subalpine grasslands. *Basic Applied Ecology* 12: 505–515. Doi: 10.1016/j.baae.2011.07.004

Kittel, T.GF., M.W. Williams, K. Chowanski, M. Hartman, T. Ackerman, M. Losleben & P.D. Blanken 2015. Contrasting long-term alpine and subalpine precipitation trends in a mid-latitude North American mountain system, Colorado Front Range, USA. *Plant Ecology and Diversity* 8: 607–625.

Körner, C. 1995. Alpine plant diversity: a global survey and functional interpretations. In: Chapin, F.S. III & C. Körner (eds.), *Arctic and alpine biodiversity: Patterns, causes and ecosystem consequences*. Ecological Studies 113: 45–62. Springer, Berlin.

Körner, C. 2004. Mountain biodiversity, its causes and function. *Ambio Special Report* 13: 11–17.

Körner, C. 2011. Coldest places on earth with angiosperm plant life. *Alpine Botany* 121: 11–22.

Körner, C. 2014. Mountain ecosystems in a changing environment. *eco.mont - Journal on protected mountain area research and management* 6(1): 71–77.

Körner, C. 2018a. Concepts in empirical plant ecology. *Plant Ecology and Diversity* 11: 405–428.

Körner, C. 2018b. Comparative, long-term ecosystem monitoring across the Alps: Austrian Hohe Tauern National Park, South-Tyrol and the Swiss central Alps. *Conference Volume, 6th Symposium for research in protected areas. Nationalpark Hohe Tauern*: 331–337. Available at: http://www.parcs.at/npa/pdf_public/2018/36275_20180523_093027_ConferenceVolume_6thSymposium_FINAL_corr.pdf (accessed 17/03/2020)

Körner, C. et al. 2020. *Langzeitmonitoring von Ökosystemprozessen im Nationalpark Hohe Tauern: Synthese der Startphase 2016–2018*. Available at: http://www.parcs.at/npht/pdf_public/2020/38764_20200901_115652_WEB_Synthesebericht.pdf (accessed 17/03/2020) Doi: 10.1553/GCP_LZM_NPHT_Synthese

Körner, C. 2021 *Alpine plant life*. Cham

Körner, C. & E. Hiltbrunner 2021. Why is the alpine flora comparatively robust against climatic warming? *Diversity* 13: 383 Doi: 10.3390/d13080383

Körner, C. & M. Ohsawa 2005. Mountain Systems. In: Hassan, R., R. Scholes & N. Ash (eds.), *Ecosystems and human well-beeing: current state and trends*: 681–716. Volume 1. Washington DC.

Körner, C., J. Paulsen & E.M. Spehn 2011. A definition of mountains and their bioclimatic belts for global comparison of biodiversity data. *Alpine Botany* 121: 73–78.

Kosonen, Z., E. Schnyder, E. Hiltbrunner, A. Thimonier, M. Schmitt, E. Seitler & L. Thöni 2019.Current atmospheric nitrogen deposition still exceeds critical loads for sensitive, semi-natural ecosystems in Switzerland. *Atmospheric Environment* 211: 214–225.

Lamprecht, A., P.R. Semenchuk, K. Steinbauer, M. Winkler & H. Pauli 2018. Climate change leads to accelerated transformation of high-elevation vegetation in the central Alps. *New Phytologist* 220: 447–459.

Lazzaro, A., D. Hilfiker & J. Zeyer 2015. Structures of Microbial Communities in Alpine Soils: Seasonal and Elevational Effects. *Frontiers in Microbiology* 6: 1330. Doi: 10.3389/fmicb.2015.01330

Lotter, A.F., O. Heiri, W. Hofmann, W.O. van der Knaap, J.F.N. van Leeuwen, I.R. Walker & L. Wick 2006. Holocene timber-line dynamics at Bachalpsee, a lake at 2265 m a.s.l. in the northern Swiss Alps. *Vegetation History and Archaeobotany* 15: 295–307.

Lürling, M., M. Mendes-Mello, F. van Oosterhout, L. de Senerpont-Domis, M.M. Marinho 2018. Response of natural cyanobacteria and algae assemblages

to a nutrient pulse and elevated temperature. *Frontiers in Microbiology* 9: 1851. Doi: 10.3389/fmicb.2018.01851

Manca, M. & M. Armiraglio 2002. Zooplankton of 15 lakes in the Southern Central Alps: Comparison of recent and past (pre-ca 1850 AD) communities. *Journal of Limnology* 61(2). Doi: 10.4081/jlimnol.2002.225

Mark, A.F., A.C. Korsten, D.U. Guevara, K.J.M. Dickinson, T. Humar-Maegli, P. Michel, S.R.P. Halloy, J.M. Lord, S.E. Venn, J.W. Morgan, P.A. Whigham & J.A. Nielsen 2015. Ecological responses to 52 years of experimental snow manipulation in high-alpine cushionfield, Old Man Range, south-central New Zealand. *Arctic, Antarctic, and Alpine Research* 47: 751–772.

Matteodo, M., S. Wipf, V. Stöckli, C. Rixen & P. Vittoz 2013. Elevation gradient of successful plant traits for colonizing alpine summits under climate change. *Environmental Research Letters* 8: 24043–24053.

Mayer, R. & B. Erschbamer 2017. Long-term effects of grazing on subalpine and alpine grasslands in the Central Alps, Austria. *Basic and Applied Ecology* 24: 9–18.

Meier, M., D. Stöhr, J. Walde & E. Tasser 2017. Influence of ungulates on the vegetation composition and diversity of mixed deciduous and coniferous mountain forest in Austria. *European Journal of Wildlife Research* 63: 1–10. Doi: 10.1007/s10344-017-1087-4

Miller, M.P. & D.M. McKnight 2015. Limnology of the Green Lakes Valley: phytoplankton ecology and dissolved organic matter biogeochemistry at a long-term ecological research site. *Plant Ecology and Diversity* 8: 689–702.

Mirtl, M., E.T. Borer, I. Djukic, M. Forsius, H. Haubold, W. Hugo, J. Jourdan, D. Lindenmayer, W.H. McDowell, H. Muraoka, D.E. Orenstein, J.C. Pauw, J. Peterseil, H. Shibata, C. Wohner, X. Yu & P. Haase 2018. Genesis, goals and achievements of Long-Term Ecological Research at the global scale: A critical review of ILTER and future directions. *Science of the Total Environment* 626: 1439–1462.

Niedrist, G.H., M. Cantonati & L. Füreder 2018. Environmental harshness mediates the quality of periphyton and chironomid body mass in alpine streams. *Freshwater Science* 37: 519–533.

Niedrist, G.H. & L. Füreder 2021. Real-time warming of Alpine streams: (re)defining invertebrates' temperature preferences. *River Research and Applications* 37: 283–293.

Pauli, H., M. Gottfried & G. Grabherr 2001. High summits of the Alps in a changing climate. The oldest observation series on high mountain plant diversity in Europe. In: Walther, G.-R., C.A. Burga & P.J. Edwards (eds.), *"Fingerprints" of climate change. Adapted behaviour and shifting species ranges*: 225–231. Kluwer Academic/Plenum, N.Y.

Pauli, H., M. Gottfried, K. Reier, C. Klettner & G. Grabherr 2007. Signals of range expansions and contractions of vascular plants in the high Alps: observations (1994–2004) at the GLORIA master site Schrankogel, Tyrol, Austria. *Global Change Biology* 13: 147–156.

Schabetsberger, R., M.S. Luger, G. Drozdowski & A. Jagsch 2009. Only the small survive: monitoring long-term changes in the zooplankton community of an Alpine lake after fish introduction. *Biological Invasions* 11: 1335–1345. Doi: 10.1007/s10530-008-9341-z

Scherrer, D. & C. Körner 2009. Infra-red thermometry of alpine landscapes challenges climatic warming projections. *Global Change Biology* 16: 2602–2613.

Scholz, K., A. Hammerle, E. Hiltbrunner & G. Wohlfahrt 2018. Analyzing the effect of growing season length on the net ecosystem production of alpine grassland using model data fusion. *Ecosystems* 21: 982–999.

Seeber, J., C. Newesely, M. Steinwandter, C. Körner, U. Tappeiner & E. Meyer 2021. Soil invertebrate diversity across steep high elevation snowmelt gradients in the European Alps. *Arctic, Antarctic, and Alpine Research* 53: 288–299. Doi: 10.1080/15230430.2021.1982665

Silvertown, J., J. Tallowin, C. Stevens, S.A. Power, V. Morgan, B. Emmett, A. Hester, P.J. Grime, M. Morecroft, R. Buxton, P. Poulton, R. Jinks & R. Bardgett 2010. Environmental myopia: a diagnosis and a remedy. *Trends in Ecology and Evolution* 25: 556–561.

Silvertown, J., P. Poulton, E. Johnston, G. Edwards, M. Heard & P.M. Biss 2006. The Park Grass experiment 1856-2006: its contribution to ecology. *Journal of Ecology* 94: 801–814.

Smith, J.G., W. Sconiers, M.J. Spasojevic, I.W. Ashton & K.N. Suding 2012. Phenological Changes in Alpine Plants in Response to Increased Snowpack, Temperature, and Nitrogen. *Arctic, Antarctic, and Alpine Research* 44: 135–142.

Søvik, G., H.P. Leinaas, R.A. Ims & T. Solhøy 2003. Population dynamics and life history of the oribatid mite *Ameronothrus lineatus* (Acari, Oribatida) on the high Arctic archipelago of Svalbard. *Pedobiologia* 47: 257–271.

Spasojevic, M.J., W.D. Bowman, H.C. Humphries, T.R. Seastedt & K.N. Suding 2013. Changes in alpine vegetation over 21 years: Are patterns across a heterogeneous landscape consistent with predictions? *Ecosphere* 4: 117.

Spehn, E.M., M. Liberman & C. Körner 2006. *Land use change and mountain biodiversity.* CRC Press, Boca Raton.

Steinger, T., C. Körner & B. Schmid 1996. Long-term persistence in a changing climate: DNA analysis suggests very old ages of clones of *Carex curula*. *Oecologia* 105: 94–99.

Stöckli, V., S. Wipf, C. Nilsson & C. Rixen 2011. Using historical plant surveys to track biodiversity on mountain summits. *Plant Ecology and Diversity* 4: 415–425.

Virtanen, R., H. Henttonen & K. Laine 1997. Lemming grazing and structure of a snowbed plant community - a long-term experiment at Kilpisjärvi, Finnish Lapland. *Oikos* 79: 155–166.

Vittoz, P., C. Randin, A. Dutoit, F. Bonnet & O. Hegg 2009. Low impact of climate change on sub-

alpine grasslands in the Swiss Northern Alps. *Global Change Biology* 15: 209–220.

Walker, M.D., D.A. Walker, J.M. Welker, A.M. Arft, T. Bardsley, P.D. Brooks, J.T. Fahnestock, M.H. Jones, M. Losleben, A.N. Parsons, T.R. Seastedt & P.L. Turner 1999. Long-term experimental manipulation of winter snow regime and summer temperature in arctic and alpine tundra. *Hydrological Processes* 13: 2315–2330.

Walker, M.D., P.J. Webber, E.H. Arnold & D. Ebert-May 1994. Effects of interannual climate variation on aboveground phytomass in alpine vegetation. *Ecology* 75: 393–408.

Williams, M.W., R.T. Barnes, J.N. Parman, M. Freppaz & E. Hood 2011. Stream water chemistry along an elevational gradient from the continental divide to the foothills of the Rocky Mountains. *Vadose Zone Journal* 10: 900–914.

Williams, M.W., P.D. Brooks & T. Seastedt 1998. Nitrogen and carbon soil dynamics in response to climate change in a high-elevation ecosystem in the Rocky Mountains, USA. *Arctic, Antarctic, and Alpine Research* 30: 26–30.

Williams, M.W., T.R. Seastedt, W.D. Bowman, D.M. McKnight & K.N. Suding 2015. An overview of research from high elevation landscape: the Niwot Ridge, Colorado Long Term Ecological Research program. *Plant Ecology and Diversity* 8: 597–605. Doi: 10.1080/17550874.2015.1123320

Williams, P.H. & R.J. Haynes 1995. Effect of sheep, deer and cattle dung on herbage production and soil nutrient content. *Grass and Forage Science* 50: 263–271. Doi: 10.1111/j.1365-2494.1995.tb02322.x

Wipf, S. & C. Rixen 2010. A review of snow manipulation experiments in Arctic and alpine tundra ecosystems. *Polar Research* 29: 95–109.

Wipf, S., V. Stöckli, K. Herz & C. Rixen 2013. The oldest monitoring site of the Alps revisited: accelerated increase in plant species richness on Piz Linard summit since 1835. *Plant Ecology and Diversity* 6: 447–455.

Yang, Y., R.T.W. Siegwolf & C. Körner 2015. Species specific and environment induced variation of $\delta^{13}C$ and $\delta^{15}N$ in alpine plants. *Frontiers in Plant Science* 6: 429. Doi: 10.3389/fpls.2015.00423

Yao, F., U. Vik, A.K. Brysting, T. Carlsen, R. Halvorsen & H. Kauserud 2013. Substantial compositional turnover of fungal communities in an alpine ridge-to-snowbed gradient. *Molecular Ecology* 22: 5040–5052.

Authors

Christian Körner[1] – corresponding author

is an emeritus Professor of Botany (1989–2014, University of Basel). He received his academic education at the University of Innsbruck. His main academic domains are alpine ecology, treeline research and forest ecology. E-mail: ch.koerner@unibas.ch See https://duw.unibas.ch/en/koerner

Ulrike-Gabriele Berninger[2]

is a Professor of Zoological Ecology at the University of Salzburg. Her research focusses on the role of plankton in nutrient and energy cycling in lakes and marine ecosystems, and on urban streams and their biota.

Andreas Daim[3]

is a Junior Researcher at the Institute of Wildlife Biology and Game Management (BOKU Vienna) where he has worked since 2015. He is currently working on his PhD, on spatio-temporal animal behaviour under different habitat and hunting regimes.

Thomas Eberl[4]

is a Vegetation Ecologist who runs a consulting company for environmental concerns. He received his academic education at the University of Salzburg. Environmental impact assessment, vegetation survey, monitoring, modelling, and statistics are his main fields of activity.

Fernando Fernández Mendoza[5]

is a Research Associate at the University of Graz (2014–). He received his academic education at the Complutense University of Madrid and the Goethe University and Senckenberg Institute in Frankfurt, and specializes in population genetics and comparative genomics of lichen symbioses.

Leopold Füreder[6]

is a Professor at the Institute of Ecology of the University of Innsbruck, and coordinates the River and Conservation Research Group. Alpine freshwater ecology, ecosystem structure and function, environmental change and restoration are the main focuses of his research.

Martin Grube[5]

is a Professor of Botany at the University of Graz (2018–), where he received his academic education. Lichenology and microbial ecology are his main domains.

Elisabeth Hainzer[7]

is responsible for research coordination at Hohe Tauern National Park, across all three provinces. She received her academic education at the University of Natural Resources and Life Sciences (BOKU, Vienna). Her main areas of activity are long-term monitoring of alpine protected areas, and data and knowledge management.

Roland Kaiser[2,4]

is a Vegetation Ecologist who runs a consulting company for environmental concerns. He received his academic education at the University of Salzburg. Environmental impact assessment, vegetation sur-

vey, monitoring, modelling, and statistics are his main fields of activity.

Erwin Meyer[8]

former Professor Emeritus of Zoology, University of Innsbruck, with a focus on soil fauna (deceased in 2020)

Christian Newesely[9]

has been a member of the Ecosystem and Landscape Ecology research group at the Department of Ecology (University of Innsbruck) since 1986. His main research topics are microclimate, alpine ecology and the ecology of ski-slopes.

Georg Niedrist[10]

works as a Researcher at Eurac Research in Bolzano, Italy (since 2006). He holds a PhD in ecology from the University of Innsbruck; his research interests include mountain agriculture, biodiversity and climate change.

Georg H. Niedrist[6]

is a Postdoctoral Aquatic Ecologist at the University of Innsbruck. Since 2011, his research has focused on understanding life in mountain waters, how species are adapted to these special conditions, and how environmental changes affect biocenosis and ecosystems.

Jana S. Petermann[2]

is an Associate Professor of Community Ecology at the University of Salzburg. She received her PhD from the University of Zurich. Her research addresses questions related to natural biodiversity and the effects of species loss on ecological communities.

Julia Seeber[10]

is a Soil Ecologist at the Institute for Alpine Environment at Eurac Research in Bolzano, Italy. Her main field of expertise are soil invertebrates in various habitats, but especially in mountain soils.

Ulrike Tappeiner[9,10]

is Professor of Ecosystem and Landscape Ecology (University of Innsbruck, Austria) and Head of the Institute for Alpine Environment (Eurac Research, Bolzano, Italy). Her research focuses on socio-ecological systems, ecosystem services, and sustainability monitoring in mountain regions.

Stephen Wickham[2]

is an Associate Professor of Aquatic Ecology at the University of Salzburg. His areas of research interest are zooplankton and protist ecology in freshwater and marine systems, multitrophic interactions, and the drivers and consequences of biodiversity.

[1] Botany and ALPFOR, Department of Environmental Sciences, University of Basel, Schönbeinstrasse 6, 4056 Basel, Switzerland
[2] Department Environment and Biodiversity, Paris-Lodron University Salzburg, Hellbrunner Str. 34, 5020 Salzburg, Austria
[3] University of Natural Resources and Life Sciences, Vienna (BOKU), Department of Integrative Biology and Biodiversity Research, Institute of Wildlife Biology and Game Management, Gregor-Mendel-Strasse 18, 1180 Vienna, Austria
[4] ENNACON environment nature consulting, Altheim 13, 5143 Feldkirchen bei Mattighofen, Austria
[5] Institute of Biology, University of Graz. Holteigasse 6, A-8010 Graz
[6] River and Conservation Research, Department of Ecology, University of Innsbruck, Technikerstr. 25, 6020 Innsbruck, Austria
[7] Nationalpark Hohe Tauern, Forschungskoordination, Kirchplatz 2, 9971 Matrei in Osttirol, Austria
[8] Department of Ecology, University of Innsbruck, Technikerstr. 25, 6020 Innsbruck, Austria
[9] Department of Ecology, Universität Innsbruck, Sternwartestr. 15, 6020 Innsbruck, Austria
[10] Institute for Alpine Environment, Eurac Research, Viale Druso 1, 39100 Bolzano-Bozen, Italy

eco.mont – Volume 14, Number 2, July 2022
ISSN 2073-106X print version – ISSN 2073-1558 online version: http://epub.oeaw.ac.at/eco.mont
https://dx.doi.org/10.1553/eco.mont-14-2s70

Avifaunal Diversity in Important Bird Areas of Western Nepal

Sony Lama, Saroj Shrestha, Ang Phuri Sherpa, Munmun Tamang & Dinesh Ghale

Keywords: avian community, bird checklist, Important Bird Area, threats

Abstract

The rural municipality of Barekot in Jajarkot district is an Important Bird Area (IBA) in Western Nepal. In recent years, illegal hunting and trapping have increased in this area. Additionally, a hydropower project with a capacity of 410 MW is being constructed within Barekot. The present study aims to update the preliminary checklist of birds and to identify the underlying threats to the bird populations in this region. The bird survey was conducted in Barekot over four days in the late winter/early spring of 2021. Direct field observation, surveys of key informants, a literature review and photography were the main tools used for data collection. The study revealed 87 bird species belonging to 10 orders and 34 families. The birds most commonly recorded belong to the Muscicapidae family, order Passeriformes. Among the recorded species, two are on the IUCN Red List of Nationally Vulnerable species, five are listed in CITES Appendix II, and one species features in CITES Appendix I. Approximately 82% of the bird species recorded were of resident types. Despite a decline in bird diversity, Barekot's unique geographical location still makes it an important IBA in Nepal. Bird numbers have plummeted due to human intrusion and disturbance, and modifications to natural systems. Based on our findings, we recommend landscape-level research on the impacts of hydropower projects, roads, poaching, and the Covid-19 pandemic. Future conservation efforts should also emphasize the prevention of habitat fragmentation and raising public awareness.

Introduction

Avifauna play a critical role in ecosystem processes and functioning, for example in pollination, control of insect pest populations and scavenging; they are indicators of ecosystem health, affect crop productivity, and are instrumental in nutrient cycling and formation (Prakash et al. 2001; Amat & Green 2010; Bensizerara et al. 2013; Sekercioglu et al. 2016; Morante-Filho & Faria 2017). Since 2020, the diversity of avifauna has decreased owing to habitat destruction and human interference.

Karnali (28° 53' 43"–30° 25' 22.06 E", 82° 0' 0.6"–82° 5' 17.02" N) in Western Nepal is the country's largest province (24,453 km^2) and has the smallest population (1,570,418) of the seven federal provinces in Nepal (26° 22' 9"–30° 24' 54" E, 81° 24' 27"–88° 1' 56" N) (CBS 2012). The altitude of Karnali province ranges from 180 m to 7,348 m. The province harbours birds (56% of the total number of species in Nepal), mammals (42%), butterflies (22%), fishes (32%), reptiles (11%), amphibians (43%), and flowering plants (42%). Several of these species are endemic to Nepal and are threatened by human activities that cause habitat loss and fragmentation (Bista et al. 2017; Lama et al. 2020; Acharya & Paudel 2020; Shrestha et al. 2021(b). Nepal is home to 886 bird species (DNPWC and BCN, 2018) and has a total of 27 Important Bird Areas (IBAs). Karnali is home to 496 different species of birds and has four IBAs: Barekot, Limi valley, Rara National Park and Shey Phokshundo National Park (Acharya & Paudel 2020).

Barekot (28° 54' 40"–29° 0' 45" E, 82° 16' 41"–82° 17' 43.53" N), Western Nepal, is in Jajarkot district (28° 59' 25"– 28° 58' 42" E, 81° 52' 52"–82° 21' 43" N), Karnali Province. The district lies in a region that is ecologically very fragile; it has an elevation range of 610 m to 5,412 m, and is ranked *very high* in the climate change vulnerability ranking index (MoFSC 2016; UNRCHCO 2021). The Government of Nepal has recently invested in hydropower projects in Jajarkot district, and one plant is currently under construction within Barekot's IBA. It is believed that this project will have adverse impacts on the local flora and fauna. Barekot is home to a number of endangered and rare mammals and birds (Bhusal & Singh 2017; Acharya & Paudel 2020). The study area is also plagued by hunting and trapping, poisoning, illegal logging, encroachment, overgrazing and overfishing (DNPWC 2017).

Despite the area's rich biodiversity and good bird habitats (Acharya & Paudel 2020), our knowledge of the status of bird species and their overall diversity in Barekot is very limited. The majority of bird studies in Nepal have focused on the southern foothills (Terai region; 60 m to 210 m). Only a handful of articles about bird species from Karnali province are available. In 2015, 146 bird species were recorded in Jajarkot district (Paudel & Bhusal 2015). The present study aims to update the bird checklists, for the first time since 2015, according to their taxa, IUCN status (i.e. critically endangered, endangered, or vulnerable), CITES Appendix status (Appendices I, II, III), occurrence status (resident or visitor), and associated threats.

Methods

Study area

Barekot, whose elevation ranges from 1,510 to 5,222 m a.s.l, is the largest rural municipality (RM) of Jajarkot district. Barekot has a total area of 57,526 hec-

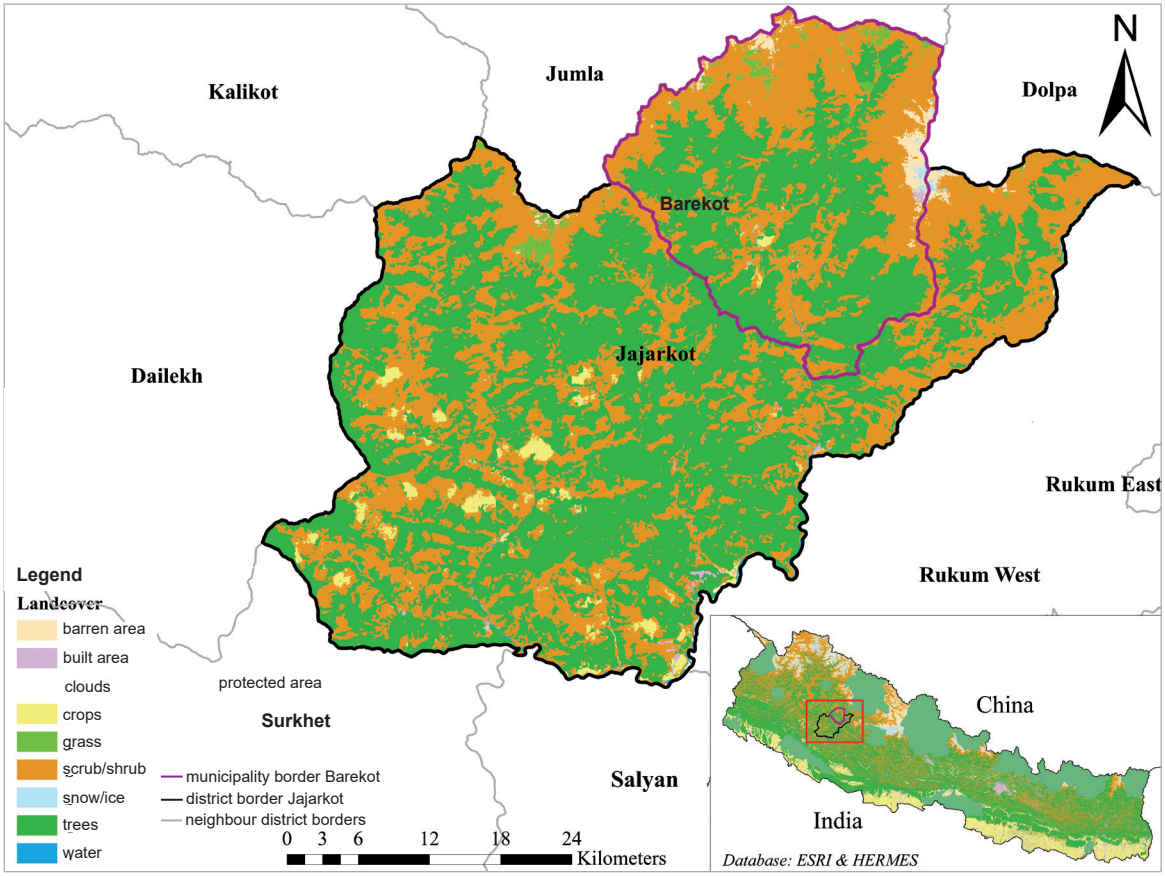

Figure 1– Study area: The rural municipality of Barekot in Nepal.

tares and a population of 18,083. The forest coverage of Barekot is 33,734 hectares, which is 0.54% of Nepal's total forest area and 10.10% of that of Karnali province (Table 1). The region is highly vulnerable to ecological challenges such as landslides and fire, as well as to epidemics, including cholera, diarrhea and influenza (Bhandari et al. 2009; Upadhyay et al. 2016; UNRCHCO 2021).

Western Himalayan subalpine conifer forests make up the majority of Barekot's habitat. There are also alpine shrub and grassland habitats in this region. The climate in most of the region is mild and temperate, with dry winters and warm summers. It also has snowy climate zones, with dry winters and cool summers.

Although this region does not have protected status, it lies in close proximity to several important protected areas, including Rara National Park, Khaptad National Park and Api Nampa Conservation Area to the west; Annapurna Conservation Area and Dhorpatan Hunting Reserve to the east; Shey-Phoksundo National Park to the north, and Bardia National Park to the south (Figure 1). Barekot's unique geographical location makes it a critical IBA in Nepal.

Table 1 – Adapted from CBS (2014) and DFRS (2018).

Region	Population (individuals)	Elevation (m a.s.l.)	Forest area (hectares)	Total area (hectares)
Barekot	18,083	1,510–5,222	33,734	57,526
Jajarkot	171,304	610–5,412	133,268	221,436
Karnali Province	1570418	180–7,348	3,061,752	1,177,033
Nepal	26,494,504	64–8,848	1,4262,567	6,230,537

Barekot is home to many threatened species, including the Himalayan red panda (*Ailurus fulgens fulgens)*, Himalayan black bear (*Ursus thibetanus*), musk deer (*Moschus spp.*), northern red deer (*Muntiacus vaginalis*), Himalayan tahr *(Hemitragus jemlahicus*), common goral (*Naemorhedus goral*), Himalayan serow (*Capricornis thar*), and blue sheep (*Pseudois nayaur)* (Acharya and Paudel 2020; Shrestha et al. 2021a; Shrestha et al. 2021b). Additionally, the study area is also home to various endangered avian species, such as the Cheer pheasant (*Catreus wallichii*), Red-headed Vulture (*Sarcogyps calvus*), and Egyptian Vulture (*Neophron percnopterus*); the nationally threatened Satyr Tragopan (*Tragopan satyra*), Bearded Vulture (*Gypaetus barbatus*), Himalayan Griffon (*Gyps himalayensis*), and Brown Fish Owl (*Bubo zeylonensis*); and the Himalayan Monal (*Lophophorus impejanus*), a Protected bird of Nepal (Paudel & Bhusal 2015). As Barekot has great conservation significance, particularly for birds, the local government has planned to designate the region a conservation area. The aim, while leveraging its tourism potential and promoting the local economy, is to preserve its rich biodiversity and landscape (NTNC 2019).

Survey methods

A number of complementary methods were used to collect information about avian fauna and associated threats. These included (i) studying the literature; (ii) unstructured interviews with community members; (iii) consultations with experts and selected key stakeholders; (iv) field visits. A questionnaire was administered to 40 households selected randomly from the records of the community forests' user group. The questionnaires, written in the Nepali language and administered orally, concerned the distribution of bird species and their habitat use.

Field survey

Field surveys were carried out over 4 days in late winter/early spring (23–26 April 2021), from 0700 hrs to 1700 hrs. A comprehensive list of the birds found in the area was recorded. We followed the Timed Species Count (TSC) approach by Bibby et al. (2000) to compile the bird survey data (see Appendix I). Additionally, we referred to a bird field guide by Richard Grimmett et al. (2016) and *Birds of Nepal* (2016) to identify the species. We surveyed birds in four blocks of Barekot RM (i.e. Eastern, Western, Southern and Northern blocks), which have an elevation range of 1,800 m to 2,400 m. These survey blocks were selected based on the land-cover patterns, potential as habitat for species, vegetation, and disturbance factors. A team of 10 individuals were involved in the survey.

Data analysis

A daily list of birds seen and heard was kept in a notebook. The final list of birds was produced using Excel by combining information from observations, consultations and surveys. Birds recorded were evaluated for their global and national importance or status (e.g. threatened), as well as their migratory status. Habitat information and bird records, particularly for threatened/migratory species, were correlated with each other.

Materials

Garmin eTrex-14 GPS and Nikon Monarch 7 8X42 binoculars were used to observe bird species closely; a Canon EOS 80D digital SLR camera with Canon RF 600mm f/11 IS STM lens was used to capture photos; measuring tapes and stationary materials were also used during the field survey. Maps and topographical sheets of the area were also used. Local people were interviewed to collect information on any prevailing threats.

Results

A total of 87 bird species (10 orders and 34 families) were recorded in the study area (see Appendix). The majority of the bird species documented belong to the order *Passeriformes* (Figure 2). *Muscicapidae* is the largest family (n=9 species), followed by *Phylloscopidae*

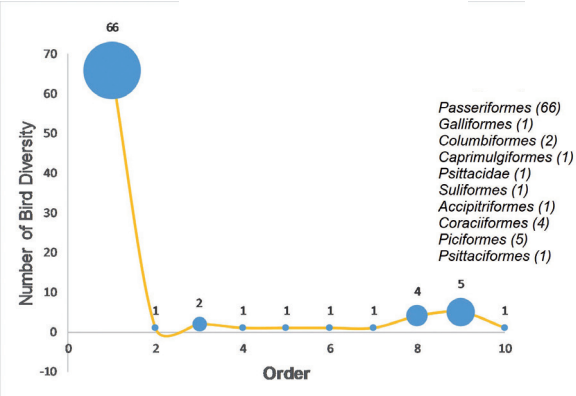

Figure 2 – Order-wise composition of birds in the rural municipality of Barekot, Jajarkot.

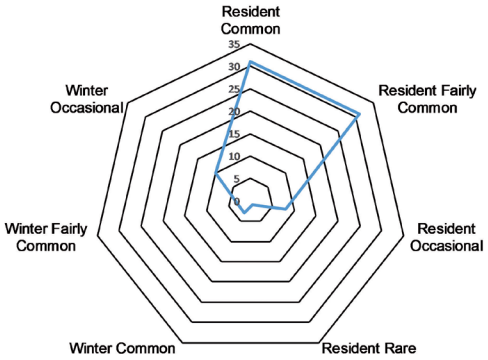

Figure 3 – Occurrence status of birds in he rural municipality of Barekot, Jajarkot.

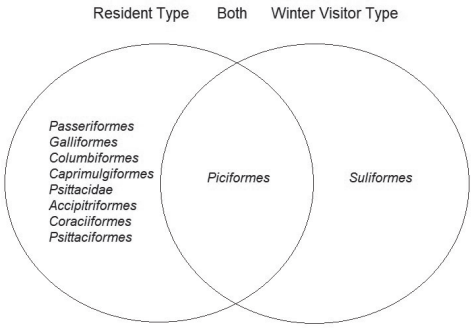

Figure 4 – Venn diagram showing bird occurrence status for species orders.

and *Leiotrichidae*, each with 7 species. Only one species was recorded for each of the following families: *Phasianidae*, *Apodidae*, *Ardeidae*, *Phalacrocoracidae*, *Psittacidae*, *Aegithalidae*, *Timaliida*, *Cinclidae*, *Sturnidae*, *Turdidae*, *Chloropseidae*, *Dicaeidae* and *Emberizidae*. Among the reported bird species, 81.61% (n=71 species) were of the resident type, and 18.39% (n=16 species) were winter visitors. 34 species (39.08%) of birds were common or fairly common; 18 species (20.69%) were sporadic/occasional, and 1 species (1.15%) was rare (Figure 3). Species belonging to the *Piciformes* order included both residents and winter visitors, whilst species belonging to *Suliformes* were winter visitors only (Figure 4).

Two species, the Himalayan Griffon (*Gyps himalayensis*) and Bearded Vulture (*Gypaetus barbatus*), have

Figure 5 – Olive-Backed Pipit (Anthus hodgsoni). © Saroj Shrestha

Figure 6 – Grey bushchat (Saxicola ferreus) © Sony Lama

nationally vulnerable status in the International Union for Conservation of Nature and Natural Resources (IUCN) Red Data Book; 85 species are of *least concern* in the Data Book. Six species were listed in the Convention on International Trade in Endangered Species of Wild Fauna and Flora (CITES); five are listed in Appendix II of the CITES Convention, and one in Appendix III of the CITES Convention. None of the recorded bird species are protected by Nepal's National Parks and Wildlife Conservation (NPWC) Act.

The field survey and interviews indicate that the primary threats to avian diversity and survival are poaching and habitat modification.

Discussion

Our study provides the first detailed checklist of birds from Barekot in Western Nepal (see Appendix), with information on species taxa, IUCN threatened species status (i. e. critically endangered, endangered, and vulnerable), CITES Appendix status (CITES Appendices I, II, III), occurrence status (i. e., resident type or visitor type), and associated threats. This study recorded 17.54% of the bird species found in the Karnali region and 9.81% of the total number of bird species found in Nepal. However, in a similar study by Paudel and Bhusal (2015), 146 bird species were identified in Jajarkot district, mostly in Barekot, indicating the drastic decrease in bird species diversity in the region.

Until 2019, the study area in Jajarkot district was not connected by a road usable by motorized vehicles, but the ongoing construction of the hydropower project within the IBA of Barekot has resulted in increased movement of vehicles and people in the area. This has been a key contributing factor to species habitat destruction. The most serious threats to Nepal's bird populations and diversity are habitat loss, degradation and fragmentation (Inskipp et al. 2017). Stephens et al. (2004) concluded that habitat fragmentation at larger scales may affect nesting success, thus reducing the bird populations. Bird species density is negatively associated with habitat fragmentation (Castelletta et al. 2005; Chace & Walsh 2006; Aronson et al. 2014). In India, dam-building has negatively affected montane birds in the Western Himalaya (Jolli 2017). Conservation biologists suggest that roads have a negative impact on adjacent habitats and their natural communities (Forman 2000; Rheindt 2003). In their study in Bhutan, Thinley et al. (2020) found that hydropower and roads pose a significant threat to wildlife. Rodrigues et al. (2018) suggest that high levels of noise adversely affect birds' behaviour and social communication. Perillo et al. (2017) found that anthropogenic noise can have a significant negative impact on bird diversity.

Illegal hunting and trapping are prevalent in this region (DNPWC & DFSC 2018). In the study area, Cheer pheasants are treated as gamebirds by local communities due to a lack of awareness and a negative attitude towards them (Biodiversity Conservancy Nepal 2016). The population of Galliformes has been reduced dramatically in many parts of Nepal, including protected areas like Kanchenjunga Conservation Area, as they are popular targets for hunters and trappers (Inskipp et al. 2008). In addition to all these factors, there are indications that the Covid-19 pandemic has forced locals to exploit forest resources more than ever, thus increasing the challenges of forest management. The majority of locals (84%) in the study area are engaged in the agricultural sector. Except for May and October (the two months of the agricultural season), most of the local youth head to India as migrant labour (UNRCHCO 2021). During lockdowns in Nepal, Covid-19-driven disruptions in global and regional supply chains, an economic recession, and negligible economic growth severely harmed the local economy and society (ILO 2020).

The impacts of the pandemic coupled with the escalating threats of poaching and habitat modification have serious implications for forest ecosystems in the region, especially bird diversity.

Conclusion

Although the study area accounts for only a small percentage of the entire Nepalese forest cover, it is rich in bird diversity. The geographical location of Barekot makes it an important IBA, despite the decrease in bird diversity. In recent years, populations of bird species in the study area have plummeted due to human activities and anthropogenic effects. This study provides information about the bird diversity of the study area during the early spring, but detailed all-season surveys are needed to evaluate precise bird diversity in Barekot. Further, in-depth longitudinal bird studies should also be carried out in Nepal, notably in Siwalik (~1,500 m) and Mahabharat lekh (600 m to 3,000 m). Also recommended are comprehensive studies of the impacts of the hydropower project, the construction of roads, illegal hunting and trapping, and Covid-19 on the local economy. Finally, awareness-raising campaigns to mitigate the effects of other harmful activities (notably killing or hunting bird species) are imperative.

References

Acharya, K.P. & P.K. Paudel 2020. *Biodiversity in Karnali Province: Current status and conservation.* Ministry of Industry, Tourism, Forest and Environment, Karnali Province Government, Surkhet, Nepal.

Amat, J.A. & A.J. Green 2010. Waterbirds as bioindicators of environmental conditions. In: Hurford, C., M. Schneider & I. Cowx, *Conservation monitoring in freshwater habitats*: 45–52. Dordrecht.

Aronson, M.F.J., F.A. La Sorte, C.H. Nilon, M. Katti, M.A. Goddard, C.A. Lepczyk, P.S. Warren, N.S.G. Williams, S. Cilliers, B. Clarkson, C. Dobbs, R. Dolan, M. Hedblom, S. Klotz, J.L. Kooijmans, I. Kühn I. MacGregor-Fors, M. McDonnell, U. Mörtberg, P. Pyšek, S. Siebert, J. Sushinsky, P. Werner & M. Winter 2014. A global analysis of the impacts of urbanization on bird and plant diversity reveals key anthropogenic drivers. *Proceedings of the Royal Society B.* 281: 20133330. Doi: 10.1098/rspb.2013.3330

Bensizerara, D., H. Chenchouni, A.S. Bachir & M. Houhamdi 2013. Ecological status interactions for assessing bird diversity in relation to a heterogeneous landscape structure. *Avian Biology Research* 6(1): 67–77.

Bhandari, G.P., S.M. Dixit, U. Ghimire & M.K. Maskey 2009. Outbreak investigation of diarrheal diseases in Jajarkot. *Journal of Nepal Health Research Council* 7(2): 66–68.

Bhusal, K.P. & G.B. Singh 2017. First Breeding record of Great Cormorant *Phalacrocorax carbo* in Nepal. Available at: https://www.researchgate.net/publication/317258934_First_Breeding_record_of_Great_Cormorant_Phalacrocorax_carbo_in_Nepal (accessed: 24/03/2022)

Bibby, C.J., N.D. Burgess, D.A. Hill, D.M. Hillis & S. Mustoe 2000. *Bird census techniques.*

Biodiversity Conservancy Nepal 2016. Cheer Pheasants Conservation Initiative. Available from: https://www.bioconnepal.org/project/detail/11/cheer-pheasants-conservation-initiative# (accessed: 24/03/2022)

Bird Conservation Nepal 2021. Bird Conservation Nepal. Available from: https://www.birdlifenepal.org/birds/important-birds-areas (accessed: 11/06/2021)

Bista, D., S. Shrestha, P. Sherpa, G.J. Thapa, M. Kokh, S.T. Lama, K. Khanal, A. Thapa& S.R. Jnawali 2017. Distribution and habitat use of red panda in the Chitwan-Annapurna Landscape of Nepal. *PloS one* 12(10): p.e0178797.

Castelletta, M., J.M. Thiollay & N.S. Sodhi 2005. The effects of extreme forest fragmentation on the bird community of Singapore Island. *Biological conservation* 121(1): 135–155.

Central Bureau of Statistics (CBS) 2012. *National Population and Housing Census*. Kathmandu, Nepal: National Planning Commission Secretariat, Government of Nepal.

Central Bureau of Statistics (CBS) 2014. Population Monograph of Nepal. Available from: https://nepal.unfpa.org/sites/default/files/pub-pdf/PopulationMonograph2014Volume1.pdf [Accessed 11 June 2021].

Chace, J.F. and Walsh, J.J., 2006. Urban effects on native avifauna: a review. Landscape and urban planning, 74(1), pp.46-69.

DFRS, 2018. Forest Cover Maps of Local Levels (753) of Nepal. Department of Forest Research and Survey (DFRS), Kathmandu, Nepal. Available from: https://www.researchgate.net/publication/338689224_Forest_Cover_Maps_of_Local_Levels_753_of_Nepal (accessed: 11/06/2021)

DNPWC 2017. *Profiling of Protected and Human Wildlife Conflicts Associated Wild Animals in Nepal.* Department of National Parks and Wildlife Conservation, Kathmandu, Nepal.

DNPWC and BCN 2018. *Birds of Nepal: An official checklist. Department of National Parks and Wildlife Conservation and Bird Conservation Kathmandu, Nepal.* Available at: http://www.himalayanwolvesproject.org/wp-content/uploads/2016/05/Birds-of-Nepal-An-Official-Checklist-2018.pdf (accessed: 11/06/2021)

DNPWC and DFSC 2018. *Pheasant Conservation Action Plan for Nepal (2019–2023).* Department of National Parks and Wildlife Conservation and Department of Forests and Soil Conservation. Kathmandu, Nepal

Forman, R.T. 2000. Estimate of the area affected ecologically by the road system in the United States. *Conservation Biology* 14(1): 31–35.

Grimmett, R., C. Inskipp, T. Inskipp & H.S. Baral 2016. *Birds of Nepal.*

Inskipp, C., H.S. Baral, T. Inskipp, A.P. Khatiwada, M.P. Khatiwada, L.P., Poudyal & R. Amin 2017. Nepal's National Red List of Birds. *Journal of Threatened Taxa* 9(1): 9700–9722.

Inskipp, C., T. Inskipp, R. Winspear, P. Collin, A. Robin, J. Thakuri & M. Pandey 2008. *Bird survey of*

Kanchenjunga Conservation Area, April 2008. Kathmandu, Nepal and Sandy, UK. Bird Conservation Nepal and Royal Society for the Protection of Birds.

International Labour Organization (ILO) 2020. COVID-19 labour market impact in Nepal. Available at: https://www.ilo.org/kathmandu/whatwedo/publications/WCMS_745439/lang--en/index.htm (accessed: 11/06/2021)

Jolli, V. 2017. Hydro power development and its impacts on the habitats and diversity of montane birds of western Himalayas. *Vestnik zoologii* 51(4): 311.

Lama, S., S. Shrestha, N.P. Koju, A.P. Sherpa & M. Tamang 2020. Assessment of the Impacts of Livestock Grazing on Endangered Red Panda (*Ailurus fulgens*) Habitat in Eastern Nepal. *Open Journal of Ecology* 10(3): 97–110.

Ministry of Forests and Soil Conservation (MoFSC) 2016. *Conservation Landscapes of Nepal*. Ministry of Forests and Soil Conservation, Singha Durbar, Kathmandu, Nepal.

Morante-Filho, J.C. & D. Faria 2017. An appraisal of bird-mediated ecological functions in a changing world. *Tropical Conservation Science* 10: 1940082917703339

National Trust for Nature Conservation (NTNC) 2019. Feasibility Study for Conservation Area in Jajarkot and Adjoining Areas. Available from: https://ntnc.org.np/sites/default/files/doc_notices/2019-02/EOI%20Document.pdf (accessed 25/03/2022)

Paudel, K. & K.P. Bhusal 2015. *Ecological Monitoring and Conservation of Vultures in Jajarkot District, Nepal*. A technical report submitted to Oriental Bird Club.

Perillo, A., L.G. Mazzoni, L.F. Passos, V.D. Goulart, C. Duca & R.J. Young 2017. Anthropogenic noise reduces bird species richness and diversity in urban parks. *Ibis* 159(3): 638–646.

Prakash, V., S. Sivakumar & J. Verghese 2001. *Avifauna as indicators of habitat quality in Buxa Tiger Reserve*. Quarterly Report IV. Bombay Natural History Society, Mumbai.

Rheindt, F.E. 2003. The impact of roads on birds: does song frequency play a role in determining susceptibility to noise pollution? *Journal für Ornithologie* 144(3): 295–306.

Rodrigues, A.G., M. Borges-Martins F. Zilio 2018. Bird diversity in an urban ecosystem: the role of local habitats in understanding the effects of urbanization. Iheringia. *Série Zoologia*: 108.

Sekercioglu, Ç.H., D.G. Wenny & C.J. Whelan (eds.) 2016. *Why birds matter: avian ecological function and ecosystem services*.

Shrestha, S., S. Lama, A.P. Sherpa, D. Ghale & S.T. Lama 2021a. The endangered Himalayan Red Panda: first photographic evidence from its westernmost distribution range. *Journal of Threatened Taxa* 13(5): 18156–18163.

Shrestha, S., A. Thapa, D. Bista, N. Robinson, A.P. Sherpa, K.P. Acharya, S. Jnawali & S. Lama 2021b. Distribution and habitat attributes associated with the Himalayan red panda in the westernmost distribution range. *Ecology and Evolution* 11(9): 4023–4034.

Stephens, S.E., D.N. Koons, J.J. Rotella, D.W. Willey 2004. Effects of habitat fragmentation on avian nesting success: a review of the evidence at multiple spatial scales. *Biological conservation* 115(1): 101–110.

Thinley, P., T. Norbu, R. Rajaratnam, K. Vernes, P. Dhendup, J. Tenzin, K. Choki, S. Wangchuk, T. Wangchuk, S. Wangdi & D.B. Chhetri 2020. Conservation threats to the endangered golden langur (Trachypithecus geei, Khajuria 1956) in Bhutan. *Primates* 61(2): 257–266.

UNRCHCO 2021. UNDAF District Profile: Jajarkot. Available at: https://un.info.np/Net/NeoDocs/View/4202 (accessed 11/06/2021)

Upadhyay, S.K., P.M.S. Pradhan, R.K. Mahato, B. Marasini, B. Upadhyaya, G. Shakya, G. Baral & K.P. Baral 2016. Outbreak Investigation of Influenza in Pajura VDC of Jajarkot District of Nepal. *Journal of Nepal Health Research Council*.

Authors

Sony Lama[1]

has been involved with the Red Panda Network (RPN) as program associate since 2018. Her expertise and interests lie in global changes and environmental governance. sonylama2016sony@gmail.com

Saroj Shrestha[1,2]

specializes in conservation ecology. One of his areas of particular concern is the protection of endangered species and the Himalayas' unique flora and fauna. His research interests include reintroduction biology, and the monitoring and management of threatened species. saroj.stha44@gmail.com

Ang Phuri Sherpa[1]

has decades of experience in the conservation sector, and has worked for WWF Nepal in different capacities for more than ten years. He has been involved with the RPN as a Country Director since 2014. ang.sherpa@redpandanetwork.org

Munmun Tamang[1]

is involved with the RPN as a program associate. Use of Arc-GIS and academic writing are her fortes. munmun.tamang@redpandanetwork.org

Dinesh Ghale[1]

previously worked with WWF Nepal in Central Nepal. He has been working for the RPN since 2016 and

is currently responsible for a red panda conservation project in Western Nepal. Project management and planning are his strong suits. Dinesh holds a Bachelor's degree in Forestry. dinesh.ghale@redpandanetwork.org

[1] Red Panda Network, 198, Dasarath Chand Marga, Baluwatar, Kathmandu, 44600, Nepal
[2] The Australian National University, Canberra ACT 0200, Australia

Appendix – Bird checklist for the study area. Notes on statutus: CITES Appendices: I – Appendix I, II – Appendix I, III – Appendix III; Conservation Status: VU – Nationally Vulnerable; Occurrence Status: R – Resident, W – Winter, 1 – Common.

SN	Order	Family	English name	Scientific name	Status
1	Galliformes	Phasianidae	Kalij Pheasant	*Lophura leucomelanos*	III, R, 2
2	Columbiformes	Columbidae	Snow Pigeon	*Columba leuconota*	R, 3
3			Oriental Turtle-dove	*Streptopelia orientalis*	R, 2
4	Caprimulgiformes	Apodidae	House Swift	*Apus nipalensis*	R, 1
5	Pelecaniformes	Ardeidae	Indian Pond-heron	*Ardeola grayii*	R, 1
6	Suliformes	Phalacrocoracidae	Great Cormorant	*Phalacrocorax carbo*	W, 1
7	Accipitriformes	Accipitridae	Crested Serpent-eagle	*Spilornis cheela*	II, R, 1
8			Himalayan Griffon	*Gyps himalayensis*	II,VU, R, 2
9			Bearded Vulture	*Gypaetus barbatus*	II,VU, R, 4
10			Black Kite	*Milvus migrans*	II, R, 1
11	Coraciiformes	Alcedinidae	Common Kingfisher	*Alcedo atthis*	R, 1
12			Crested Kingfisher	*Megaceryle lugubris*	R, 2
13			White-breasted Kingfisher	*Halcyon smyrnensis*	R, 1
14	Picipormes	Megalaimidae	Great Barbet	*Psilopogon virens*	R, 1
15			Blue-throated Barbet	*Psilopogon asiaticus*	R, 1
16		Picidae	Scaly-bellied Woodpecker	*Picus squamatus*	R, 2
17			Black-naped Woodpecker	*Picus guerini*	R, 2
18	Psittaciformes	Psittacidae	Slaty-headed Parakeet	*Psittacula himalayana*	II, R, 3
19	Passeriformes	Campephagidae	Long-tailed Minivet	*Pericrocotus ethologus*	R, 2
20			Scarlet Minivet	*Pericrocotus flammeus*	R, 2
21		Corvidae	Yellow-billed Blue Magpie	*Urocissa flavirostris*	R, 2
22			Grey Treepie	*Dendrocitta formosae*	R, 1
23			Large-billed Crow	*Corvus macrorhynchos*	R, 1
24		Stenostiridae	Yellow-bellied Fairy-fantail	*Chelidorhynx hypoxanthus*	R, 2
25			Grey-headed Canary-flycatcher	*Culicicapa ceylonensis*	R, 2
26		Paridae	Green-backed Tit	*Parus monticolus*	R, 1
27			Great Tit	*Parus major*	R, 1
28			Black-lored Tit	*Machlolophus xanthogenys*	R, 1
29			Yellow-browed Tit	*Sylviparus modestus*	R, 3
30		Cisticolidae	Common Tailorbird	*Orthotomus sutorius*	R, 1
31			Grey-breasted Prinia	*Prinia hodgsonii*	R, 1
32		Hirundinidae	Barn Swallow	*Hirundo rustica*	R, 1
33			Red-rumped Swallow	*Cecropis daurica*	R, 2
34		Pycnonotidae	Himalayan Bulbul	*Pycnonotus leucogenys*	R, 1
35			Black Bulbul	*Hypsipetes leucocephalus*	R, 1
36			Mountain Bulbul	*Ixos mcclellandii*	R, 2
37			Red-vented Bulbul	*Pycnonotus cafer*	R, 1
38		Phylloscopidae	Ashy-throated Warbler	*Phylloscopus maculipennis*	W, 3
39			Grey-hooded Warbler	*Phylloscopus xanthoschistos*	R, 1
40			Lemon-rumped Leaf-warbler	*Phylloscopus chloronotus*	W, 3
41			Buff-barred Warbler	*Phylloscopus pulcher*	W, 3
42			Chestnut-crowned Warbler	*Phylloscopus castaniceps*	R, 3
43			Blyth's Leaf-warbler	*Phylloscopus reguloides*	W, 3
44			Chestnut-headed Tesia	*Cettia castaneocoronata*	R, 3
45		Aegithalidae	Red-headed Tit	*Aegithalos iredalei*	R, 1
46		Zosteropidae	Oriental White-eye	*Zosterops palpebrosus*	R, 1
47			Stripe-throated Yuhina	*Yuhina gularis*	R, 2
48			Whiskered Yuhina	*Yuhina flavicollis*	R, 2
49		Timaliidae	Black-chinned Babbler	*Cyanoderma pyrrhops*	R, 3
50		Leiotrichidae	Chestnut-crowned Laughingthrush	*Trochalopteron erythrocephalum*	R, 2
51			Striated Laughingthrush	*Grammatoptila striata*	R, 2
52			White-throated Laughingthrush	*Garrulax albogularis*	R, 1
53			Blue-winged Minla	*Siva cyanouroptera*	R, 2
54			Bar-throated Minla	*Chrysominla strigula*	R, 2
55			Rufous Sibia	*Heterophasia capistrata*	R, 1
56		Sittidae	White-tailed Nuthatch	*Sitta himalayensis*	R, 2
57			Wallcreeper	*Tichodroma muraria*	W, 3
58		Cinclidae	Brown Dipper	*Cinclus pallasii*	R, 2
59		Sturnidae	Common Myna	*Acridotheres tristis*	R, 1
60		Turdidae	Long-billed Thrush	*Zoothera monticola*	W, 3

SN	Order	Family	English name	Scientific name	Status
61	Passeriformes	Muscicapidae	Blue Whistling-thrush	*Myophonus caeruleus*	R, 1
62			Himalayan Bush-robin	*Tarsiger rufilatus*	W, 3
63			White-capped Water-redstart	*Phoenicurus leucocephalus*	R, 1
64			Blue-fronted Redstart	*Phoenicurus frontalis*	W, 1
65			Plumbeous Water-redstart	*Phoenicurus fuliginosus*	R, 1
66			Black-backed Forktail	*Enicurus immaculatus*	R, 3
67			Little Forktail	*Enicurus scouleri*	R, 2
68			Rufous-gorgeted Flycatcher	*Ficedula strophiata*	R, 2
69			Grey Bushchat	*Saxicola ferreus*	R, 2
70			Pied Bushchat	*Saxicola caprata*	R, 2
71		Chloropseidae	Orange-bellied Leafbird	*Chloropsis hardwickii*	R, 2
72		Dicaeidae	Fire-breasted Flowerpecker	*Dicaeum ignipectus*	R, 2
73		Nectariniidae	Green-tailed Sunbird	*Aethopyga nipalensis*	R, 2
74			Black-throated Sunbird	*Aethopyga saturata*	R, 2
75			Purple Sunbird	*Cinnyris asiaticus*	R, 1
76		Passeridae	Russet Sparrow	*Passer cinnamomeus*	R, 3
77			Eurasian Tree Sparrow	*Passer montanus*	R, 1
78			House Sparrow	*Passer domesticus*	R, 1
79		Motacillidae	Grey Wagtail	*Motacilla cinerea*	R, 2
80			Olive-backed Pipit	*Anthus hodgsoni*	W, 1
81			Rosy Pipit	*Anthus roseatus*	W, 2
82		Fringillidae	Pink-browed Rosefinch	*Carpodacus rodochroa*	W, 2
83			Dark-breasted Rosefinch	*Procarduelis nipalensis*	W, 2
84			Spot-winged Rosefinch	*Carpodacus rodopeplus*	W, 3
85			Scarlet Finch	*Carpodacus sipahi*	W, 3
86			Yellow-breasted Greenfinch	*Chloris spinoides*	R, 2
87		Emberizidae	Rock Bunting	*Emberiza cia*	W, 3

eco.mont – Volume 14, Number 2, July 2022
ISSN 2073-106X print version – ISSN 2073-1558 online version: http://epub.oeaw.ac.at/eco.mont
https://dx.doi.org/10.1553/eco.mont-14-2s78

Report on the Southern African Mountain Conference 2022, Southern African mountains – their value and vulnerabilities

Günter Köck (Austrian MAB National Committtee), Guy Broucke & Francisco Gómez Durán (both UNESCO Regional Office Harare)

From 14 to 17 March 2022, the first Southern African Mountain Conference (SAMC 2022) was held at the transboundary Maloti-Drakensberg World Heritage Site, which straddles South Africa and Lesotho. The conference, under the patronage of UNESCO, was the first regional mountain research conference focusing specifically on the Southern African region, which includes the areas south of the Congo Rainforest and Lake Rukwa in Angola, Botswana, Comoros, Democratic Republic of Congo (southern mountains), Eswatini, Lesotho, Madagascar, Malawi, Mauritius, Mozambique, Namibia, La Réunion, South Africa, southern Tanzania, Zambia and Zimbabwe.

With the conference theme *Southern African mountains – their value and vulnerabilities*, the organizers used the UN's International Year of Sustainable Mountain Development 2022 to raise awareness of the importance of the conservation and sustainable use of African mountain ecosystems.

Organized by the Afrimontane Research Unit (ARU) of the University of the Free State (South Africa), the African Mountain Research Foundation (AMRF; United Kingdom) and Global Mountains Safeguard Research (GLOMOS; a joint initiative of EURAC Bolzano and the Institute for Environment and Human Security of the UN University, Italy and Germany), and supported by several sponsors, including the Mountain Research Initiative (MRI), the conference was a great success, with over 250 participants from 21 countries. Many of the presenters, who numbered nearly 200 in all, were young MSc and PhD students.

The importance of the conference was underlined by several prominent keynote speeches, for example by Caroline Adler (MRI), Martin Price (University of the Highlands, Scotland) and Lyn Wadley (University of Witwatersrand, South Africa). A total of 17 sessions covering a wide variety of topics (including Protected Areas & Conservation, Biodiversity: Plants, Biodiversity: Animals, Mountain Invasives, Communities & Livelihoods, Education & Research Management and Water Resource Management) and about 200 scientific contributions brought together stakeholders from governments, international organizations, academic institutions, research institutes, NGOs and private individuals. The conference also hosted two workshops, on how to write scientific articles and competitive project proposals. This forward-thinking idea of the conference organizers is certainly an example of best practice example for knowledge transfer and capacity building; it could thus serve as a model for future conferences as well.

The UNESCO Special Session on Regional Collaboration, organized by the UNESCO Regional Office in Harare (Zimbabwe), aimed to highlight the benefits of regional cooperation from the perspectives of African stakeholders and of the Austrian National Committee for UNESCO's Man and the Biosphere (MAB) programme. The subsequent discussion focused on looking beyond a one-off conference and provided an excellent opportunity to exchange ideas, establish connections, and explore possibilities for cooperation, such as the newly created UNESCO World Network of Mountain Biosphere Reserves.

From this author's point of view, the conference was definitely a great success and is a positive sign for the future. However, the fact that science and research in the southern part of Africa are severely underfunded was confirmed in numerous presentations and discussions with African colleagues. For example, a number of talks can be interpreted as *emergency calls* for much-needed research funding. The effects of the lack of money are so varied that only a few examples can be given here, but for readers interested in an overview of the conference as a whole, the Book of Abstracts can be downloaded from https://www.samc2022.africa/Documents/Abstracts.pdf

In Southern Africa as a whole, there are still many mountain areas that have not been explored at all in terms of biodiversity research, or where such research has been very limited (for example, the mountainous areas in southern Angola or the inselbergs in northern Mozambique). It is very likely that many species will become extinct before they are even discovered. Since the possibilities for long-term biodiversity monitoring studies are usually severely limited, it is also difficult to make statements about changes in mountain ecosystems, for example caused by climate change. Illustrative of the difficulties is the failure, due to lack of funding, to establish a permanent monitoring plot in the Maloti-Drakensberg as part of the renowned global climate change monitoring network GLORIA (Global Observation Initiative in Alpine Environments) region (Ralph Clarke, ARU, personal communication).

Due to underfunding, protected areas in southern Africa are often unable to fulfil their basic mission of protecting fauna and flora, and may be just so-called *paper parks* – i. e., areas which have been established legally as PAs but which do not function as such in reality. Frequently, very few staff are available, so that the PA management (if it exists at all) is unable to address adequately or to solve many problems, such as poaching, pressure from the rapid increase in the rural population, or wildlife-population conflicts (e. g., damage to agricultural land by elephants).

Significantly and perhaps encouragingly, the conference showed that collaborations with research institutions from this region would have a comparatively large impact on environmental science in southern Africa. Let us end, therefore, with a quotation from a conversation with a colleague from the University of Malawi: *„You can't imagine how much we could do here with a few thousand euros!"*

eco.mont – Volume 14, Number 2, July 2022
ISSN 2073-106X print version – ISSN 2073-1558 online version: http://epub.oeaw.ac.at/eco.mont
https://dx.doi.org/10.1553/eco.mont-14-2s79

GI (Green Infrastructure) goes business

The EU Strategy for the Alpine Region (EUSALP) initiated the "GI (Green Infrastructure) goes business" award and during the ceremony in May 2022 in Bozen six businesses won and two initiatives not related to the private sector received special recognition. More information available on: www.gi-goes-business.eu/

CIPRA celebrates 70 years of Alpine protection

Connecting people, overcoming borders, protecting the Alps: For 70 years CIPRA has been working for a good life in the Alps. What might the Alps of the future look like? CIPRA takes a fresh look at itself and presents various visions of the future in the current AlpsInsight issue "The Alps of Tomorrow". More information available on: www.cipra.org/en/news/cipra-celebrates-70-years-of-alpine-protection

Climate bridges to south-eastern Europe

The "Climate Bridges" project strengthens cooperation for transnational climate protection in the Western Balkans and is looking for good climate protection examples from south-eastern Europe until June 30. More information available on: www.cipra.org/climate-bridges

Parks discussed in this issue

Abbreviations: NP – National Park; p. – page